western australian marine science institution

Terrestrial-Ocean Linkages: the role of rivers and estuaries in sustaining marine productivity in the Kimberley

Andrew T. Revill[1,4], Nicole L. Jones[2,4], Matthew R. Hipsey[2,4], Louise C. Bruce[2,4], Richard P. Silberstein[2,4], Miles Furnas[3,4], Michael Donn[1,4], Alexis Espinosa[2,4], Renee Gruber[2,4], Wencai Zhou[2,4]

[1]*CSIRO Oceans and Atmosphere, Hobart, Tasmania*

[2] *University of Western Australia, Perth, Western Australia*

[3]*Australian Institute of Marine Science (AIMS), Townsville, Queensland, Australia*

[4]*Western Australia Marine Science Institution (WAMSI), Perth, Western Australia a*

WAMSI Kimberley Marine Research Program

Final Report

Project 2.2.6

September 2017

western australian marine science institution

CSIRO

THE UNIVERSITY OF WESTERN AUSTRALIA

Australian Government

Australian Institute of Marine Science

WAMSI Kimberley Marine Research Program

Initiated with the support of the State Government as part of the Kimberley Science and Conservation Strategy, the Kimberley Marine Research Program is co-invested by the WAMSI partners to provide regional understanding and baseline knowledge about the Kimberley marine environment. The program has been created in response to the extraordinary, unspoilt wilderness value of the Kimberley and increasing pressure for development in this region. The purpose is to provide science based information to support decision making in relation to the Kimberley marine park network, other conservation activities and future development proposals.

Front cover images (L-R)

Image 1: Satellite image of the Kimberley coastline (Image: Landgate)

Image 2: Preparing the bottom mounted ADCP for deployment (Source: Andy Revill, CSIRO)

Image 3: RV Dorado operating in Walcott Inlet (Source: Andy Revill, CSIRO)

Image 4: Inside Walcott Inlet (Source: Andy Revill, CSIRO)

Year of publication: September 2017

Metadata: http://catalogue.aodn.org.au/geonetwork/srv/eng/metadata.show?uuid=fc8bbadc-3242-06db-e043-08114f8c34f5
and http://catalogue.aodn.org.au/geonetwork/srv/eng/metadata.show?uuid=76d88713-0a15-4936-a0ff-ec9ac259d78d

Citation: Revill AT, Jones NL, Hipsey MJ, Bruce LC, Silberstein RP, Furnas M, Donn M, Espinosa A, Gruber R, Zhou W (2017) Terrestrial-Ocean Linkages: the role of rivers and estuaries in sustaining marine productivity in the Kimberley. Report of Project 2.2.6 prepared for the Kimberley Marine Research Program, Western Australian Marine Science Institution, Perth, Western Australia, 102 pp.

Author Contributions: ATR and NLJ prepared project plans, ATR oversaw organic chemistry component. NLJ, MJH, LCB, RG, WZ and AE undertook hydrodynamic and biogeochemical modelling, RPS and MD prepared catchment export models and climate scenarios. MF provided Kimberley river nutrient data. ATR, NLJ, MJH, LCB and RPS prepared the final report.

Corresponding author and Institution: Andy Revill (CSIRO, Hobart, Australia)

Funding Sources: This project was funded (commissioned) by the Western Australian Marine Science Institution as part of the WAMSI Kimberley Marine Research Program, a $30M program with seed funding of $12M provided by State government as part of the Kimberley Science and Conservation Strategy. The Program has been made possible through co-investment from the WAMSI Joint Venture partners and further enabled by data and information provided by Woodside Energy Ltd.

Competing Interests: The commercial investors and data providers had no role in the data analysis, data interpretation, the decision to publish or in the preparation of the manuscript. The authors have declared that no competing interests exists.

Kimberley Traditional Owner agreement: This research was enabled by the Traditional Owners through their advice, participation and consent to access their traditional lands.

Acknowledgements: We would like to thank James Brown and staff at the Kimberley Marine Research Station for their support and assistance in conducting fieldwork in a challenging environment and Mina Brock for laboratory analyses.

Collection permits/ethics approval: No collection requiring permits occurred in the production of this report.

Contents

Executive Summary

River mouths and estuaries can be highly productive habitats that support biodiversity and potentially targeted species for commercial, recreational, and cultural purposes. Productivity in the inshore environment is sensitive to terrestrial runoff that generates turbidity, deposits sediments, and subsidizes marine carbon and nutrient pools. While the western Kimberley is among the most pristine in Australia, abundant water and energy resources will likely be developed in the near future with important implications for linked river, estuarine and inshore environments.

The Kimberley Marine Research Program (KMRP) Project 2.2.6 represents the first attempt to characterise the interaction between largely undeveloped catchments and the coastal environment of the Kimberley and the role large coastal inlets play in transforming material transported from those catchments during large flows before it reaches the coast. This project also attempted to provide the first assessment of how future changes in climate might impact these processes. Walcott Inlet, which flows into Collier Bay, was the focus estuary used for the development of catchment-based modelling tools that estimate freshwater discharge and the delivery of carbon and nutrients to inshore coastal environments.

Walcott Inlet appears to be a carbon poor environment where labile carbon from algae is rapidly re-mineralised by bacteria. There is evidence that large amounts of more recalcitrant terrestrial material may be transported into the inlet during high flow events, but there is little evidence that this becomes incorporated into sediments suggesting it is most likely transported directly through the inlet. Water quality data for streams and rivers flowing into Walcott Inlet are very limited, which hampered the ability to relate flow to the input of material. However, this project represents the first serious attempts to generate modelled flows and loads to the inlet for the estuarine modelling and as such, we have a good base on which to plan future investigations in the region.

The project also required simulation of stream flows under projections of future climate. Global climate models (GCMs) available from the Fifth IPCC Assessment Report have been run under a number of future emission scenarios, referred to as Representative Concentration Pathways (RCP). Pathway RCP8.5 was selected and the scenario was projected forward to 2050 for the purposes of the comparisons undertaken in this project.

The future climate scenarios suggest there is not a great difference in mean rainfall or flows between the three possible future climates and the historical sequence. The projections for all future climates, even the driest one, are for an increase in mean annual rainfall and flow. However, the projections are also for a greater inter-annual variability, so that while the average flows may increase, there will be a greater range between wet and dry years and low flow years will be more severe. Because of the limitations in the historical water quality data we are cautious about drawing strong conclusions on the future trends of water quality parameters.

Circulation of the estuary/ bay system was explored using ROMS simulations We demonstrated that bathymetric variation in different directions (lateral or longitudinal) had different impacts on the interaction between tides and freshwater inflow. Salt (a tracer) was to trace the cross-shore exchange of water within the estuary/bay system, identifying the important patterns of exchange flows with the open ocean. This detailed hydrodynamic understanding of the nature of the bay and estuarine hydrodynamics provided an important foundation for the more complex assessment of carbon and nutrient fate and transport.

To investigate the physical-biogeochemical interactions in this region, a second model was established with a focus on the coastal margin and estuarine portion, and then additionally configured to simulate turbidity (including particle resuspension), and inorganic and organic carbon and nutrients. The model was validated and then used to assess how far terrestrial nutrients might extend from the river into Walcott Inlet and possibly Collier Bay. Flows greater than 300m^3/s were shown to dominate nutrient loads within Walcott Inlet itself (>50% of total load) and significantly contribute to the inner reaches of Collier Bay (>15% of total load).

Implications for management

Terrestrially derived nutrients can constitute significant proportions of total nutrient load in Walcott Inlet and Collier Bay. Seasonal cyclonic events and the associated high river flows bring sediments and nutrients into the coastal environment in a way that doesn't happen at other times of the year. Deposition of these sediments may influence habitat availability and there is evidence that a significant proportion of nutrients being delivered could be in the form of dissolved organic nitrogen (DON) about which little is known. If catchment derived nutrients are a significant contribution to nearshore coastal environments, then any changes in catchment use or flow restrictions could impact on delivery of this material. Until we better understand the linkages with coastal production it is unclear what the ecosystem level impacts could be.

Management of catchments and/or rivers needs to consider the system as a whole and requires a greater understanding of the origins of the material being delivered into the coastal environment.

Key residual knowledge gaps

The results from this project have provided the first insight to key questions around the role of terrestrial material entering the Kimberley coastal environment. Uncertainty remains in several aspects of the available observations and subsequent model predictions which will require further refinement to enable key questions such as the role this material might play in the coastal food web to be answered:

- the results in this report are based on two field campaigns, one of which was restricted by vessel issues. To develop further understanding into the future it will be important to extend the temporal range of available observation data. One mechanism for this could be through knowledge transfer and training of traditional owner rangers based on country to facilitate on-going observation programs for parameters such as nutrient concentrations;
- data from several Kimberley rivers suggests that dissolved organic nitrogen (DON) may be a significant nutrient input in high flow events. Presently little is known about the composition or availability of DON or whether it is associated with the first-flush or later in the flow event. It is important to understand more about this component and what role it may play in coastal productivity;
- results from enhanced benthic mapping could be used to better configure spatial regions within the model domain with distinct sediment properties and/or benthic structures and communities.
- improved focus on sediment resuspension and sedimentation will allow for improved prediction of suspended sediment and turbidity. Outputs from remote sensing efforts can be used to help calibrate such a model to better capture the turbidity gradient from the coast to offshore. Additional effort is required to better understand the rate of particulate carbon resuspension;
- sediment nutrient fluxes, including denitrification estimates and nitrate/ammonium fluxes is important to better resolve the sediment derived nutrient loading to the water column. This includes recommendations for laboratory based sediment flux studies, and additional effort to apply/develop an improved sediment biogeochemical model; and
- water quality data from the streams flowing into the estuaries in the region are very limited. Only the Fitzroy River has anything approaching a reasonable dataset but does not flow into Walcott Inlet. It is strongly recommended that a concerted campaign of water sampling be undertaken, and that water sampling and analysis be introduced as part of the current stream gauging and monitoring programme. Given the resources required to maintain the current level of stream monitoring in the Kimberley, adding the cost of water sampling at each site visit or gauge attendance would be a minor additional expense that would yield enormous benefit for future understanding.

1 Introduction

Significant freshwater (30,000 GL/y) and associated carbon (C) and nutrients are delivered to Kimberley coastal marine environments (in Western Australia) during a short period of the summer monsoon season. This ensures inshore and estuarine environments are tightly linked to river flows, exhibiting strong seasonality as well as high inter-annual variability. River mouths and estuaries are known to be highly productive habitats that support broad biodiversity as well as species targeted by commercial, recreational and indigenous fishers. Productivity in the inshore environment is likely to be sensitive to terrestrial runoff that generates high levels of water column turbidity, deposits sediments, and potentially subsidises marine carbon and nutrient pools. While the western Kimberley is regarded as one of the most pristine environments in Australia, the abundant water and energy resources will likely come under increasing development pressure in the near future with potentially important implications for linked river, estuarine and inshore environments.

The Kimberley Marine Research Program (KMRP) Science Plan identified "*Understanding key ecosystem processes*" and "*predicting the biological implications to climate change*" as key research priorities. The monsoonal climate of the Kimberley generates seasonal flows and element fluxes that are highly variable from year to year, yet we have little understanding of total export rates and how carbon and nutrients sustain primary production and higher trophic levels. Rivers and estuaries represent critical biogeochemical hotspots that link terrestrial ecosystems to the coastal ocean, and estuarine processes determine the net export of sediment and nutrients to coastal regions.

The KMRP Project 2.2.6 was undertaken to help guide planning and management of the Kimberley region by providing catchment-based modelling tools that estimate freshwater discharge and the delivery of carbon and nutrients to inshore coastal environments. The project has developed a high-resolution hydrodynamic-biogeochemical model validated with field observations that integrates catchment exports, tidal forcing and biogeochemical process rates into a numerical model for a focus estuary ecosystem (Walcott Inlet) and synthesises a conceptual model of terrestrial-ocean linkages based on biogeochemical isotope fingerprinting and functional relationships identified by the coupled model. This project links with KMRP Projects 2.2.1 (Ivey et al. 2017) and 2.2.2 (Hipsey et al. 2017) to better understand how freshwater discharge influences marine food web structure and sustains the productivity of Kimberley inshore ecosystems.

Specific project objectives were to:

1. Estimate freshwater discharge and Carbon (C), Nitrogen (N), Phosphorus (P) delivery (including dissolved and particulate forms) from major Kimberley rivers to the coastal zone under current and future climate;
2. Distinguish C, N, P derived from terrestrial sources (e.g. mangroves and catchment sources) from marine sources (e.g. phytoplankton, seagrass, macroalgae) in a focus estuary-inshore environment using biogeochemical tracing tools and techniques (including stoichiometric, fluorescence and multi-isotopic techniques);
3. Determine the net export rate of C, N, P from estuaries by developing a coupled hydrodynamic-biogeochemical model that includes freshwater discharge, tidal forcing, and biogeochemical cycling in a focus estuary, and to formulate general relationships between catchment loading and estuarine export for wider use across Kimberley coastal waters; and
4. Determine how terrestrial C, N, P influences key ecological processes (e.g. decomposition, production, and C,N,P flow into higher trophic levels) in a focus estuary and inshore environment.

This project combined expertise in climate science, catchment rainfall-runoff modelling, and estuarine hydrodynamic-biogeochemical processes to better understand how the Kimberley inshore environments are influenced by terrestrial carbon and nutrient sources. Major outputs include estimates of terrestrial runoff and C, N, P export under current and future climate scenarios, and conceptual and numerical models of linked catchment-river-estuary biogeochemistry. This study provides some of the first critical information on linkages

between terrestrial and marine ecosystems and the start of a scientific basis for improved management to promote resilience and minimize the impacts of climate change, catchment development, and commercial and recreational fishing.

2 Field and Laboratory Methodology

In order to achieve the project objectives estimates of freshwater runoff and C, N, P export from major Kimberley rivers were determined through the use of historical rainfall records as well as Global Climate Model (GCM) downscaled projections of future rainfall. Projections of future climate and catchment rainfall-runoff modelling were based on hydrologic modelling platforms from CSIRO Pilbara Water Resources Assessment (CSIRO 2012). Biogeochemical fluxes were developed from available data (Water Information Reporting, Department of Water, January 2015) of particulate and dissolved C, N and P concentrations. Linear interpolation of concentrations and, where sufficient data existed, concentration-discharge relationships were used to estimate fluxes. Estimates of catchment export provided input into shelf-scale physical-biogeochemical oceanography models.

A conceptual model of linked catchment-river-estuary biogeochemistry was built based on nutrient concentrations, stable isotopes and lipid/fatty acid composition and linked with estimates of primary production. The goal of this approach was to:

i) discriminate C, N, P and organic matter derived from different catchment/estuary sources (e.g. mangroves, native plants, pastoral activities);
ii) examine the persistence and fate of terrestrially derived C, N and P in collaboration with KMRP Project 1.4 Remote Sensing (Fearns et al. 2017) and KMRP Project 2.2.3 Oceanography (Lowe et al. 2016); and
iii) establish how terrestrially-derived nutrients sustain primary production by comparing estuarine chemistry with process rates from near shore benthic and oceanographic cruises and in collaboration with KMRP Project 2.2.3 Oceanography (Lowe et al. 2016) and KMRP Project 2.2.4 Benthic primary production (Kendrick et al. 2017).

An understanding of Kimberley estuarine hydrodynamics and physical-biogeochemical interactions was used to develop a representative Kimberley estuary such as Walcott Inlet that flows into Camden Sound. The study considered the circulation, mixing mechanisms, and biogeochemistry that influence the transport and transformation of terrestrially derived C, N and P to coastal waters. This was achieved using a combination of hydrodynamic observations (from field instruments deployed in the estuary and boat-based sampling), concurrent water sampling for dissolved and particulate matter, and determination of key pelagic ecosystem variables and rate processes (primary production and respiration) to support the development of a coupled biogeochemical-physical numerical model, built with Regional Ocean Modelling System (ROMS) and the AED2 biogeochemical platform. ROMS was first used to gain a detailed understanding of the hydrodynamics controlling the transport of scalars within the estuary and bay system. Using ROMS a detailed understanding of the cross-shore fluxes of scalars both within the estuary/ bay system and across the bay/ ocean boundary was developed. The biogeochemistry model within ROMS was found to be deficient in terms of the details of the complex estuarine biogeochemistry and light controlled by the large suspended sediment load. The AED2 model with the bathymetry grid, initial and boundary conditions developed in the ROMS model was therefore used to explore the biogeochemical response. General export relationships from the high- resolution model for the focus site were developed to allow the findings to be applied across the region and link with KMRP Project 2.2.1 Oceanography (Ivey et al. 2017) for the larger scale coastal and shelf models.

2.1 Field work

Two cruises were undertaken to sample Walcott Inlet, one in the dry season (November 2013) and one immediately following the wet season (March 2014) using vessels chartered from the Kimberley Marine Research Station (KMRS).

2.1.1 Dry Season sampling (November 2013)

A ten day cruise (including transit time) was undertaken in November 2013 aboard the Cygnet Bay KMRS vessels *Dorado* and *Escapade*, with *Escapade* being substituted half way through the trip for *Atlanta IV*. These cruises were conducted in parallel with the AIMS research vessel R.V. *Solander* operating as part of KMRP Projects 2.2.1 and 2.2.2, with two days of *Solander* time dedicated to measuring process rates at the mouth and within Walcott Inlet.

A series of water column and sediment samples were collected along a series of transects during the ten day cruise (Figure 2-1 and Table 2-1). Water samples were analysed for the parameters indicated in Table 2-2. Two oceanographic moorings were deployed within the estuary consisting of an Acoustic Doppler Current Profiler (ADCP) and a pressure transducer (Figure 2-1). One ADCP was lost when recovery was attempted 6 months later (during wet season sampling trip) (location not shown). See section 2.1.2 for replacement ADCP data. The other ADCP was recovered at the end of the ten day field trip. A pressure sensor (PT on Figure 2.1) was deployed to provide data for tidal correction of the collected bathymetry data.

Table 2-1. Field activity during the Walcott Inlet November 2013 (dry season) field trip.

Date	Activity
27/10/2013	Water sampling along transect
28/10/2013	Water sampling at 12 hour station
29/10/2013	Sediment sampling
30/10/2013	Sediment sampling/bathymetry
31/10/2013	Bathymetry
1/11/2013	Water sampling at 12 hour station
2/11/2013	Water sampling along transect

Table 2-2. Water column parameters analysed during the November 2013 (dry season) field trip.

Parameter analysed	Details
Particulate Organic Matter	
Total suspended solids	
Extracted chlorophyll *a*	
Nutrients	NH_4; NO_2; NO_3; Total dissolved nitrogen (TDN); Dissolved organic nitrogen (DON); Particulate nitrogen (PN); Dissolved inorganic phosphorus (DIP); Total dissolved phosphorus (TDP); Dissolved organic phosphorus (DOP); Particulate phosphorus (PP); Si; Dissolved organic carbon (DOC); Particulate organic carbon (POC); Dissolved inorganic carbon (DIC)

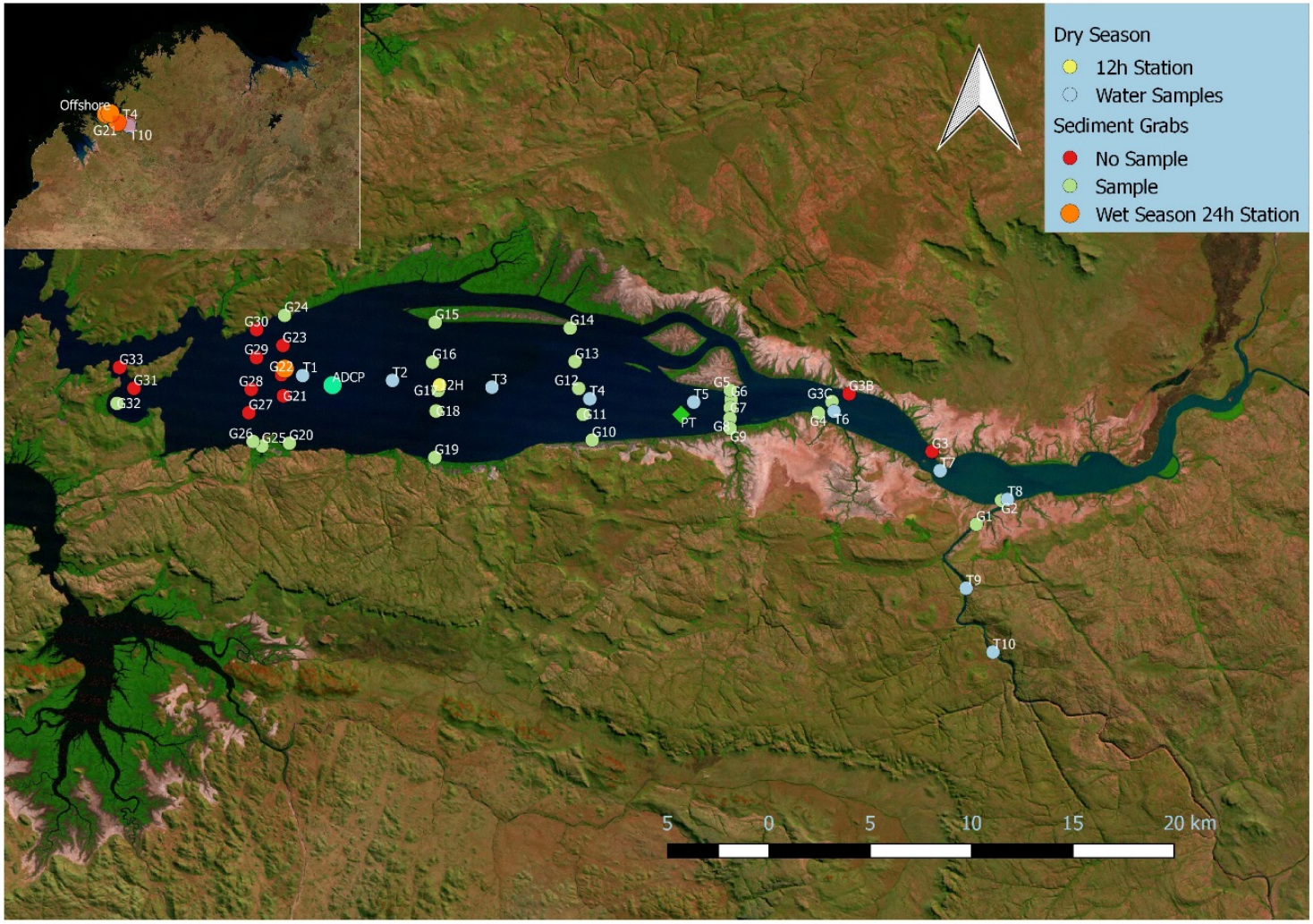

Figure 2-1. Walcott Inlet field sampling sites.

2.1.2 Wet Season sampling (March 2014)

A wet season field trip was initially planned for January 2014. Due to boat engine issues on the first day, the cruise had to be postponed. In order to obtain samples as close to the preceding wet season as possible, KMRP 2.2.6 project team members participated on a R.V. *Solander* cruise (March 2014) for water column sampling and a separate mooring deployment (ADCP) /sediment sampling trip on *Dorado* (April/May 2014). Sediment samples were collected from sites which were successful during the dry season trip (Figure 2-1). Water samples were collected from sites approaching Walcott Inlet (KMRP Project 2.2.2) and at a single site over a 24 hour period within Walcott Inlet (Figure 2-1) in an attempt to assess the variability of material being exported.

Extensive bathymetry data was collected throughout Walcott Inlet from the *Dorado* and R.V. *Solander*. This data was corrected for the tide and compiled into one data set and used in the creation of the hydrodynamic/ biogeochemical model of Walcott Inlet.

Wet season cruises were also undertaken on R.V. *Solander*, allowing the collection of nutrient samples from the freshwaters of King George River, Drysdale River, Prince Regent River, Isdell River, and in adjacent coastal (but non-estuarine) waters.

Table 2-3. Field activity during the Walcott Inlet March 2014 (wet season) field trip.

Date	Activity
March 2014	Offshore transect and 24 hour station water sampling
01/05/2014	ADCP deployment
02/05/2014	Grab samples repeat of 2013 transect
03/05/2014	Water samples repeat of 2013 transect
14/06/2014	ADCP recovery

2.2 Organic Matter Characterisation Methodology

Sediment and water particulate samples were collected at sites shown in Figure 2-1. Water particulates were collected by filtering water through 47 mm GFF filters. Sediment samples were collected using a box corer and the surface (1 cm) removed into pre-cleaned glass jars. All samples were frozen immediately and transported to Hobart (Tasmania) for analysis.

2.2.1 Stable Isotope Analysis

Samples on glass fibre filters were fumed over HCl to remove any carbonate present and dried at 60°C for several hours, before being divided using a scalpel and tweezers and packed into tin cups for analysis (Elemental Microanalysis Ltd., Okehampton, UK). Sediment samples for stable isotope analysis were dried in an oven overnight at 60°C, before being ground with a mortar and pestle. Samples were weighed into tin cups for nitrogen isotope analysis. For the analysis of carbon, samples were weighed into aluminium cups and acidified using sulphurous acid (6% w/w min; Australian Chemical Reagents, Queensland; Verardo et al. (1990)) to remove any mineral carbonate. Samples were then analysed for nitrogen and carbon contents, $\delta^{15}N$ and $\delta^{13}C$ using a Carlo Erba NA1500 CNS analyser interfaced via a Conflo IV to a Thermo Scientific Delta V Plus isotope ratio mass spectrometer operating in the continuous flow mode. Combustion and oxidation were achieved at 1090°C and reduction at 650°C. Samples were analysed at least in duplicate. Results are presented in standard δ notation:

$$\delta^{13}C = \frac{R_{sample}}{R_{standard}} - 1$$

Where R = $^{13}C/^{12}C$ or $^{15}N/^{14}N$. The standard for carbon is Vienna PDB limestone and Air for nitrogen. Average

reproducibility of the stable isotope measurements was ~0.2‰.

2.2.2 Analysis of Lipid Biomarkers

Sediment samples (or filters) were extracted three times by a one-phase chloroform-methanol-water mixture (1:2:0.8 v/v/v) according to a modified version of the Bligh and Dyer method (Bligh & Dyer 1959). Samples were ultrasonicated for 10 min during each extraction, then centrifuged and the supernatant extracts combined. After phase separation, the lipids were recovered in the lower chloroform layer (solvent removed *in vacuo*) and were made up to a known volume and stored sealed under nitrogen at 4°C. An aliquot of the total extract was taken for alkaline saponification with 3 mL of 5% KOH in methanol:water (80:20 v/v). The test tubes were vortex mixed and heated at 80°C for 2 h. The neutral fraction was extracted 3 times into hexane:chloroform (4:1). The fatty acid fraction was subsequently extracted in the same manner after the saponified total extract had been acidified to pH < 3 with HCl. Fatty acid methyl esters (FAMEs) were formed by treating the fatty acid fraction with MeOH:HCl at 80°C for 2 h and extracted into hexane: chloroform (4:1). The neutral fractions were treated with *bis*(trimethylsilyl)trifluoroacetamide (BSTFA, 100 μL, 60°C, 60 min) to convert hydroxylated compounds such as sterols and alcohols to their TMSi-ethers.

Gas chromatography (GC) was initially performed using a Thermo Scientific Trace 1310 controlled by Chromeleon software. For the analysis of the neutral fraction, the gas chromatograph was equipped with a 50 m × 0.32 mm i.d. cross-linked 5% phenyl-methyl silicone (HP5, Hewlett Packard now Agilent) fused-silica capillary column; hydrogen was the carrier gas. Samples were injected through a hot injector. The initial oven temperature was 45°C with a 30°C min^{-1} ramp rate to 140°C and then a 3°C min^{-1} ramp rate to 310°C which was held for 5 min. The fatty acid fraction was analysed on the same instrument, except that the samples were injected through a programmable temperature injector (heated at 200°C min^{-1}) onto a 50 m × 0.32 mm i.d. cross-linked 1% phenyl-methyl silicone (HP1, Hewlett Packard) fused-silica capillary column, with hydrogen as the carrier gas. The initial oven temperature was 45°C with a 25°C min^{-1} ramp rate to 180°C, then a 2°C min^{-1} ramp rate to 290°C followed by a 10°C min^{-1} ramp rate to 310°C, which was held for 10 min. Compounds were detected using a flame ionisation detector, with 5β(H)-cholestan-24-ol as the internal standard for sterols and the methyl ester of tricosanoic acid as the internal standard for fatty acids. Peak identifications were based on retention times relative to authentic and laboratory standards and subsequent GC-MS analysis. The detection limit for individual sterols and fatty acids was approximately 0.2 mg m^{-2} sediment (to a depth of 0.5 cm).

Verification of the identity of individual sterols and fatty acids by GC-MS analyses was performed on a Thermo Scientific TSQ8000 benchtop mass spectrometer fitted with a direct capillary inlet and a programmable temperature injector. Data were acquired in scan acquisition mode and processed using Xcalibur software supplied with the instrument. The non-polar column (HP5) and operating conditions were similar to that described above for GC-FID analyses, except that samples were injected on-column and helium was used as the carrier gas. Compounds were identified from their retention times and mass spectra by comparison with reference standards and data from compounds previously analysed in our laboratories.

3 Catchment-Ocean Modelling Methodology

3.1 Catchment hydrology methodology

3.1.1 Climate data analysis and preparation

Daily climate data were obtained from the CSIRO SILO archive, for the period ending in March 2015. The data are available on a 0.05° x 0.05° latitude x longitude grid (Jeffrey et al. 2001), and from these individual climate sequences were developed for each catchment. Climate sequences refer to the dataset created from the climate variables that include rainfall, temperatures (daily minimum and maximum), humidity, solar radiation, wind speed, and, if it has been calculated, potential evaporation. The gridded data have been analysed to extract the statistics and patterns presented below.

A “water year” is used in hydrology beginning and ending with a natural break between wet seasons, with

September to October the driest two consecutive months in the Kimberley, the water year commences on the 1st October and ends on 30th September. This water year was also adopted in the CSIRO Pilbara Water Resource Assessment (Charles et al. 2015).

The data from all the 0.05° cells were mapped into the catchments in the region and then area weighted average climate sequences derived. These sequences were used as input to the catchment modelling to generate runoff and stream flow. This methodology is substantially simpler than using distributed cell climates into the model and saves a major computational resource. There is the potential for loss of spatial and temporal accuracy in runoff generation using this method, but since the catchment simulations are required at the outlet only, provided the method produces adequate accuracy for this process it is deemed appropriate. The impact of using a single input climate sequence as opposed to using the individual climate cells as distributed input was tested by Silberstein and Aryal (2015a) who found that the difference in streamflow at the catchment outlet was negligible and, given the time and resources saved, was adopted.

3.1.2 Stream flow and water quality data

Eighty eight streamflow gauging stations exist across the Kimberley (http://wir.water.wa.gov.au) and are mostly managed by the Department of Water (DoW). The data from these stations were examined, with 13 stations assessed to have reasonable stream flow records. Of these, only the Isdell River (Gauge 804001) and Charnley River (Gauge 804002) flow into Walcott Inlet, hence only limited analyses were possible. In addition to these two stations, Gauge 803001 (Lennard River at Mt Joseph) was used as it is close to the divide with the Isdell catchment and has been assessed as similar in hydrologic response, thus adding extra information about catchment rainfall—runoff response to improve confidence in stream flow estimates. Gauges 803001 and 804001 have a good recent flow record (Figure 5-3). Unfortunately, Gauge 804002, the closest to the inlet, ceased operation in 1999.

As a consequence of the lack of complete measured flow record during the period of field work in the estuary, the inflows to the inlet needed to be simulated with a calibrated model. The calibrated model was also used to provide estimates of long-term inlet inflows. The three gauges identified above were used to calibrate the model, discussed below for the stream flow estimates to the Walcott Inlet, and for future projections under climate change scenarios.

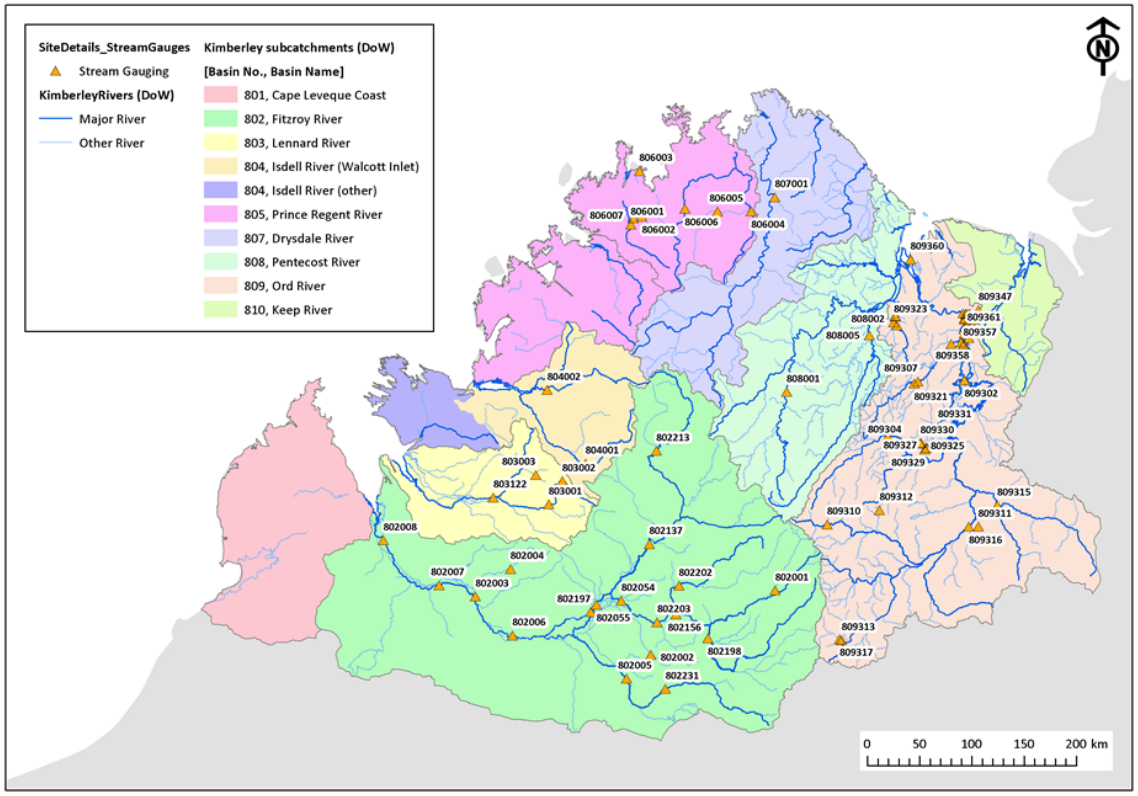

Figure 3-1. Location of stream gauging stations in the Kimberley. While only basin 804 (Isdell) is mapped as flowing into the Walcott Inlet, clearly some southern parts of 805 (Prince Regent) do also.

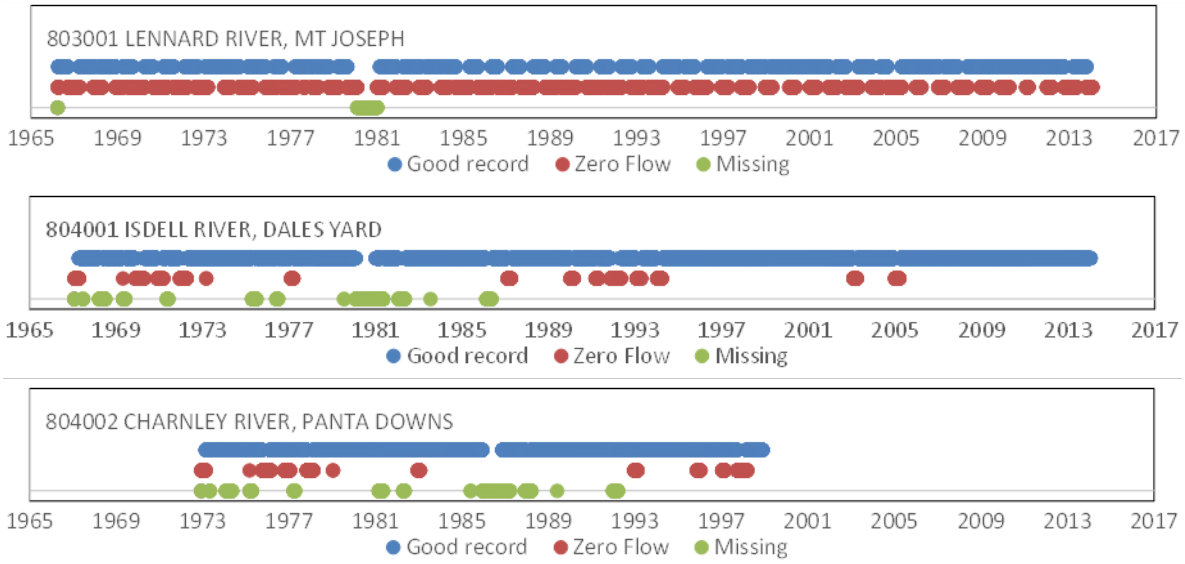

Figure 3-2. The period of good record with flow, days with no-flow, and days of missing record for the stream gauges flowing into Walcott Inlet plus the Lennard River

Water quality records were obtained from the DoW database (Water Information Reporting, Department of Water, January 2015). Unfortunately, as shown in Section 5.1.4 these are extremely limited, and as a result no river flow—water quality correlations could be derived, nor temporal changes associated with catchment or climate trends. As a consequence the river loads of nutrients and carbon were obtained by simply multiplying daily flow volumes by the mean or median quality parameters and, in some case, some ranges. However, coupled with the estuarine measurements these values were examined for scale of reliability and preliminary conclusions drawn.

3.1.3 Catchment runoff modelling

The need for catchment runoff modelling arose because not all streams flowing to Walcott Inlet are gauged, and those that are gauged have imperfect records or records ceased some years prior to the estuarine field programme. By using a model inflows to the estuary can be estimated using the best available knowledge, to complement the marine field work. With the model we can also 'hind cast' the flows over previous years to generate an understanding of how the water and nutrient balances of the estuary have resulted in current conditions. The calibrated model also facilitates analysis of estuarine dynamics under future climate projections.

3.1.4 Model description

Several catchment modelling approaches were tested following methods used in the CSIRO Pilbara Water Resources Assessment project (CSIRO 2012). The method adopted was a modification of the methodology used in the Northern Australian Sustainable Yields (NASY) (CSIRO, 2009) project. This improved methodology (CSIRO 2012) uses a relatively simple catchment runoff generation model based on the nine parameter SIMHYD model (Chiew & McMahon 2002, Chiew et al. 2002, Chiew & Siriwardena 2005, Tan et al. 2005). SIMHYD simulates catchment runoff using rainfall and potential evaporation (PE) with a daily time step. The model, now referred to as SIMHYDGW (Silberstein & Aryal 2015b), has been modified to incorporate groundwater connections. The model, coded in Matlab (MathWorks[tm]), while simple, has enough hydrological detail and process representation to give a reasonable representation of catchment behaviour over large areas, and particularly as there are inadequate data to justify a detailed model application which could not be adequately calibrated. Stream flow generated with this model has four flow components: surface runoff, interflow, base flow and leakage to ground water representing water lost from the stream into riparian or deeper aquifers. The hydrological modelling simulates conditions up to the end of water year 2014.

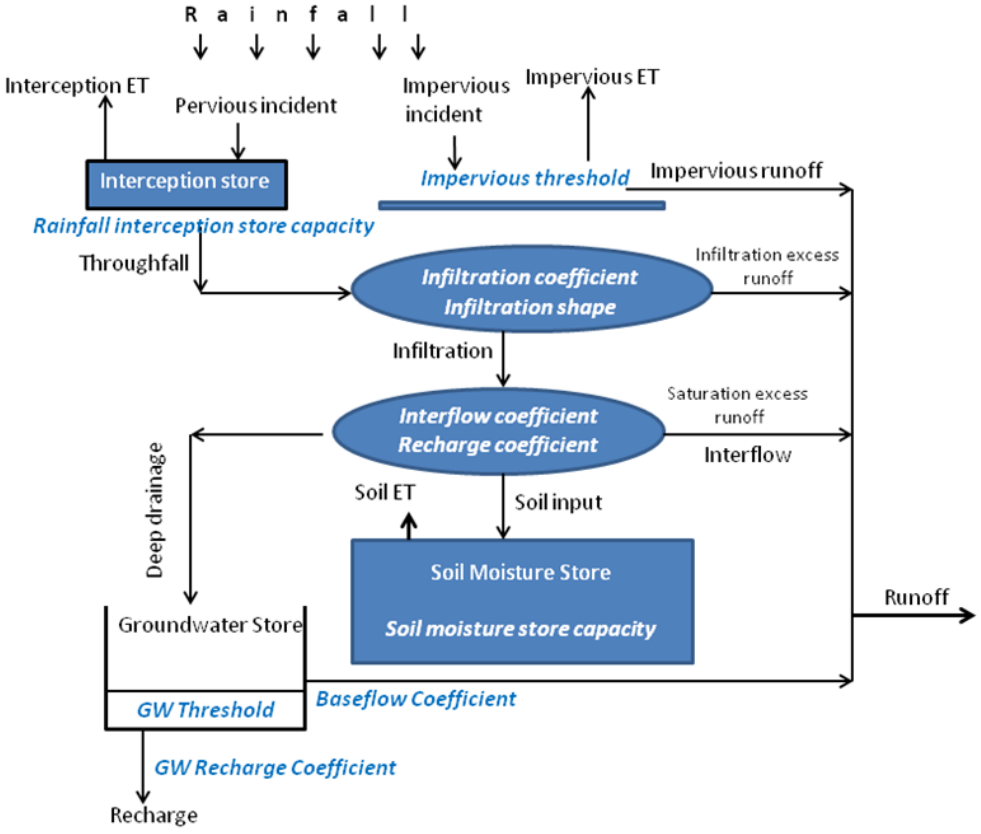

Figure 3-3. Schematic diagram of the SIMHYDGW hydrological model, a modified version of SIMHYD, with additional parameters for groundwater threshold required for baseflow to occur and a groundwater recharge rate out of the stream zone. Variables in italics are parameters able to be optimised (Silberstein & Aryal 2015b).

3.1.5 Model Input data - Rainfall and areal potential evaporation

The historical daily rainfall and areal potential evaporation (PE) data to drive the model were obtained from the Queensland Government's Environmental Protection Agency SILO gridded data (Data Drill) derived from selected stations (<http://www.longpaddock.qld.gov.au/silo> (Jeffrey et al. 2001)]) as described in Section 3.1.1. PE is defined as the total evaporation, including transpiration that would take place if there was unlimited water supply from a large area that has come to equilibrium with conditions in the overlying air. It is not as high as would be possible from small wet areas surrounded by dry surfaces, such as isolated springs or pools, and is less than that measured from standard Class A pans, but is representative of large areas under similar conditions, such as would occur after major rainfall events. PE was calculated using Morton's wet environment PE formulation available from http://www.bom.gov.au/averages (Morton 1983, Chiew & Leahy 2003). The daily rainfall and PE sequences for each catchment were calculated from the 0.05 x 0.05 degree grid and these catchment average sequences input to the model. Stream flow data from the gauging stations in the region were obtained from the DoW and used for calibrating the model.

3.1.6 Model calibration and parameter estimation

The SIMHYDGW model is calibrated using daily rainfall and daily potential evaporation as input data from the water years 1961 to 2014. The model was calibrated against all available stream flow data using the shuffled complex evolution (SCE) (Duan et al. 1992) automated optimiser. A 10 year 'warm up' period was used to achieve convergence in the model. In the calibration, the parameters were optimised to maximise an objective function that incorporated a range of goodness-of-fit criteria together with the Nash-Sutcliffe efficiency (NSE) (Nash & Sutcliffe 1970) of daily runoff. Since the frequency and duration of flow from the stream flow modelling is of particular interest, to provide estimates of recharge to alluvial aquifers in the groundwater analysis, the precise timing of flow events is considered less significant than the frequency distribution. Thus after testing several alternatives, a composite objective function, that included the flow duration curve, number of flow days each year, the daily flow hydrograph, and overall simulation bias, was derived. This use of an alternative objective function was also adopted in the study of rainfall-runoff modelling in northern Australia (Petheram et al. 2012). Further details of the analysis of other objective function performance are given by Silberstein and Aryal (2015a).

The model parameter values are unique to the input climate and catchment characteristics on which they are calibrated. The stream flow for uncalibrated catchments was simulated using model parameters from nearest calibrated catchments which has been shown to perform as well as any other parameter transfer techniques (Chiew & Siriwardena 2005, Zhang & Chiew 2009). Flows from uncalibrated streams are required to give an estimate of the total flow into the inlet, not just that from the main streams which have been calibrated. The errors involved are likely to have a small influence as the uncalibrated catchments are substantially smaller than the Charnley catchment.

3.1.7 Future climate scenarios

The project also required simulation of stream flows under projections of future climate. There were eighteen global climate models (GCMs) available from the Fifth IPCC Assessment Report that deliver daily output suitable for generating future climate daily sequences (Charles et al. 2015). The GCMs have been run under a number of future emission scenarios, referred to as Representative Concentration Pathways (RCP). Pathway RCP8.5 is equivalent to a globally averaged increased radiation balance of 8.5 W/m^2. This was selected following previous analysis in a project based in the Pilbara (Charles et al. 2015). This emission scenario was projected forward to 2050 and for the purposes of the comparisons undertaken in this project, the changed climate assumed to take place instantaneously on the first day of the future climate scenario simulation, conceptually this was 1 October 2015.

To generate future climate sequences the historical sequences were transformed by rescaling each daily rainfall and potential evaporation value according to the changes projected by the GCMs. The projections for future potential evaporation requires a scaling of the historical sequence by projected seasonal trends; each month of

the historical sequence was rescaled according to the projected changes in the monthly mean under each GCM. This is adequate for all variables except rainfall which is a much more stochastic process and requires a different approach to render a more reasonable estimate of future sequence. It is expected that the daily frequency distribution of rainfall will be affected by climate change at least as much as the annual mean. Hence, for this, the historical frequency distribution (determined for each season separately) was transformed according to the projection by the GCMs, and then the full sequence rescaled so that the projected change in mean annual rainfall was captured. Thus the future climate sequences present seasonal changes in mean rainfall and in daily frequency distribution from the historical. This treatment was coded in Matlab^{tm} and followed the methodology presented by Charles et al. (2015).

The calibrated hydrological model was then run for each catchment under the new scenarios to generate future stream flow projections. The results are reported as a degree of change from the historical, rather than actual quantity projections, as this removes, to some extent, errors and biases in the model, by assuming that these will have similar effects under all climate scenarios, whereas the differences will be representative of the future climate impacts. There is some uncertainty about this approach, but the uncertainty in relative change is considered less than the uncertainty in the absolute values (Chiew et al. 2009a, Chiew et al. 2009b, Chiew et al. 2010). Thus, we get a simple comparison of conditions in an average year around 2050 with those of the historical period of record.

3.1.8 Simulation of water quality of inflow under future climate scenarios

To simulate the quality of flows under future climate we really only had recourse to presume the flow-parameter relationships would be remain consistent with the historical record and scale future water quality on the basis of projected flows. As discussed elsewhere, the water quality data were very sparse and the relationships derived have a high degree of uncertainty. It was not considered worthwhile to include temperature related processes in modifying possible water quality parameters as the data did not justify what would have been a highly speculative approach.

3.2 Methodology for Characterising Estuary and Bay Hydrodynamics

3.2.1 Model Description

To begin to understand the hydrodynamic control of cross-shore fluxes and transport of scalars for the complex bay/ estuary topography we first examined scalar transport using hydrodynamic simulations with ROMS (Allen et al. 2003, Warner et al. 2005a, Warner et al. 2005b). The simulations were carried out on the domain shown in Figure 3-4 from November 2013 to May 2014. The averaged horizontal resolutions of the domain are 660 m in the lateral and 535 m in the longitudinal, and 30 sigma-layers were configured in the vertical. Wind forcing was not applied in order to exclude the interference of wind-driven processes when analysing salt fluxes with the simulation results. More details can be found in the KMRP 2.2.1 Final Report (Ivey et al. 2017).

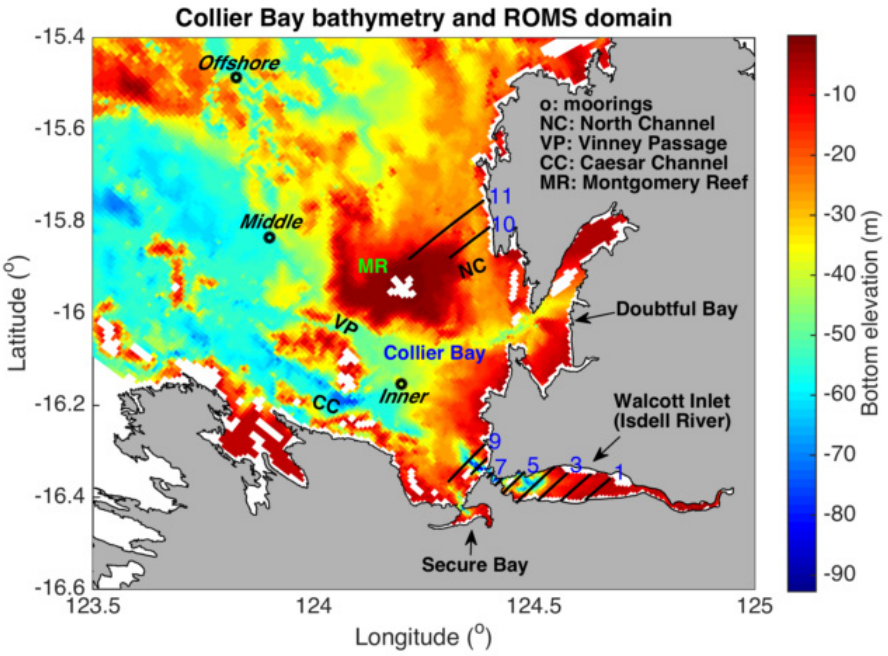

Figure 3-4. Collier Bay bathymetry and ROMS domain. The short solid lines are cross-sections (parallel to grid mesh) where the analysis of salt flux decomposition is carried out. The arrows point to the three estuaries.

The freshwater input was from Section 5.2.1 (Figure 3-5). The analysis applies an Eulerian salt-flux decomposition and isohaline salt-flux decomposition approach to a group of cross-sections distributed longitudinally from the river mouth to the open ocean (Figure 3-34).

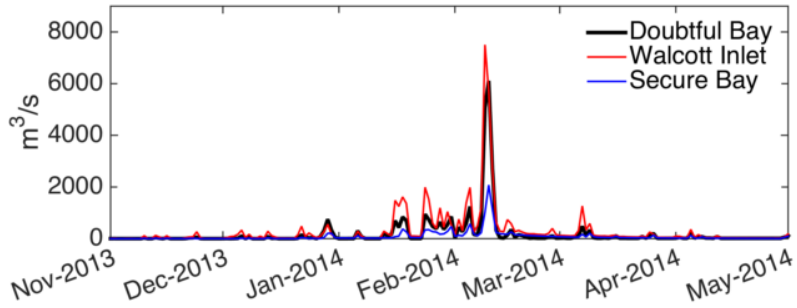

Figure 3-5. Total river runoff at Collier Bay. There are three estuaries that flow into Collier Bay (Figure 3-33): Doubtful Bay, Walcott Inlet (Isdell River) and Secure Bay.

3.2.2 Salt flux decomposition

Water exchange and mass transport between the shallower inshore water in Collier Bay and the deeper offshore water occurs through three channels separated by islands and reefs, however, it remains unclear how the tides, topography and inflows interact to shape the net mass flux (Figure 3-33). Here we focus on the mechanisms controlling the salt flux, which is a scalar. Mechanisms driving the salt flux include advection, steady shear dispersion and tidal oscillations (Lerczak et al. 2006). To distinguish the salt flux components driven by each of these mechanisms, Eulerian salt flux decomposition (Lerczak et al. 2006, MacCready 2011) was applied:

$$F = FR + FE + FT = u_0 s_0 A_0 + \int u_1 s_1 dA_0 + < \int u_2 s_2 dA > \quad (2)$$

Where <> denotes a Godin-type low-pass filter; $\int$ denotes integration over the cross-section area; F is the total salt flux; FR, FE, FT are the advective, steady shear dispersion and tidal oscillatory salt flux, respectively; dA is the differential area element in the vertical; u_0, s_0, A_0 are the tidally and spatially averaged velocity,

salinity and cross-sectional area that are calculated as:

$$u_0 = \frac{<\int udA>}{A_0},\ s_0 = \frac{<\int sdA>}{A_0},\ A_0 =< \int dA > \quad (3)$$

Variables u and s are the normal velocity and the salinity at the cross section. Normal velocity is considered positive when directed towards the open ocean and negative when directed landwards (Figure 3-33). Note that A (or dA) is the cross-sectional area that calculated with depth without being filtered, so it varies with sea surface height. To the contrary, A_0, u_0, s_0 and thus FR are quantities with significant fluctuations due to sub-tidal variation of sea surface height excluded. Variables u_1, s_1 are the tidally averaged and sectionally varying horizontal velocity and salinity, and dA_0 is the tidally averaged differential area element:

$$u_1 = \frac{<udA>}{dA_0} - u_0,\ s_1 = \frac{<sdA>}{dA_0} - s_0,\ dA_0 =< dA > \quad (4)$$

The remainders are the tidally and sectionally varying horizontal velocity and salinity that are associated with the tidal oscillatory salt flux:

$$u_2 = u - u_0 - u_1,\ s_2 = s - s_0 - s_1 \quad (5)$$

The Eulerian decomposition shows that salt fluxes are driven by different mechanisms, but it does not provide further information about simultaneous fluxes that occur up the salinity gradient (towards the open ocean) or down the salinity gradient (landward). Therefore, we also undertook an isohaline salt flux decomposition to characterize the up-gradient and downgradient fluxes as functions of salinity (MacCready 2011). Firstly, it defines the tidally averaged volume flux of water with salinity above a specific salinity s as

$$Q(s) =< \int_{A_s} udA > \quad (6)$$

Where A_s is the area of the portion of the cross-section with salinity above certain specific salinity s. Then the upgradient and downgradient fluxes are calculated as

$$-\frac{\partial Q}{\partial s} = -\lim_{\delta s \to 0} \frac{Q\left(s+\frac{\delta s}{2}\right) - Q\left(s-\frac{\delta s}{2}\right)}{\delta s} \quad (7)$$

$$Q_{up/downgradient} = \int -\frac{\partial Q}{\partial s}|_{up/downgradient} ds \quad (8)$$

$$F_{up/downgradient} = \int s(-\frac{\partial Q}{\partial s}|_{up/downgradient}) ds \quad (9)$$

Here, $-\frac{\partial Q}{\partial s}$ is the differential isohaline volume flux (the volume flux at a specific salinity) and F is the salt flux. The flux-weighted salinities of the upgradient and downgradient fluxes are then calculated as

$$s_{up/downgradient} = \frac{F_{up/dwongradient}}{Q_{up/downgradient}} \quad (10)$$

Both the Eulerian decomposition and isohaline decomposition were carried out at the three channels and Walcott Inlet. Specific attention was paid to comparing North Channel and Walcott Inlet, as the bathymetry of the two regions consists of shallow and deep sections, but varies laterally at North Channel while longitudinally at Walcott Inlet.

3.3 Methodology for Characterising Estuary and Bay Biogeochemistry

3.3.1 Model description

In addition to the ROMS simulations described in Section 3.2, a high-resolution coupled hydrodynamic-biogeochemical model platform was also setup for the Collier Bay and Walcott Inlet region. This model adopted a finite volume (FV) hydrodynamic model that was applied to better capture the complex coastal morphometry, allowing for focused prediction of turbidity, nutrients and productivity around the coastal margin of this region. The TUFLOW-FV hydrodynamic model was used with a flexible mesh (in plan view), consisting of triangular and quadrilateral elements of different size (Figure 3-6). The model was configured to be 3-D by adopting a vertical mesh discretization with z-coordinates below the tidal range and sigma-coordinates within the tidal (26 vertical layers in total). See Bruce et al. (2014) and Jovanovic et al. (2015) for recent descriptions of the TUFLOW FV hydrodynamic and turbulence modelling approach.

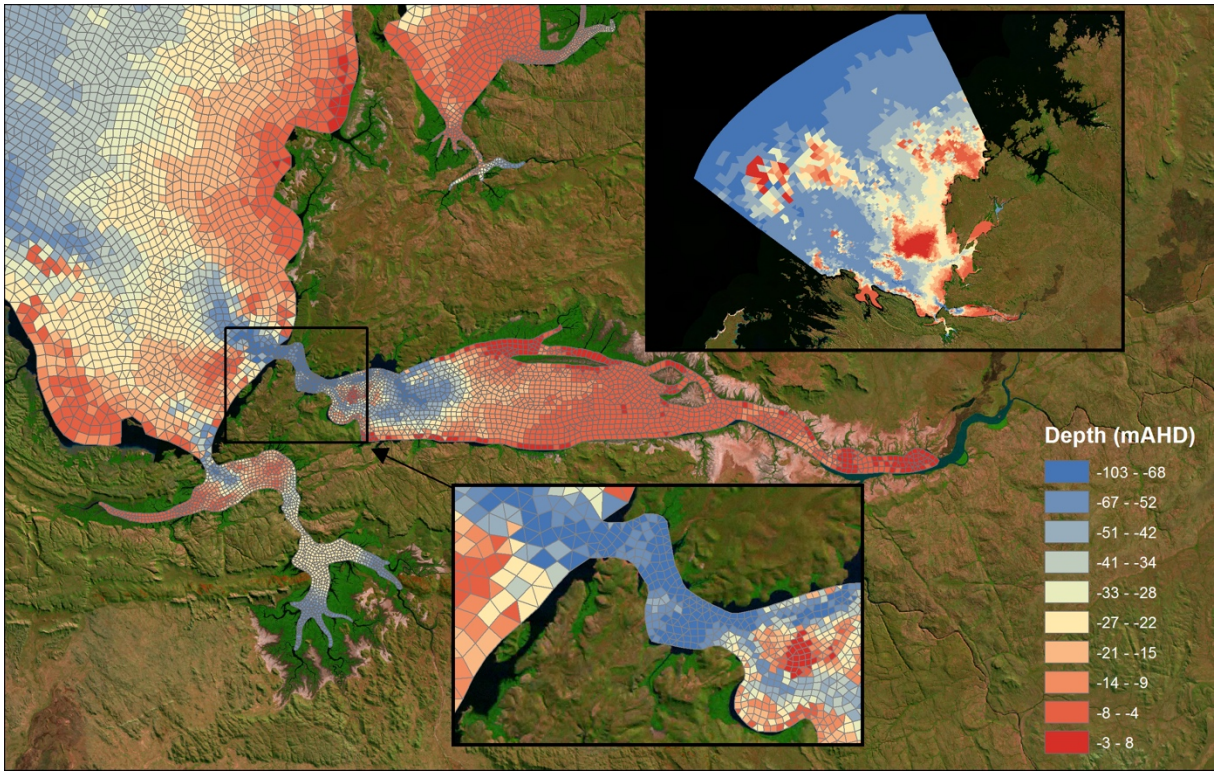

Figure 3-6. Finite volume mesh used for the hydrodynamic-biogeochemical model of Walcott Inlet and Collier Bay.

The TUFLOW-FV hydrodynamic model was dynamically linked with the Aquatic Ecosystem Dynamics (AED2) biogeochemical model library (Hipsey et al. 2013) for simulation of sediment, biogeochemistry and algal productivity. The AED2 Model has ability to simulate a range of physical, chemical and biological processes relevant to computing biogeochemical dynamics for the region that can be generally described as:

- water column kinetic (time-varying) chemical / biological transformations (e.g., denitrification or algal growth);
- water column equilibrium (instantaneous) chemical transformations (e.g., PO_4 adsorption);
- vertical sedimentation or migration of particulates;
- biogeochemical transformations in the sediment or biological changes in the benthos;
- fluxes across the air-water interface;
- fluxes across the sediment-water interface; and
- feedback of chemical or biological attributes to physical properties of water (e.g. light extinction).

The model is organised as a series of interconnected "modules" each with a set of state variables, kinetic equations and associated parameters. State variables used in the Walcott Inlet/Collier Bay TUFLOW-FV AED2 model (Figure 3-6) are summarized in Table 3-1.

3.3.2 Model setup and parameterisation

The main model simulation period was configured to run over a 6 months simulation period, spanning the two field campaigns described in Section 2.1, from 1/10/2013 – 31/3/2014, and providing a suitable spin-up time based on advective timescales. The model was forced on the land-side of the domain by 4 river inflows, based on predictions from the hydrology model described in Section 5.1, and values for flow, salinity, turbidity and nutrients were prescribed for each. At the ocean boundary, and the surface meteorological boundary, data was prescribed based on ROMS simulation derived boundary conditions as outlined in Section 3.2. Nutrient initial conditions were spatially interpolated from the observations. Nutrient values at the ocean boundary were specified as outlined in the KMRP Project 2.2.2 (Hipsey et al. 2017).

Table 3-1. Variables used in the Walcott Inlet / Collier Bay model configuration.

Variable	Units *	Common Name	Process Description
Physical variables			
V	m/s	Velocity	Velocity modelled by TUFLOW-FV, subject to inflows, tide and wind forcing
T	°C	Temperature	Temperature modelled by TUFLOW-FV, subject to surface heating and cooling processes
S	psu	Salinity	Salinity simulated by TUFLOW-FV, impacting density. Subject to inputs and evapo-concentration
EC	µS cm^{-1}	Electrical conductivity	Derived from salinity variable
I_{PAR}	mE m^{-2} s^{-1}	Shortwave light intensity	Incident light, I_0, is attenuated as a function of depth
I_{UV}	mE m^{-2} s^{-1}	Shortwave light intensity	Incident light, I_0, is attenuated as a function of depth
η_{PAR}	m^{-1}	PAR extinction coefficient	Extinction coefficient is computed based on organic matter and suspended solids
η_{UV}	m^{-1}	UV extinction coefficient	Extinction coefficient is computed based on organic matter and suspended solids
Core biogeochemical variables			
DO	mmol O_2 m^{-3}	Dissolved oxygen	Impacted by photosynthesis, organic decomposition, nitrification, surface exchange, and sediment oxygen demand
FRP	mmol P m^{-3}	Filterable reactive phosphorus	Algal uptake, organic mineralization, sediment flux
PIP	mmol P m^{-3}	Particulate inorganic phosphorus	Adsorption/desorption of/to free FRP
NH_4^+	mmol N m^{-3}	Ammonium	Algal uptake, nitrification, organic mineralization, sediment flux
NO_3^-	mmol N m^{-3}	Nitrate	Algal uptake, nitrification, denitrification, sediment flux
DOC	mmol C m^{-3}	Dissolved organic carbon	Mineralization, algal mortality/excretion
DON	mmol N m^{-3}	Dissolved organic nitrogen	Mineralization , algal mortality/excretion
DOP	mmol P m^{-3}	Dissolved organic phosphorus	Mineralization, algal mortality/excretion
POC	mmol C m^{-3}	Particulate organic carbon	Breakdown, settling, algal mortality/excretion
PON	mmol N m^{-3}	Particulate organic nitrogen	Breakdown, settling, algal mortality/excretion
POP	mmol P m^{-3}	Particulate organic phosphorus	Breakdown, settling, algal mortality/excretion
TP	mmol P m^{-3}	Total Phosphorus	Sum of all P state variables
TN	mmol N m^{-3}	Total Nitrogen	Sum of all N state variables
TKN	mmol N m^{-3}	Total Kjedahl Nitrogen	Sum of all N state variables
Plankton groups			
BAC	mmol C m^{-3}	Heterotrophic bacteria (*)	
PIPICO	mmol C m^{-3}	Photo-inhibited picoplankton (<2µm)	Chlorophytes including Prasinophytes and
PICO	mmol C m^{-3}	Non photo-inhibited picoplankton	Cyanobacteria including Synechoccus
MICRO	mmol C m^{-3}	Marine diatom and flagellates	Pseudo-nitzschia spp., Chaetoceros spp and Haptophytes (incl. coccolithophorids)
TCHLA	µg L^{-1}	Total Chlorophyll-a	Sum of relevant phytoplankton groups
ZOO_z	mmol C m^{-3}	Zooplankton groups (*)	Grazing, excretion, respiration and mortality
Sediment and related properties			
SS	g SS m^{-3}	Suspended solids (inorganic)	Resuspension and sedimentation
Turbidity	NTU	Turbidity	Computed based on SS, POC and TCHLA concentrations

(*) – indicates a variable defined in the 2.2.2 project conceptual model but not simulated here

BOLD – indicates a simulated state variable, other variables are derived

3.3.3 Model evaluation, analysis and scenario assessment

Model evaluation

Given the relatively low amount of data for setting up the model and its validating, the analysis of model performance was calculated by comparing the mean and standard deviation of data collected during the week long cruise for each station along a transect from Isdell inflow to ~120 km from the congruence of Walcott Inlet. Measures of model performance were calculated for each of three depths, 0-5 m, 5-2 m and >20 m. The eleven state variables used in model evaluation were: salinity, dissolved oxygen, NH_4, NO_3, PO_4, DOC, POC, DON, DOP, TChla and TSS.

Measures of model fit used to evaluate model performance included six alternative formulae Root mean square error (RMSE):

$$RMSE = \sqrt{\frac{\sum_{i=1}^{N}(P_i - O_i)^2}{N}} \tag{11}$$

1) Model Efficiency (MEFF; Murphy, 1988; Nash and Sutcliffe, 1970):

$$MEFF = 1 - \frac{\sum_{i=1}^{N}(P_i - O_i)^2}{\sum_{i=1}^{N}(O_i - \bar{O})^2} \tag{12}$$

2) Model Skill Score (MSS; Willmott 1981):

$$MSS = 1 - \frac{\sum_{i=1}^{N}(P_i - O_i)^2}{\sum_{i=1}^{N}(|P_i - \bar{O}| + |O_i - \bar{O}|)^2} \tag{13}$$

3) Correlation coefficient (r):

$$r = \frac{\sum_{i=1}^{N}(P_i - \bar{P})(O_i - \bar{O})}{[\sum_{i=1}^{N}(P_i - \bar{P})^2 \sum_{i=1}^{N}(O_i - \bar{O})^2]^{1/2}} \tag{14}$$

4) Percent relative error (PRE) :

$$PRE = \frac{\sum_{i=1}^{N}(P_i - O_i)/O_i}{N} * 100 \tag{15}$$

5) Normalised mean absolute error (NMAE) :

$$NMAE = \frac{\sum_{i=1}^{N}|(P_i - O_i)/O_i|}{N} \tag{16}$$

where N is the number of observations, O_i and P_i, the "i^{th}" observed and model predicted data and $\bar{O}$ and $\bar{P}$ the mean observed and model predicted data respectively as described below. Alternative measures of model fit enable us to better scrutinize aspects of model performance, track the nature of trends in deviations from observed data, as well as provide a comprehensive set to compare against similar modelling studies. A further advantage of calculating alternative measure of model fit is that different methods of model evaluation highlight different aspects of model performance. RMSE is a standard measure of the average deviation of simulated values from observations with values near zero indicating a close match, units correspond to those of

the variable. MEFF and MSS are measures of the square of the deviation of simulated values from observations, normalized to the standard deviation of the observed data where a maximum value of one indicates perfect fit; zero indicates that the model provides equal predictive skill as assuming mean observed data. MEF can be an unreliable measure of model fit, however we have included this metric as it is commonly used allowing us to compare model fit with similar estuary modelling studies. The correlation coefficient gives an indication of the linear relationship between observed and predicted data and is the most common measure for assessing aquatic models. PRE is a measure of the relative deviation of simulated from observed values and can be used to determine the bias or under or over prediction of reality. Finally, since NMAE is normalised to the mean it is useful to compare against different variables and by using the absolute avoids over and under error values cancelling each other out.

Computing the realm of influence: the extent of terrestrial contribution to ocean nutrients

In this study terrestrially derived nitrogen is defined as that entering the model domain via one of three river inflows, Walcott Inlet, Secure Bay and Doubtful Bay. To elucidate the terrestrial influence in the estuarine and coastal environments, three tracers were used in this study:

1) TRC1 - Inert tracer equal in value to the total nitrogen (in mmol/m^3) in each of three inflows;
2) TRC2 - Inert tracer set to a value of 1.0 in each of three inflows; and
3) TRC3 - Tracer set to a value of 1.0 in each of three inflows, and set to double in concentration each day.

The percent terrestrially derived nitrogen was then calculated in each model cell as:

$$\%N_{terr} = \frac{\mathrm{TRC1}}{NH_4 + NO_3 + DON + PON + \sum_{i=1}^{3} \chi_{NCON}^{PHY} PHY_i} * 100 \qquad (7)$$

where *i* represents one of three simulated phytoplankton functional groups. The residence time in days for terrestrially derived nitrogen within the domain was then calculated from the following:

$$RT\_N_{terr} = \log_2 \left(\frac{TRC3}{TRC2}\right) \qquad (8)$$

Additionally, two length scales were computed from model output to represent the lateral extent of terrestrial nitrogen – the 'realm of influence'. The first, L_1, was defined as the distance from the mouth of Walcott Inlet (Figure 3-6) to the point at which the fraction of terrestrially derived nitrogen, $\%N_{terr}$ of the water drops below 1%. This length scale represents the ocean extent, or maximum realm of influence, of inflow nitrogen. The second, L_{50}, is the distance from the mouth of Walcott Inlet to the point at which at least half of the total nitrogen of the surface waters is terrestrially derived (i.e. $\%N_{terr}$> >50%). This region represents the area where at least half of the nutrients have been derived from river inflows and therefore terrestrial sources.

Nutrient budget

We explored the nutrient budget by assessing the relative contribution of different sources of nutrients (terrestrial/ recycled and open ocean) to gross primary production using a transect extending from within Walcott Inlet, out Caesar channel into the open ocean. We also compared time series of fractions of nitrogen at different regions of the larger domain, specifically within Walcott Inlet and the Bay.

Climate change scenario assessment

One of the objectives was to ascertain the extent to which ocean biogeochemistry in this region may be impacted by projected changes in climate. Due to computational constraints we were not able to run decade-long simulations using the modified inflow rates; however, we were able to extrapolate the relationship

between flow rate and terrestrial nitrogen influence to assess the sensitivity to climate changes in the catchment.

4 Organic matter characterization

4.1 Sediment samples

During the dry season sampling, we attempted to obtain sediment grab samples from a total of 33 sites with 24 being successful (Figure 2-1; Table 4-1). In general, sediment sampling was most successful in the shallow, eastern end of the Walcott Inlet with samples being a mixture of mud and muddy sand (Table 4-1). The deeper western end of the inlet was characterised by muddy sediments close to shore with scoured rocky bottom in the central deep sections. For comparison purposes, only sites with successful samples in the dry season were re-sampled in the wet.

Sediment carbon content was very low, generally much less than 1% with stable isotope values around -22‰ to -24‰ which is typically for material originating from grasslands. Exceptions to this are several sites at the western end (G17, G20 and G26) which have slightly higher %C contents and more depleted isotope values, suggesting a higher proportion of organic matter derived from mangroves. In addition, there was no clear effect of wet season flow on sediment carbon content, with some sites becoming slightly elevated while others decreased, presumably due to enhanced flow rates removing material.

It was not possible to obtain reliable values for nitrogen content or stable isotopes due to the low amounts present and the maximum sample size that could be analysed via the online continuous flow system. We did estimate C:N ratios to be of the order of 20:1. The carbon values and very low nitrogen content reported here are in keeping with those previously reported for the Ord River estuary in the eastern Kimberley (Volkman et al. 2007).

Table 4-1. Walcott Inlet dry season sediment samples

Sample	Date	Time	Depth (m)	Comments
1	29/10/2013	10:15	7	Isdell River, mangrove lined, sand + mud
2	29/10/2013	10:48	4	Mouth of Isdell River, sand + mud
3a	29/10/2013	11:15	7	Towards N bank between Is and main land. NO SAMPLE, gravel
3b	29/10/2013	11:20	5	N Bank, NO SAMPLE
3c	29/10/2013	11:30	6.8	Centre channel, muddy sand
4	29/10/2013	12:00	10	South bank, Mud
5	29/10/2013	12:20	1.8	N bank, Mud
6	29/10/2013	12:26	8	Towards centre, mud
7	29/10/2013	12:34	6	Centre, mud
8	29/10/2013	12:45	5.8	towards s bank, mud
9	29/10/2013	12:55	2.2	S bank, firm mud
10	29/10/2013	13:30	2.8	N bank, firm mud
11	29/10/2013	13:45	5.9	transect away from bank, soft mud
12	29/10/2013	13:52	1.9	centre, sandy mud
13	29/10/2013	14:00	8	transect to south, mud
14	29/10/2013	14:15	2.2	S bank
15	29/10/2013	14:42	2.2	N bank, firm mud
16	29/10/2013	15:00	16	transect away from N, mud
17	29/10/2013	15:10	10	centre, sandy mud
18	29/10/2013	15:20	10	transect to south, muddy sand
19	29/10/2013	15:40	3.3	S bank, mud
20	29/10/2013	16:15	2.2	S bank, mud
21	29/10/2013	16:30	48.6	transect to north, NO SAMPLE rock
22	29/10/2013	16:45	68.4	Centre, NO SAMPLE
23	29/10/2013	17:00	47	Transect to north, NO SAMPLE - pebbles
24	29/10/2013	17:10	38	N Bank Anchorage, Mud
25	30/10/2013	8:45	3.6	Creek near mouth, mud
26	30/10/2013	9:15	3	S Bank, Mud
27	30/10/2013	9:30	37.4	Transit away from S, NO SAMPLE rock
28	30/10/2013	9:50	50.7	Centre, NO SAMPLE
29	30/10/2013	10:10	60	Transit to N, NO SAMPLE
30	30/10/2013	10:22	32	N Bank, NO SAMPLE, grab damaged
31	30/10/2013	14:52	54	Channel, NO SAMPLE
32	30/10/2013	16:35	17	towards S bank, mud with shells
33	30/10/2013	16:55	52	Channel, NO SAMPLE, nearly lost grab

Table 4-2. Carbon content and stable isotope values for Walcott Inlet sediments.

	%C		$\delta^{13}C$ (‰ VPDB)	
Site	Dry	Wet	Dry	Wet
G 01	1.4	1.0	-21.3	-24.5
G 02	0.1	0.6	-23.0	-22.8
G 03	0.2	0.4	-24.6	-19.6
G 04	1.0	0.6	-22.1	-22.7
G 05	0.5	0.5	-22.1	-25.1
G 06	0.6	1.1	-22.6	-22.3
G 07	0.9	0.9	-22.4	-23.6
G 08	0.9	0.9	-22.7	-27.7
G 09	1.0	1.2	-22.2	-29.7
G 10	0.5	0.8	-21.9	-28.5
G 11	0.7	0.3	-21.3	-28.9
G 12	0.3	0.7	-24.9	-26.6
G 13	0.5	0.5	-22.2	-26.5
G 14	0.6	0.0	-23.0	n.d.
G 15	0.3	0.3	-21.6	-23.1
G 16	0.6	0.8	-24.2	--25.1
G 17	0.7	0.3	-30.6	-30.4
G 18	0.4	0.9	-21.1	-35.1
G 19	1.0	0.5	-26.2	-27.0
G 20	0.6	0.7	-27.1	-31.2
G 24	0.8	0.8	-25.1	-27.5
G 25	1.0	0.9	-25.4	-24.9
G 26	0.7	0.7	-27.6	-24.2
G 32	0.5	0.6	-26.1	-25.2

Total sediment fatty acid concentrations (a proxy for labile carbon) are shown in Figure 4-1. As with total carbon, concentrations are highly variable across the inlet as is the effect of wet season flows with some sites (G11, G19 and G20) exhibiting a large increase in concentration post wet season flows (Figure 4-1).

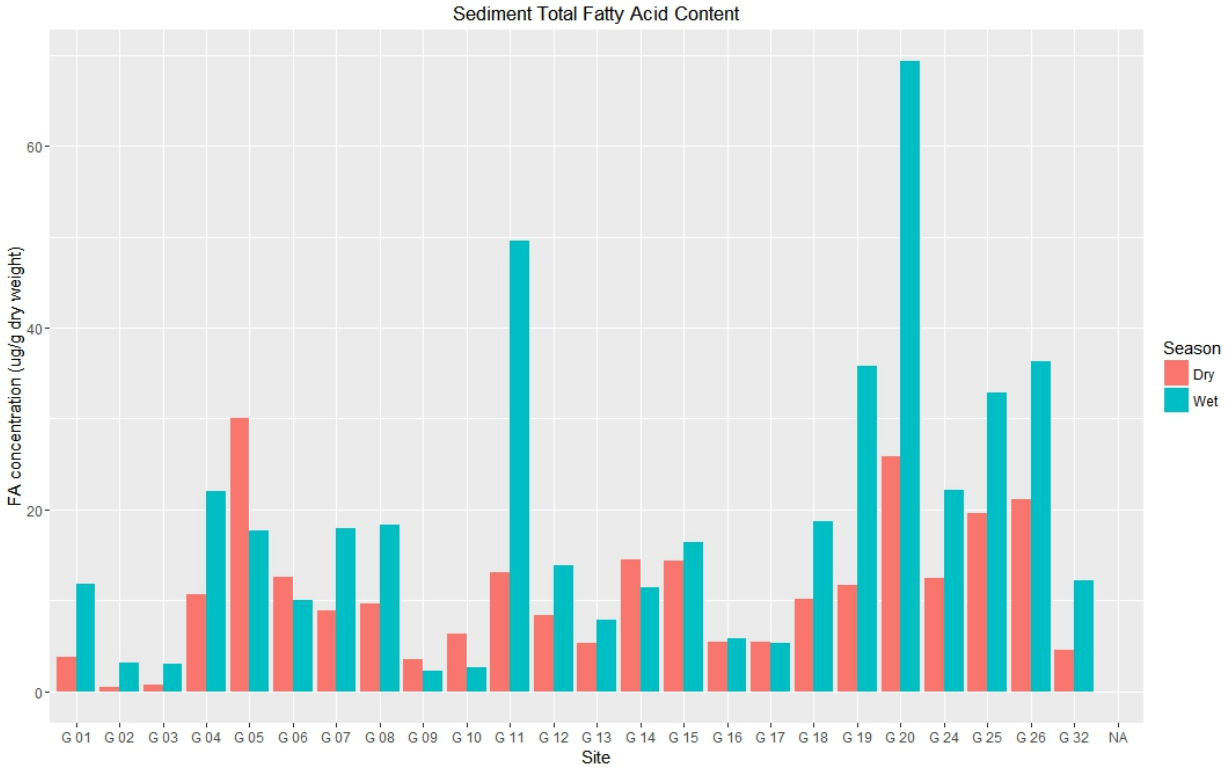

Figure 4-1. Total fatty acid content in Walcott Inlet sediments expressed as µg/g dry weight of sediment for dry (November 2013) and wet (March 2014) samples.

The overall fatty acid profile of the combined sites is dominated by the $C_{16:0}$ hexadecanoic acid (common name palmitic acid) which is unsurprising as this is the most common fatty acid (Figure 4-2). Other dominant fatty acids are $C_{18:0}$, another common compound and then a series of compounds which can be associated with bacteria $C_{14:0}$, straight chain and *iso* and *anteiso* branched $C_{15:0}$, $C_{16:1w7}$ *cis*, $C_{18:1w9}$ *cis*, $C_{18:1w7}$ *cis* (Figure 4-2). This pattern appears to be relatively consistent between the dry and wet sampling periods, even for the site which exhibited the largest increase in total Fatty acid content, G20 (Figure 4-3). The relatively enhanced contribution of bacterial derived fatty acids and the lack of longer chain polyunsaturated compounds which would indicate algae suggests rapid re-working of most labile organic matter. There is also some contribution from plant derived long chain fatty acids ($C_{22:0}$, $C_{24:0}$ and $C_{26:0}$) though still at low relative abundance for what is essentially a terrestrially dominated system. This could be due to most terrestrial material being transported rapidly through the system during high flow events when the input is also highest and/or slow degradation and incorporation of this material into sediments.

When the results are used to investigate which sites might be varying in similar ways via hierarchical cluster analysis (Figure 4-4) the results indicate that the major clusters mostly occur along a wet/dry division rather than geographic position within the inlet, suggesting that site characterization depends on where material happens to be deposited during large events rather than specific localised inputs.

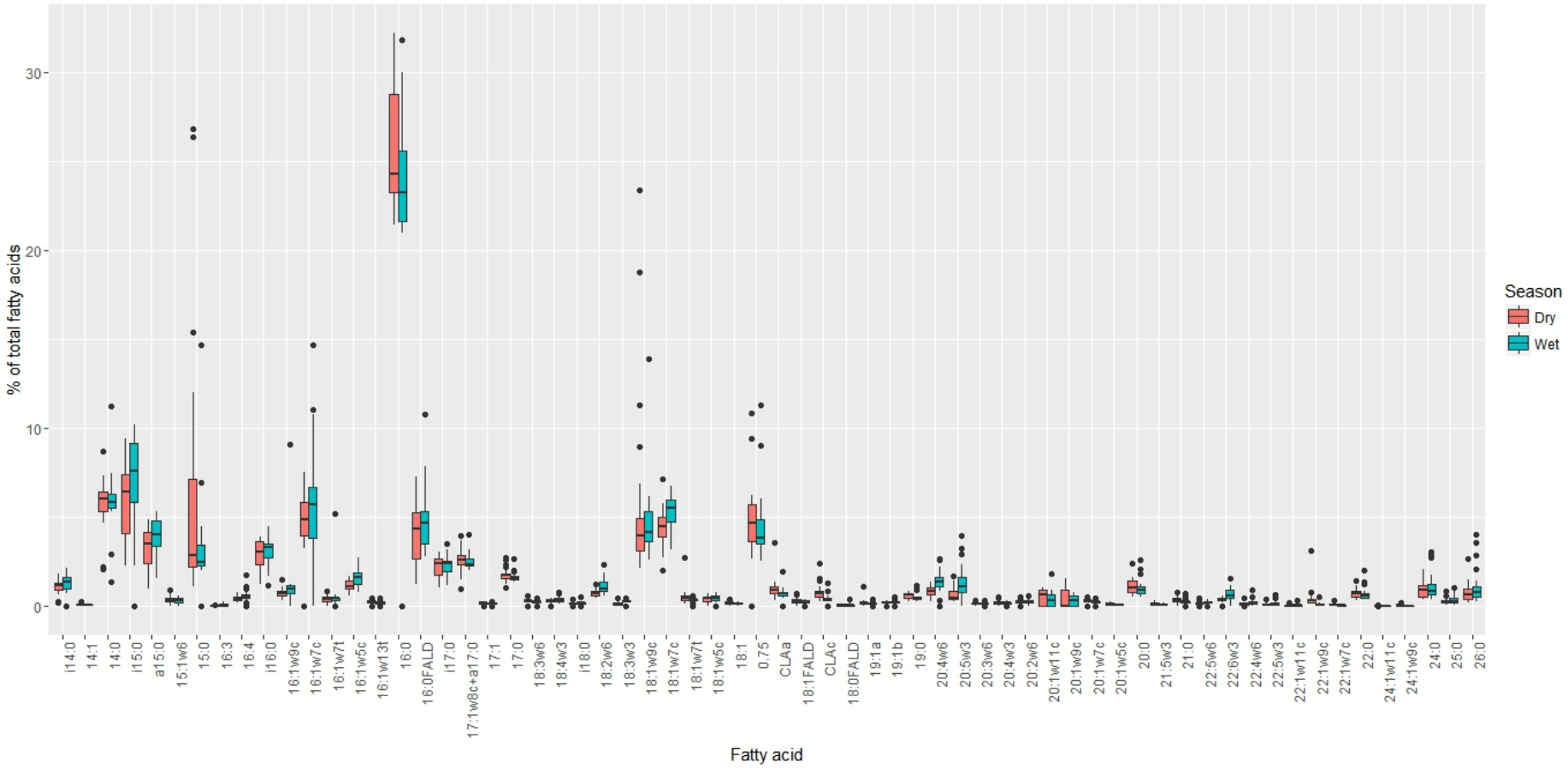

Figure 4-2. Overall percent composition of fatty acid profiles from sediments collected at all sites during the dry (November 2013) and wet (March 2014) field trips. Compounds are denoted in the form Cn:x□y where C = number of carbon atoms, n = number of double bonds, □y = position of first double bond

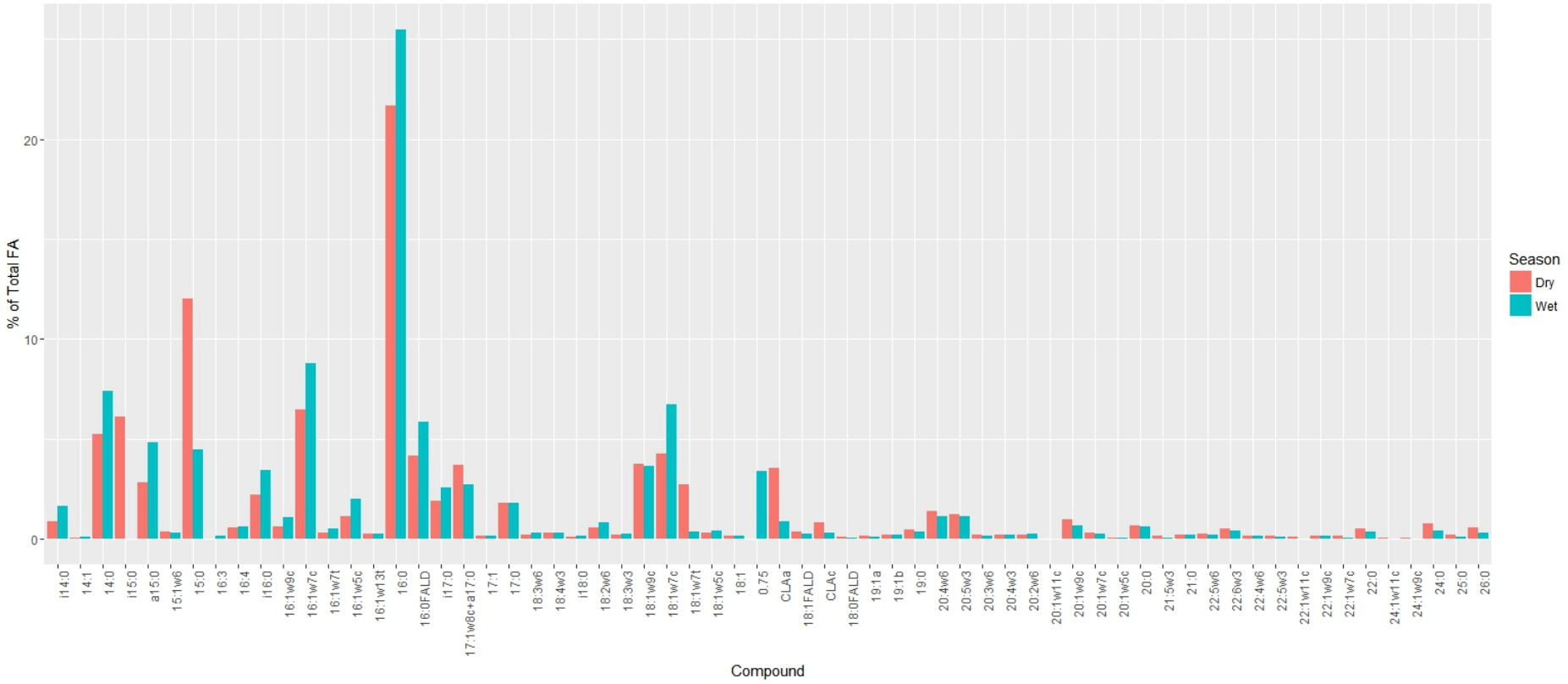

Figure 4-3. Percent fatty acid composition of sediment collected at site G20 during the dry (November 2013) and wet (Marhc 2014) sampling periods. Compounds are denoted in the form $C_{n:x}\omega_y$ where C = number of carbon atoms, n= number of double bonds, ω_y= position of first double bond.

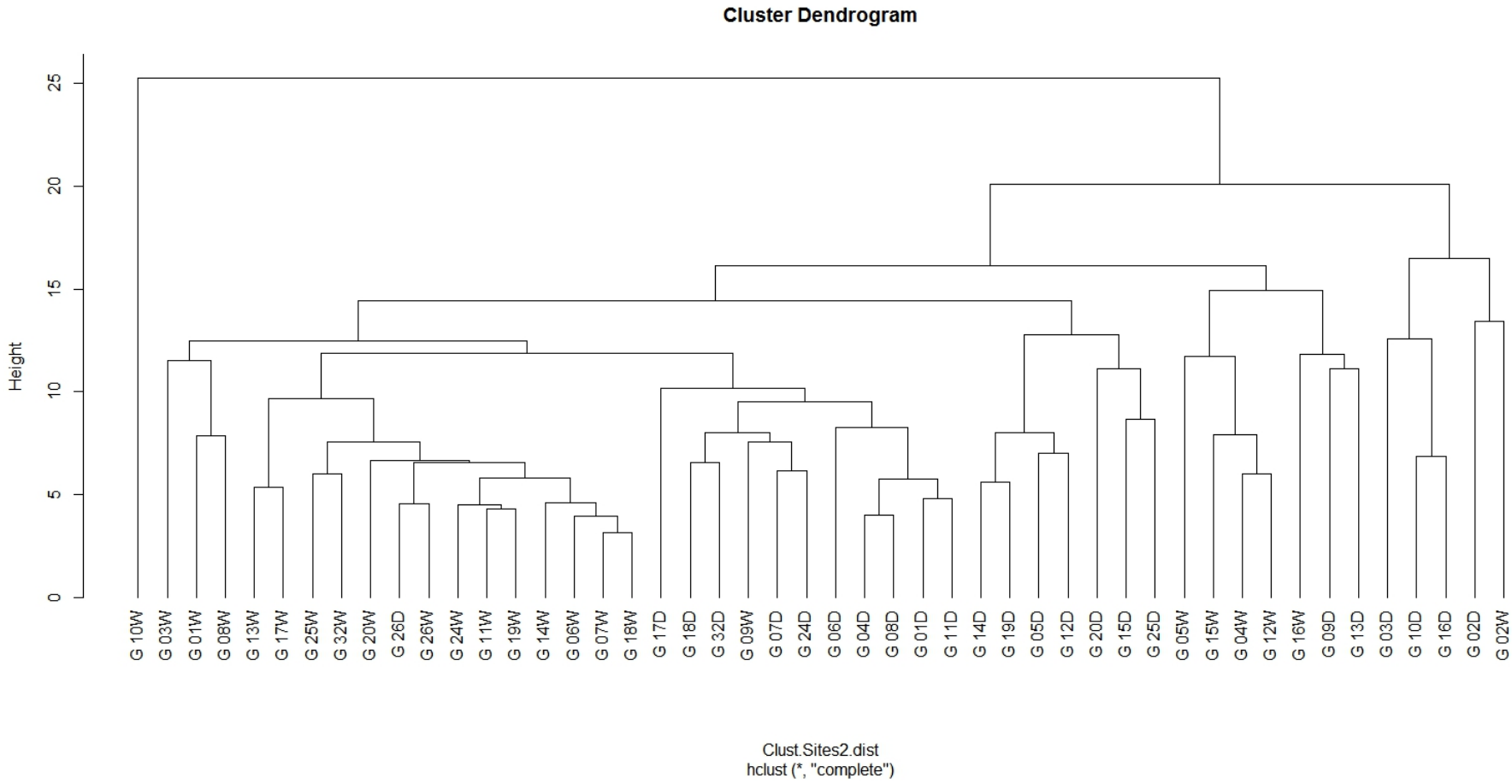

Figure 4-4. Hierarchical cluster diagram for Walcott Inlet sediment samples collected during the dry (November 2013) and wet (March 2014) sampling periods. Sample sites are denoted as Gxx with D=dry and W=wet

Note: Clusters are created from normalized % fatty acid composition using Euclidean distances and complete linkage.

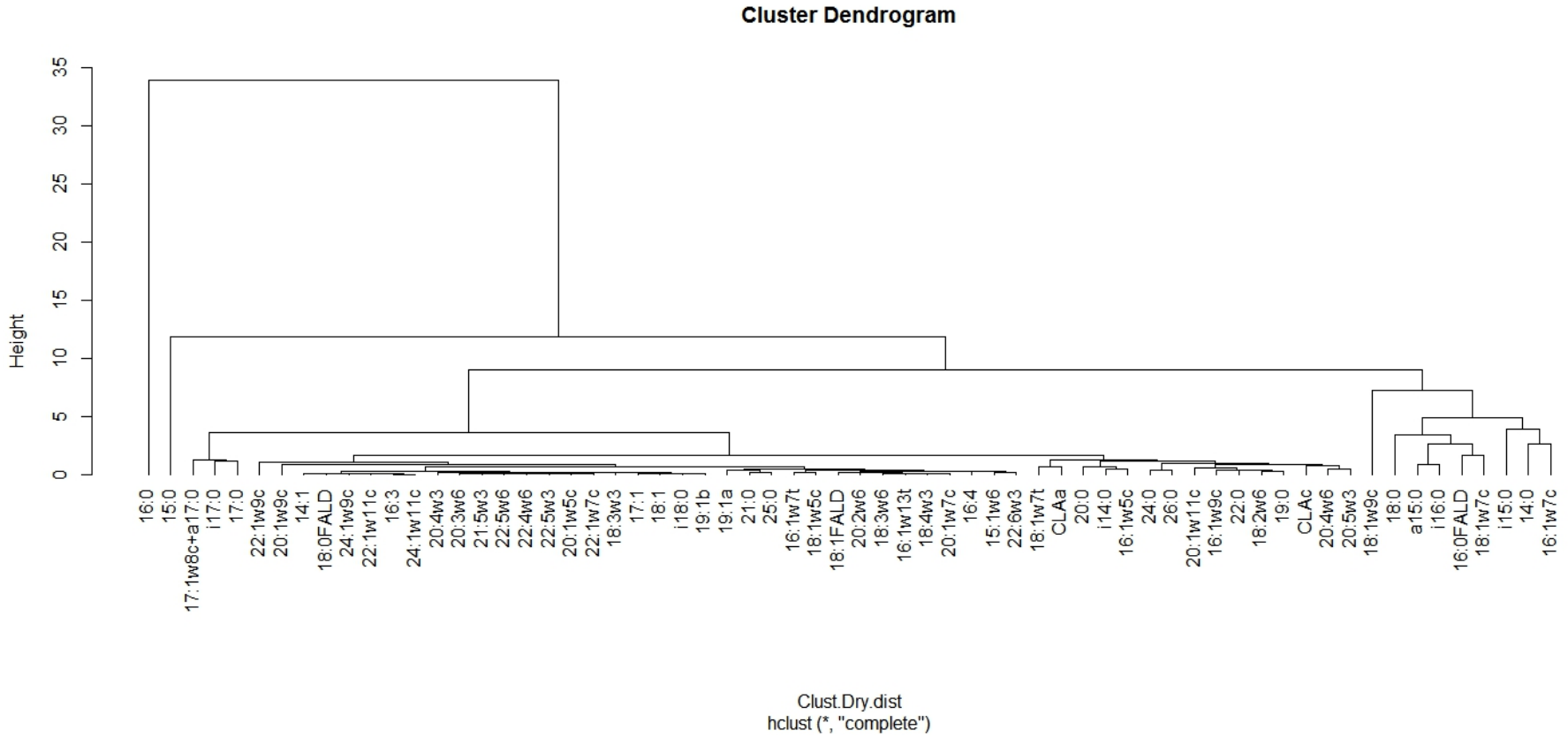

Figure 4-5. Hierarchical cluster analysis of individual fatty acids in sediments collected during the dry (November 2013) field trip.

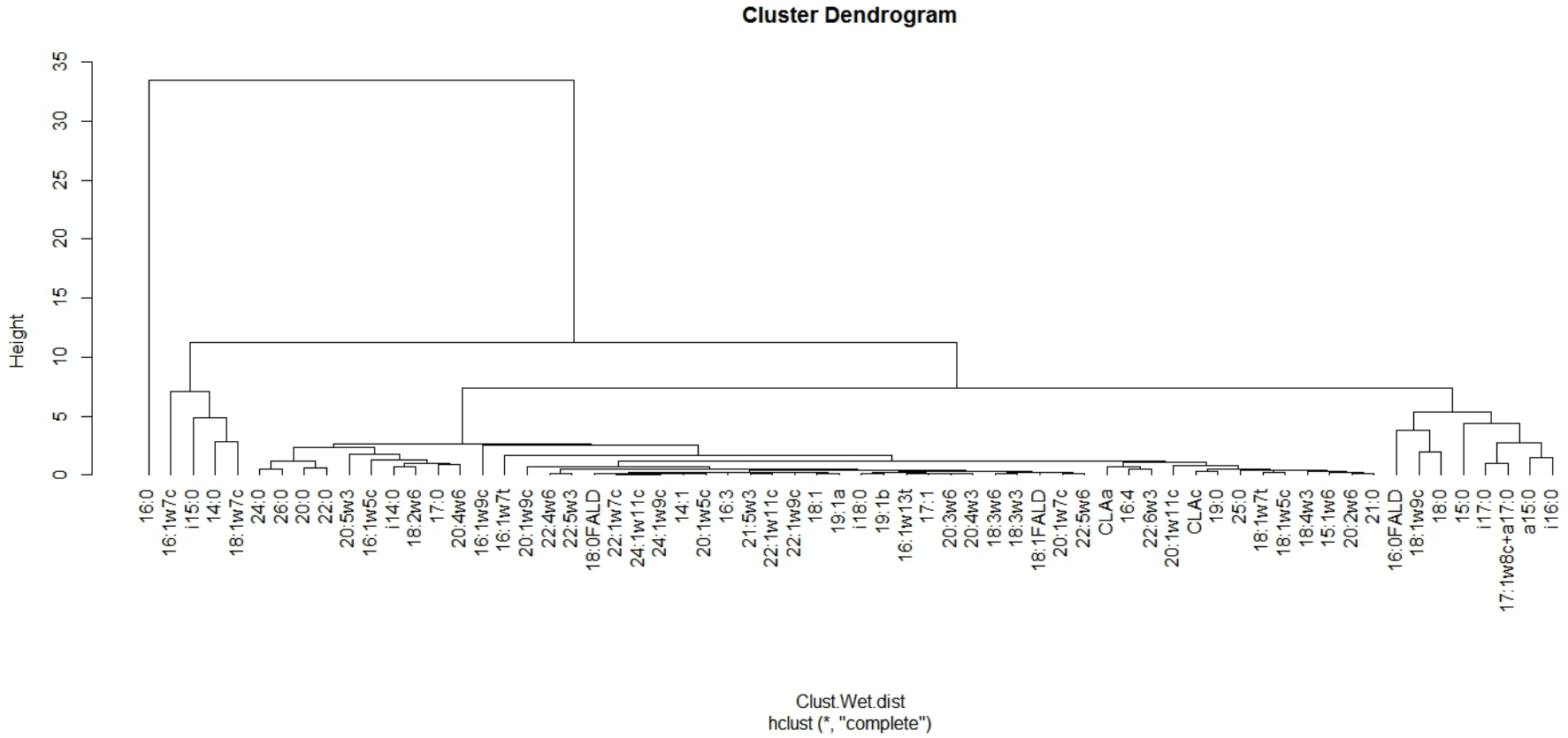

Figure 4-6. Hierarchical cluster analysis of individual fatty acids in sediments collected during the wet (March 2014) field trip.

4.2 Water column samples

During the dry season sampling, water column samples were collected along a transect from close to the mouth of Walcott Inlet (T01) finishing within the Isdell River (T10; Figure 2-1). There was a general trend of increasing fatty acid concentration along the transect with a marked increase within the Isdell River (T9 and T10; Figure 4-7)

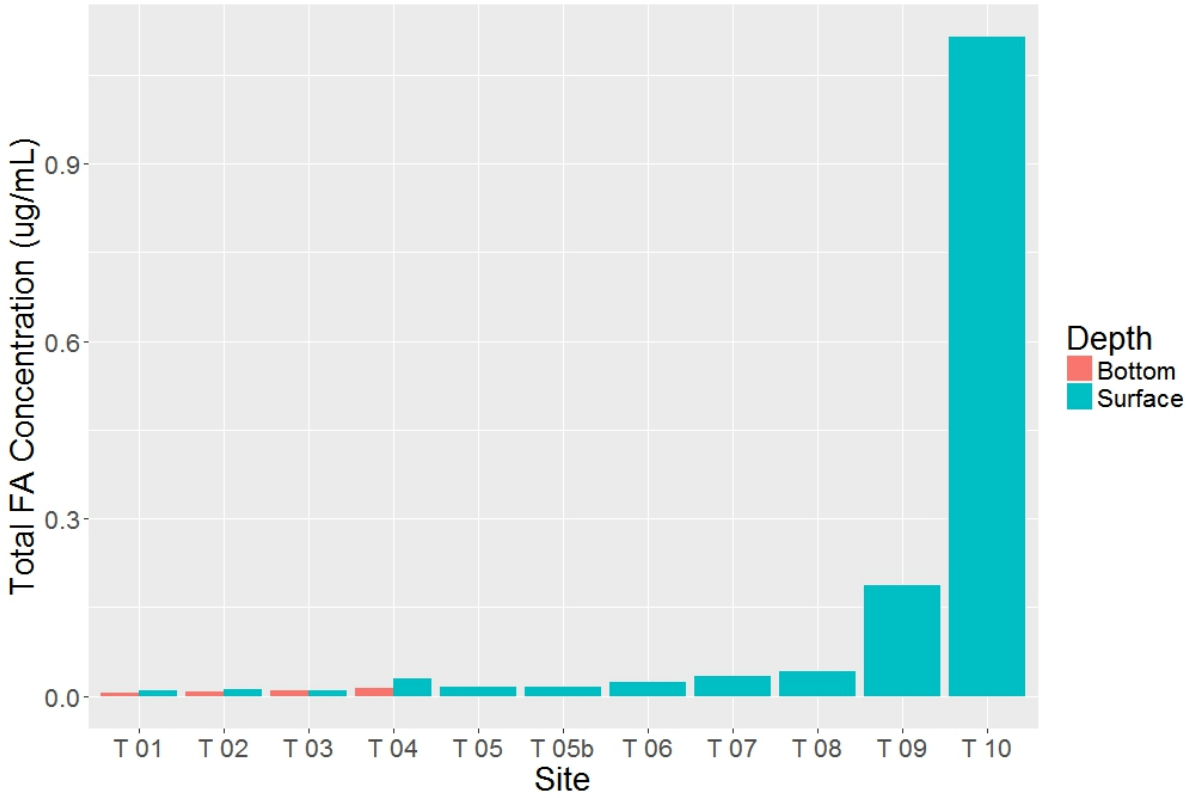

Figure 4-7. Concentrations of fatty acids (ug/mL) in water column samples collected along a transect during the dry season (November 2013) field trip.

In general, the average fatty acid profile in the water column is dominated by 16:0 fatty acid, which is a common constituents of many sources of organic matter (Figure 4-8). Unlike the sediment samples, the water column samples also contained significant proportions of 18:0 and 22:1w9 fatty acids. Octadecanoic acid ($C_{18:0}$) is a common constituent of both animal and vegetable oils whilst docosenoic acid ($C_{22:1w9}$) is often associated with members of the *Brassicaceae* family of flowering plants suggesting inputs from plant sources. There is also a significant contribution of $C_{18:1w9}$ which can be associated with freshwater algae.

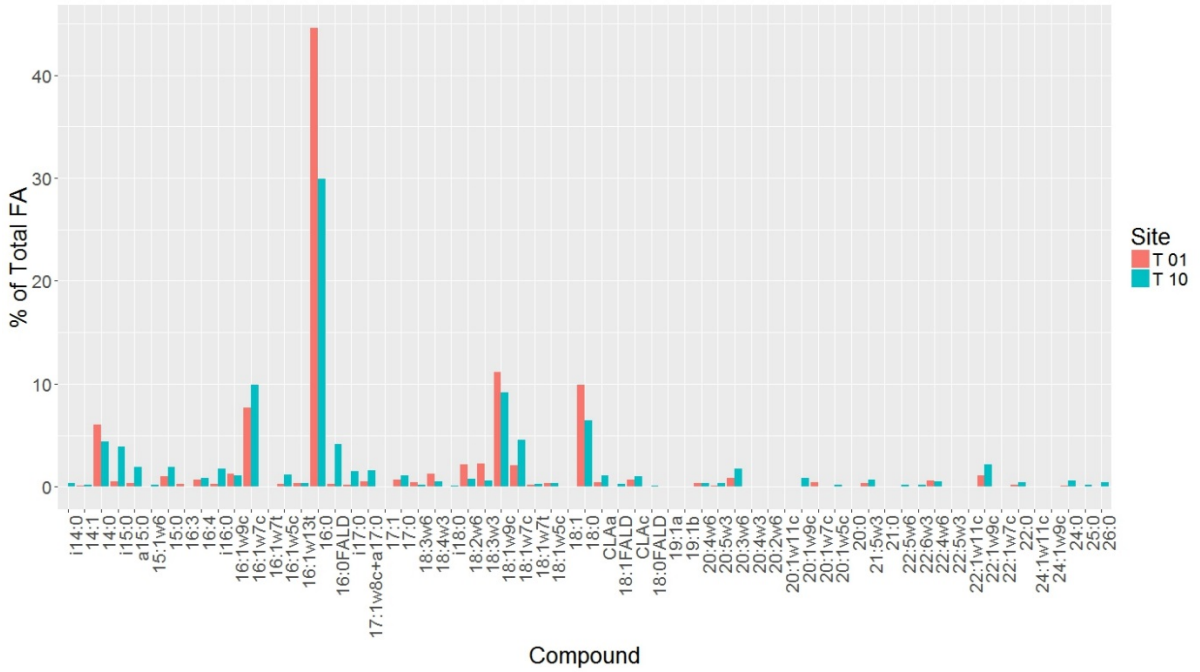

Figure 4-8. Average fatty acid profile as percent composition of water column samples collected during the dry season (November 2013).

A comparison of the fatty acid profiles at each end of the transect shows that while concentrations at the Isdell River were elevated (Figure 4-7) there was no obvious major difference in the source material that would account for the elevated concentrations (Figure 4-9), suggesting in general that the lower concentrations down the inlet are mostly due to dilution.

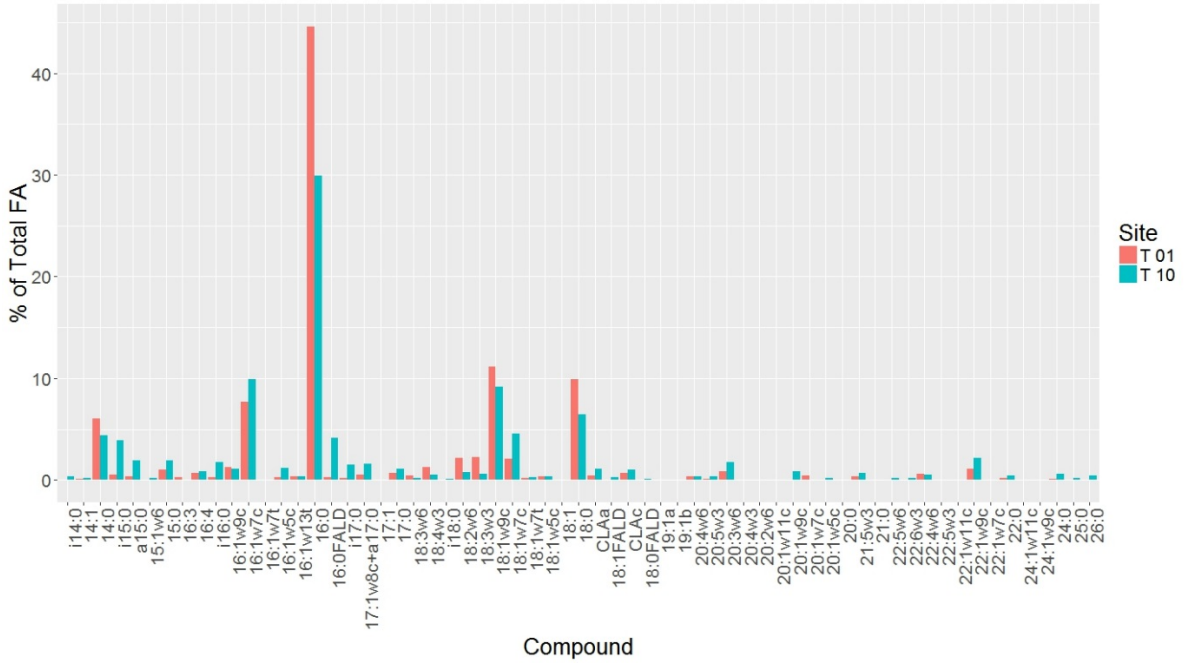

Figure 4-9 Comparison or percent fatty acid composition of water column samples collected from opposite ends of the dry season (November 2013) transect.

However, samples from the Isdell River do appear to have a greater contribution of bacterial sources as indicated by relatively enhanced *i*$C_{15:0}$, *ai*$C_{15:0}$ and $C_{16:1w7}$ as well as more influence from higher plant sources ($C_{22:0}$, $C_{24:0}$ and $C_{26:0}$), (Figure 4-9).

Due to vessel issues during the wet season survey (March 2014), water column samples were only collected at one site, outside of Walcott inlet. However samples were collected hourly over a 24 hour period, and provided information on export from the inlet during this time. Interestingly, maximum concentrations of fatty acids occurred just prior to high water at Shale Island (Figure 4-10), possibly due to export from the inlet being restricted.

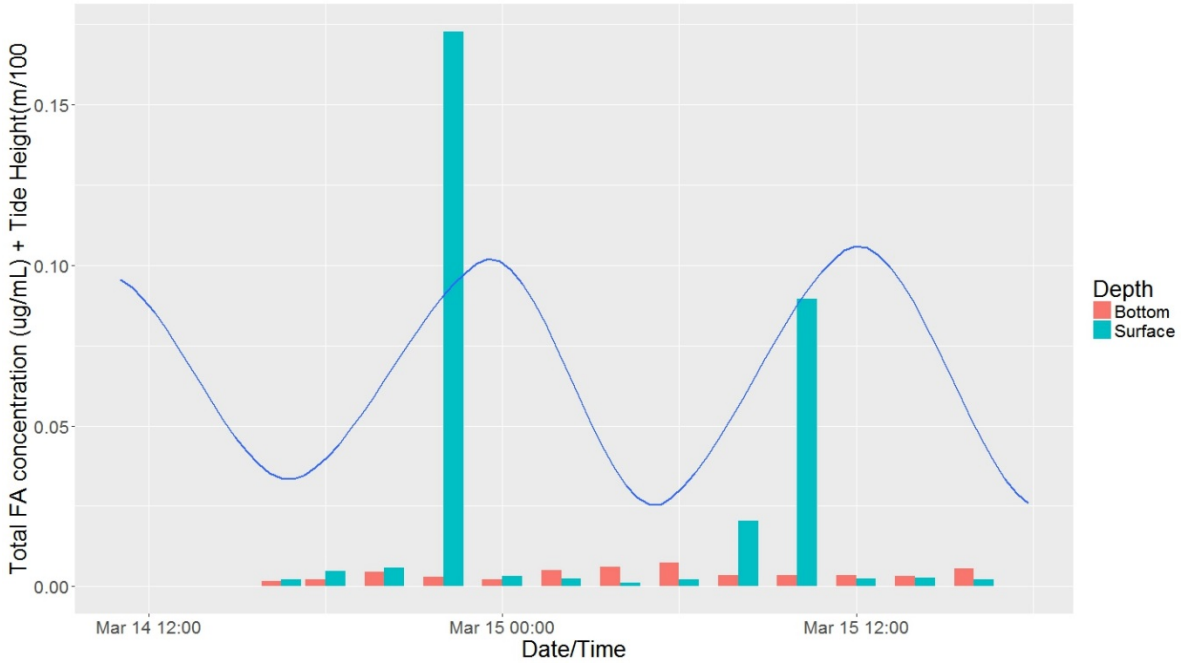

Figure 4-10. Total water column fatty acid concentrations in surface and bottom waters over a 24h period during the wet season (March 2014) sampling superimposed with Shale Island tidal curve.

There were some slight differences in average composition with depth (Figure 4-11) and state of the tide (Figure 4-12). Fatty acid profiles were relatively simple generally containing a mix of algal, bacterial and terrestrially derived compounds though those from bacteria appear to dominate the exported material as they do within Walcott inlet.

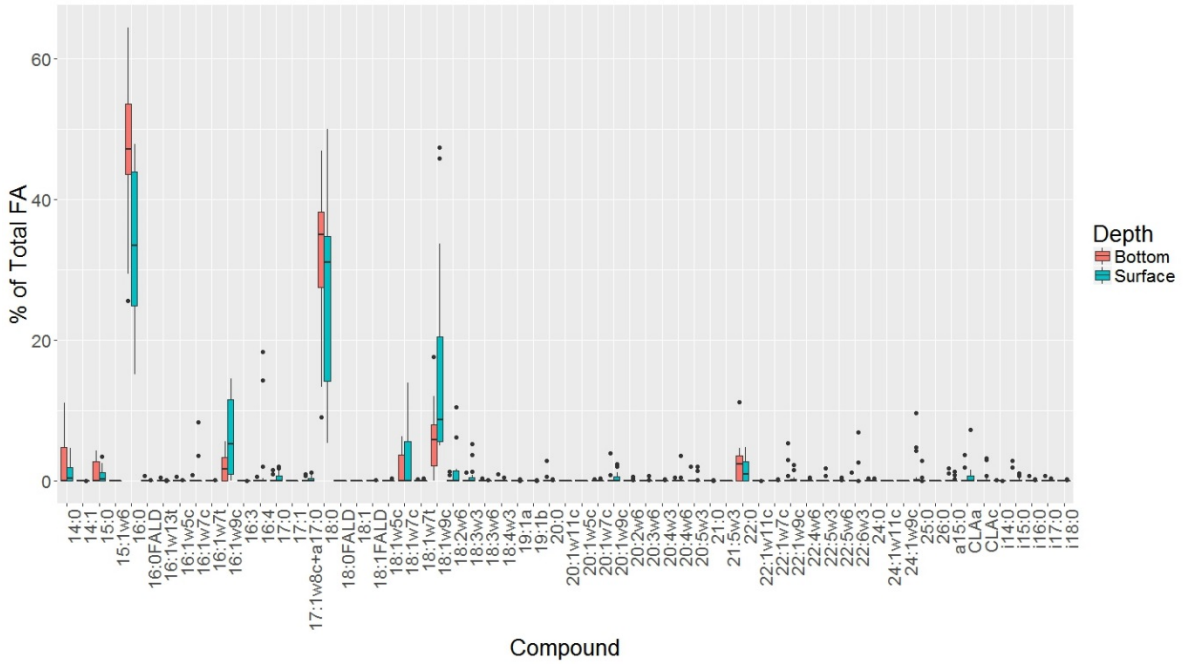

Figure 4-11. Variation in average fatty acid composition (%) of water samples collected from the surface and near bottom at the wet season (March 2014) 24 hour station.

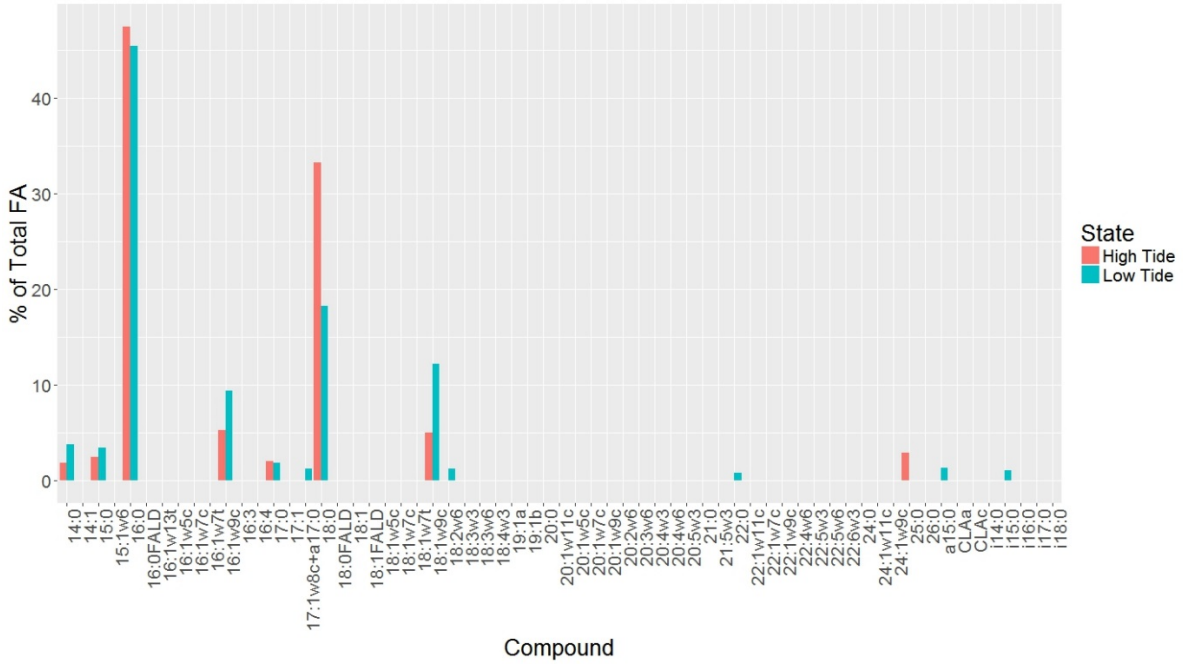

Figure 4-12. Variation in average fatty acid composition (%) of water samples collected at high and low tide at the wet season (March 2014) 24 hour station.

4.3 Summary

From the biomarker data, it appears Walcott Inlet is generally a carbon poor environment in which any labile carbon is rapidly broken down by bacteria. There are circumstantial observation data of large quantities of recalcitrant terrestrially derived material (leaves and twigs) entering the inlet via rivers during times of high flow but this material doesn't appear to become incorporated into sediments, most likely being removed from the inlet during periods of high flow before it can be degraded.

5 Catchment-Ocean Modelling

5.1 Catchment Hydrology

5.1.1 Climate analysis

The climate of the Kimberley covers a wide range in conditions, with a wide spatial and temporal range and variability. Average annual rainfall across the region is 808 mm, but with a range from 1341 mm, in the north-west, to 449 mm inland in the south-east (Figure 5-1). About 85% of rain falls during the summer (December to March). Rainfall during the remainder of the year is usually light and sporadic. Mean annual rainfall across the catchments of the Walcott Inlet is around 950mm (CSIRO, 2009) and ranges from around 650mm to 1250mm. There are two dominant seasons: a hot, wet season from November to April and a warm, dry season from May to October and potential evaporation exceeds rainfall in all but two months (January and February) (Figure 5-2).

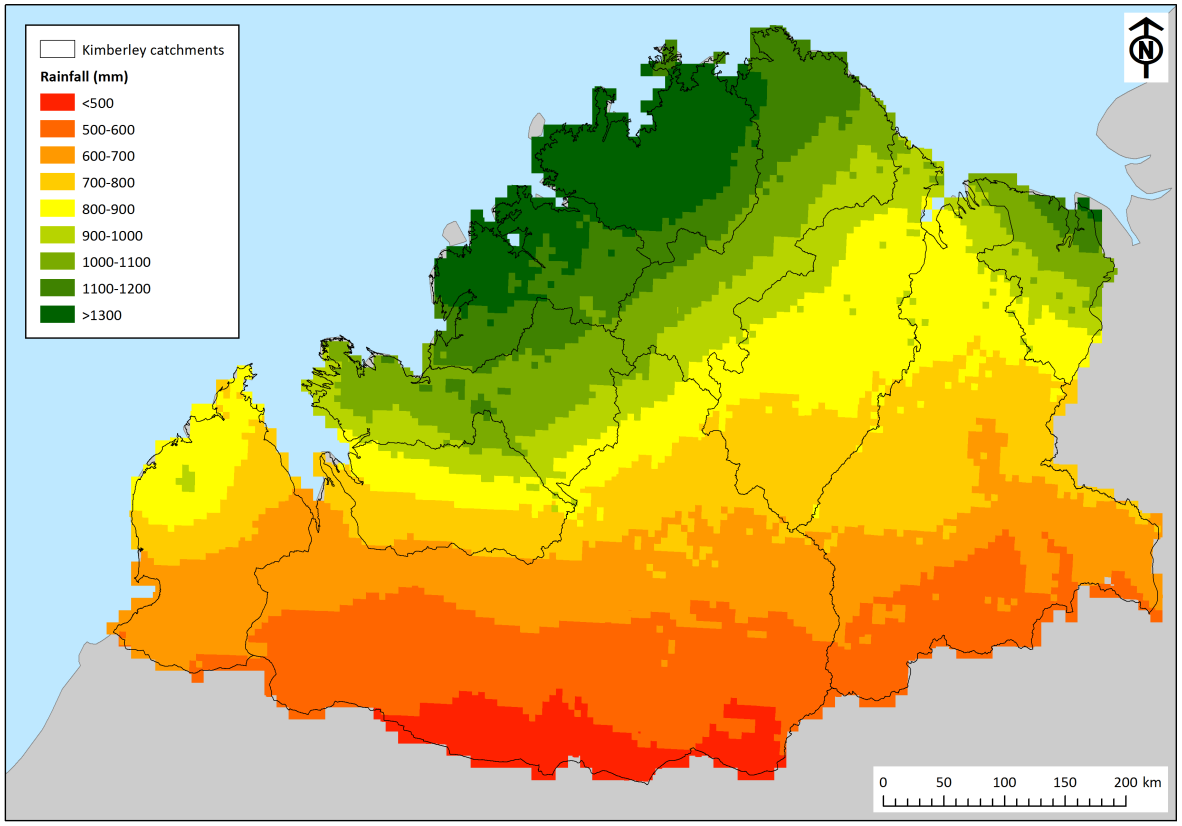

Figure 5-1. Map showing the mean annual rainfall across the Kimberley, derived from SILO 0.05o x 0.05o grid cells. Statistics taken for water years 1961 to 2014.

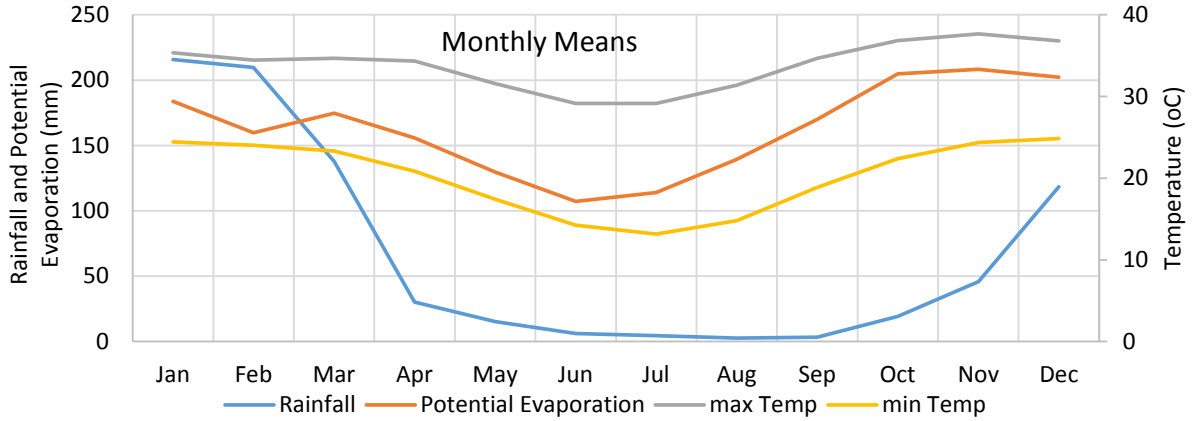

Figure 5-2. Mean monthly rainfall, temperature and potential evaporation across the Kimberley during the water years 1961 to 2014. The data are averages across the entire Kimberley.

5.1.2 Catchment runoff

The spatial and temporal variability in rainfall leads to similar variability in runoff generation and stream flow. While there have been few, if any, direct measurements of runoff generation processes in the Kimberley, there is anecdotal evidence for the occurrence of a number of key hydrological processes. The duration and maximum flow of rivers in the region Kimberley depend on the intensity and spatial extent of rain and on landscape characteristics such as geology, vegetation and soil moisture. The infiltration capacity of the soil is a significant determinant of runoff generation, and this is affected by soil type and land use, such as grazing which removes vegetation and can compact riverine soils. These factors can influence runoff generation thresholds which, therefore, are spatially and temporally variable. A thunderstorm typically results in rapid runoff and but relatively small total flow volumes to the ocean, while monsoonal rain falling over several days may produce a moderate but sustained flow, and depression systems associated with tropical cyclones generate widespread heavy rain and floods. Flood flows in the major Kimberley rivers are among the largest in the world for similar sized catchments (DoW 2008). The duration and intensity, that is, quantity of rainfall, of the 'wet' season varies from year to year. The combination and distribution of floods, smaller, more regular flows and the long dry season, all influence the characteristics and hydrological function of the Kimberley rivers. These factors then govern adaptation of the flora and fauna resulting in the Kimberley rivers being valuable natural wilderness assets.

The Kimberley streams have many perennial pools maintained by groundwater discharge; rainfall may infiltrate upslope through fractures in rock, or possibly sink holes in calcareous formations, and then returns to the surface down slope through groundwater seepages and springs (Lindsay & Commander 2005, Harrington et al. 2011). This mechanism is interpreted from groundwater bores as an important source of water to springs and for groundwater dependent ecosystems, maintaining flow in perennial streams. The long flow periods in some streams in the region, despite the intermittency of rainfall, indicates the importance of groundwater discharge. Some of this water comes from high in catchments and some infiltrates into the alluvium adjacent to rivers during periods of high flow and later returns to the river when flow levels reduce.

The fresh water that flows from the rivers into the sea is crucial to the lifecycle of many coastal species and ocean fish. It is these functions that are the focus of this project.

5.1.3 River flow statistics

The full record of daily flows for the three stream gauges used in this analysis are shown in Figure 5-3. Most streamflow in the region is related to heavy rainfall, occurring mainly in the summer, with approximately 80% occurring in the five months between December and April (Figure 5-5 to Figure 5-7). It is this link to the heavy rainfall events, and a largely rocky catchment with skeletal soils, that leads to the high runoff coefficients referred to above. In larger river channels, flow can persist for weeks, and sometimes months, following major rainfall such as associated with tropical cyclones. During the summer, average discharge by Kimberley is about

32,000 GL to the Timor Sea (CSIRO 2009). Annual flows are highly variable, especially in the southern Kimberley. The summary details of the three gauges are shown in Table 5-1 and Table 5-2.

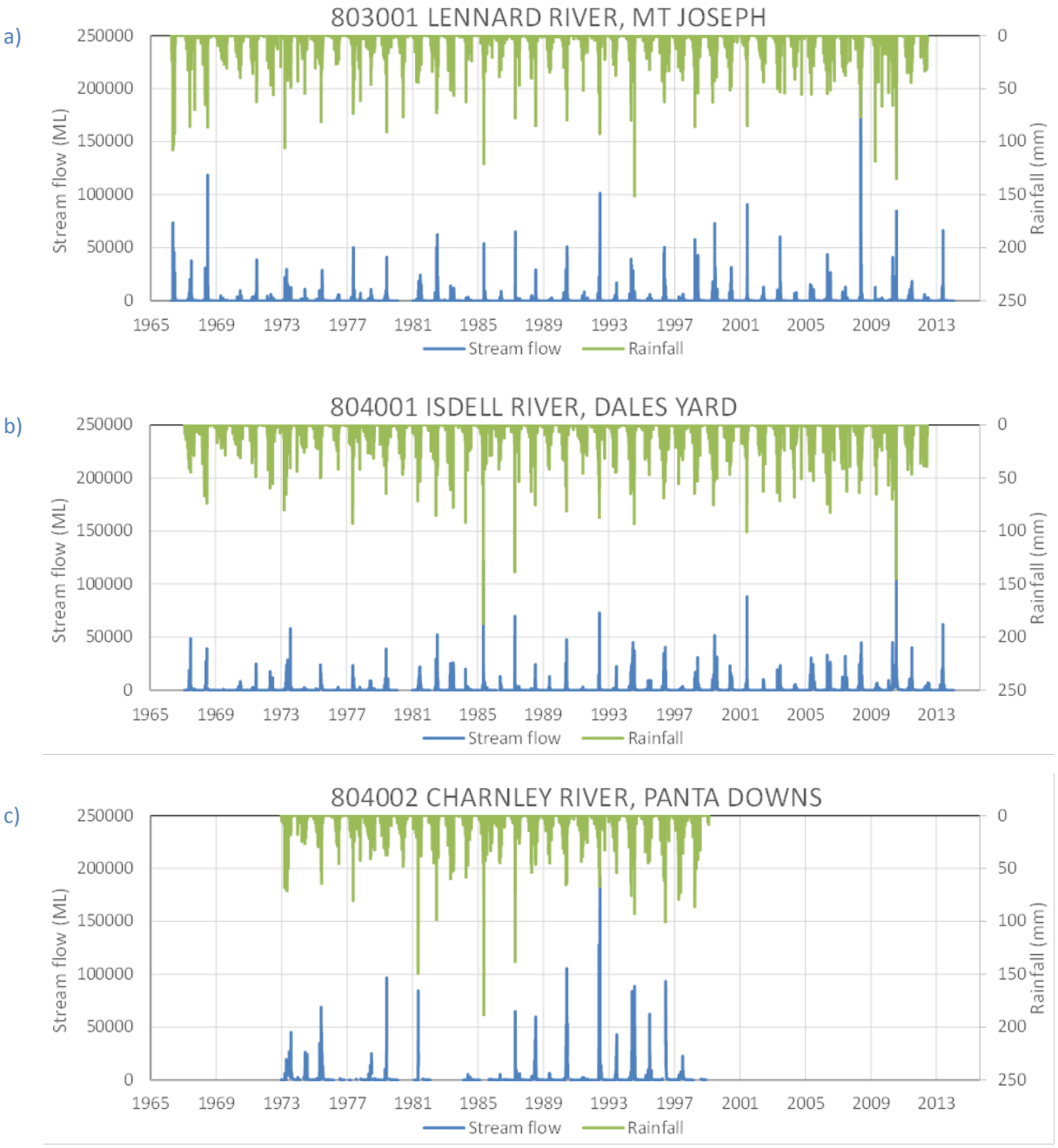

Figure 5-3. Daily rainfall and stream flow hydrographs of the three catchments used in the modelling and for inlet inflow volume estimates.

Table 5-1. List of stream gauges used in the project, with catchment area and dates of commencement and cessation (if closed).

Australian Water Resources Council (AWRC) code	Station Name	Catchment Area (km2)	Station Commence	Station Close	Length of record (Years)
803001	LENNARD RIVER, MT JOSEPH	1049.8	15/12/1966		48.5
804001	ISDELL RIVER, DALES YARD	1829.3	19/10/1967		47.7
804002	CHARNLEY RIVER, PANTA DOWNS	3984.6	30/08/1973	13/08/1999	26.0

Table 5-2. Summary statistics for the gauges in the Kimberley streams used in this project.

AWRC station code	Mean annual rainfall (mm)	Mean annual discharge (GL)	Mean annual runoff (mm)	Mean annual runoff coefficient	Max daily flow (GL)	Mean flow days per year	Most zero flow days in a year
803001	856	233	222	0.26	202	198	270
804001	926	328	179	0.19	178	341	133
804002	973	390	98	0.10	192	269	149

Figure 5-4 indicates that over the long term, these catchments yield between 14 and 26 percent of annual rainfall as stream flow, the runoff coefficient, which is high relative to catchments in the south west and much higher than those in the Pilbara, just a short distance south (Silberstein & Aryal 2015b). However, Figure 5-4a shows that in any single year, once the threshold rainfall of about 500 mm has been reached, the effective runoff coefficient for stream flow generating events can be as high as 57 percent. It should be noted here that in hydrology the term "runoff" is usually quantified in area normalised units, as millimetres, which facilitates comparison between catchments of different sizes. A runoff of 1 mm is equivalent to 1 L m^{-2} and 1 ML km^{-2}. Runoff of 1 mm from a catchment with area of 1,000 km^2 is, therefore, 1 GL. The three main discharges to Collier Bay are via Walcott Inlet (catchment area 12,580 km^2), Doubtful Bay (catchment area 5,533 km^2) and Secure Bay (catchment area 2,665 km^2) with about 1,000 km^2 of other catchment inflows. Considering just Walcott Inlet flow, median daily runoff is 0.06 mm day^{-1} or 0.8 GL day^{-1}.

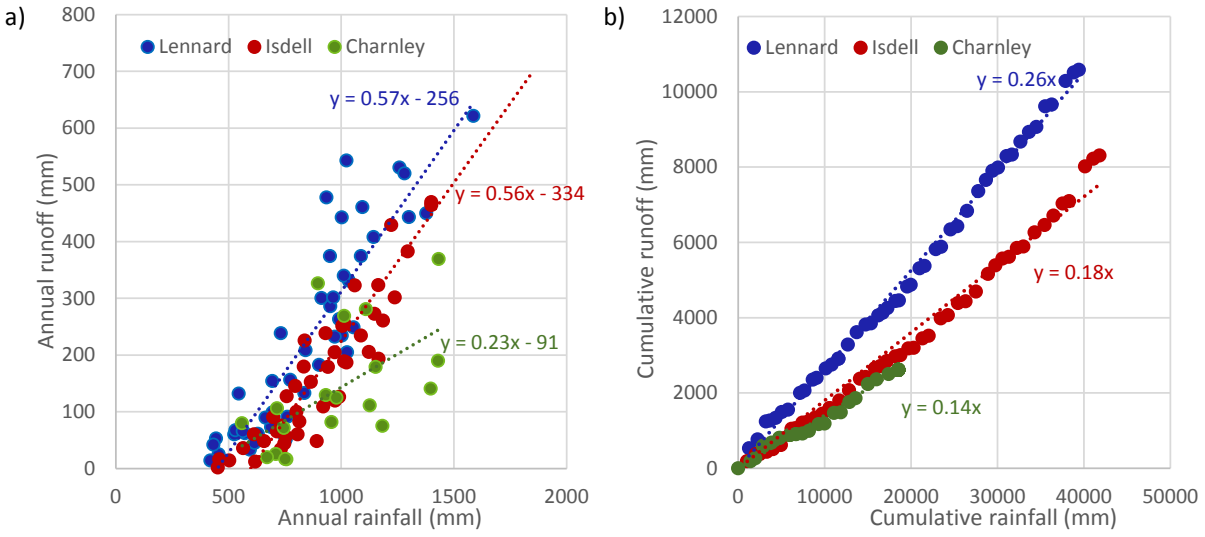

Figure 5-4. a) Mean annual runoff against rainfall, and b) cumulative runoff against cumulative rainfall for the three stream gauges given in Figure 5-3.

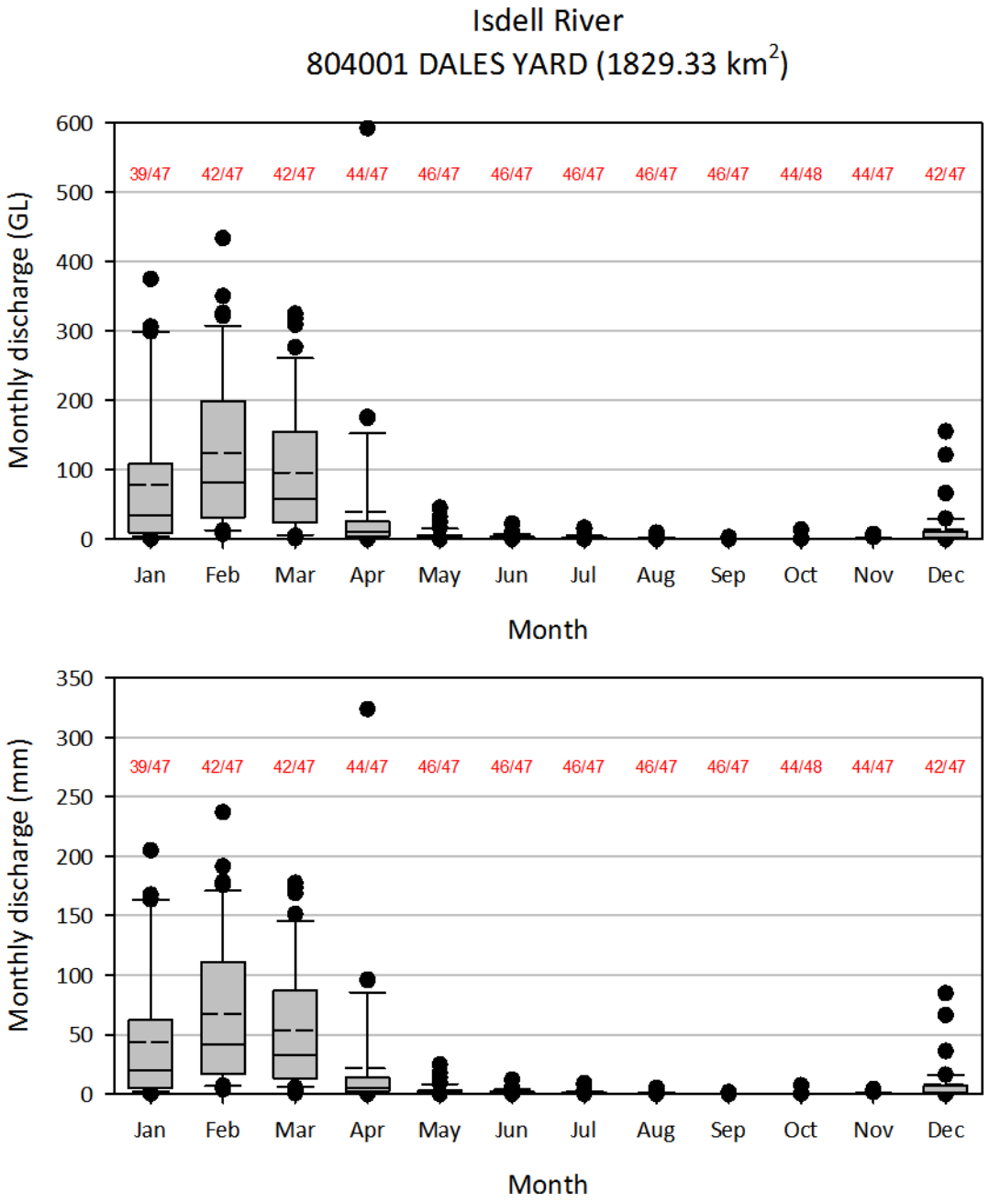

Figure 5-5. Isdell River monthly catchment discharge at station 804001 (Dales Yard). Data only included if full monthly record available with red numbers indicating the proportion of the total months in the data record. Points represent outliers; error bars, the 10th and 90th percentiles; boxes, the 25th and 75th percentiles; solid line in box the 50th percentile and the dashed line the mean.

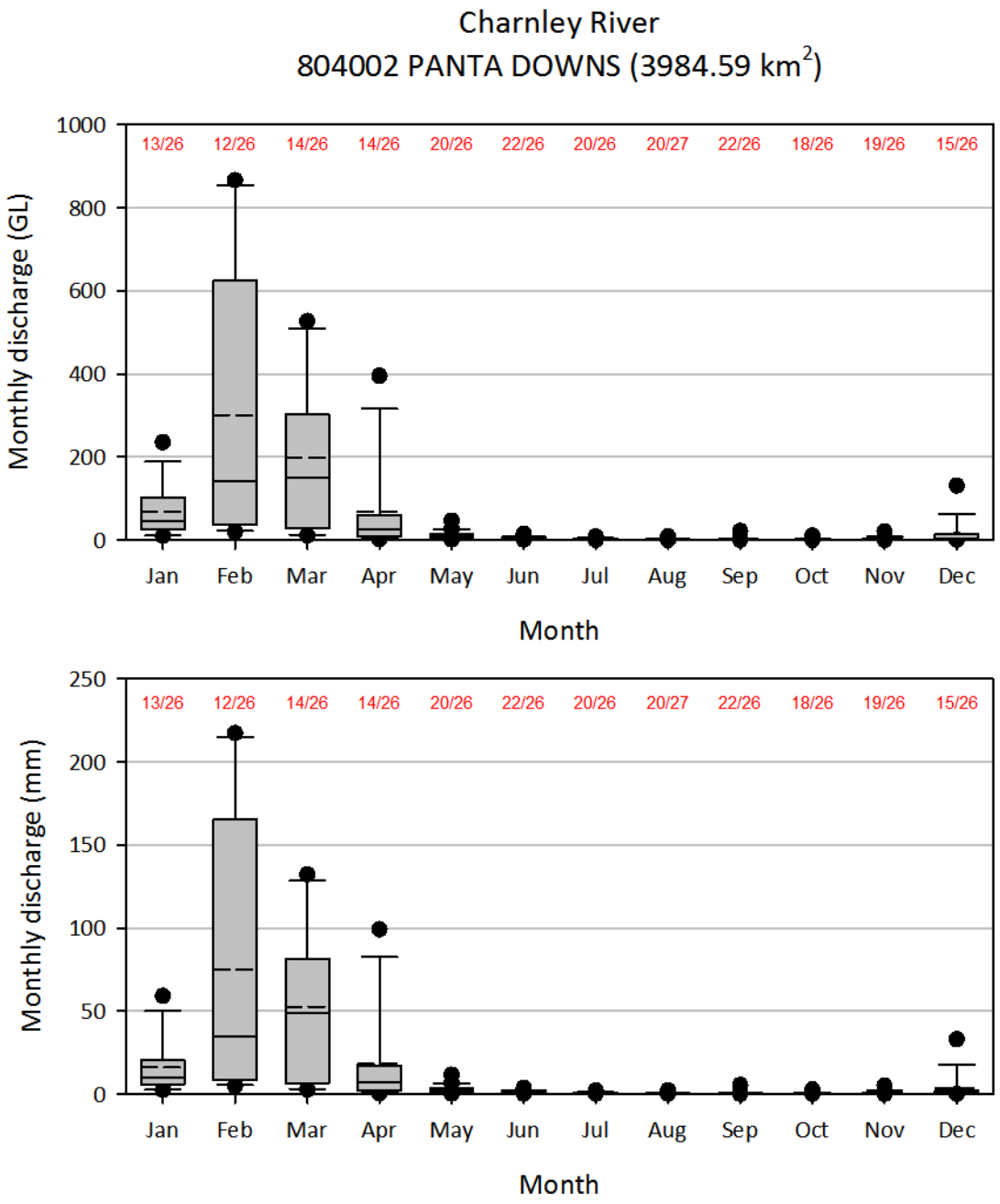

Figure 5-6. Charnley River monthly catchment discharge at station 804002 (Panta Downs). Data only included if full monthly record available with red numbers indicating the proportion of the total months in the data record. Points represent outliers; error bars, the 10th and 90th percentiles; boxes, the 25th and 75th percentiles; solid line in box the 50th percentile and the dashed line the mean.

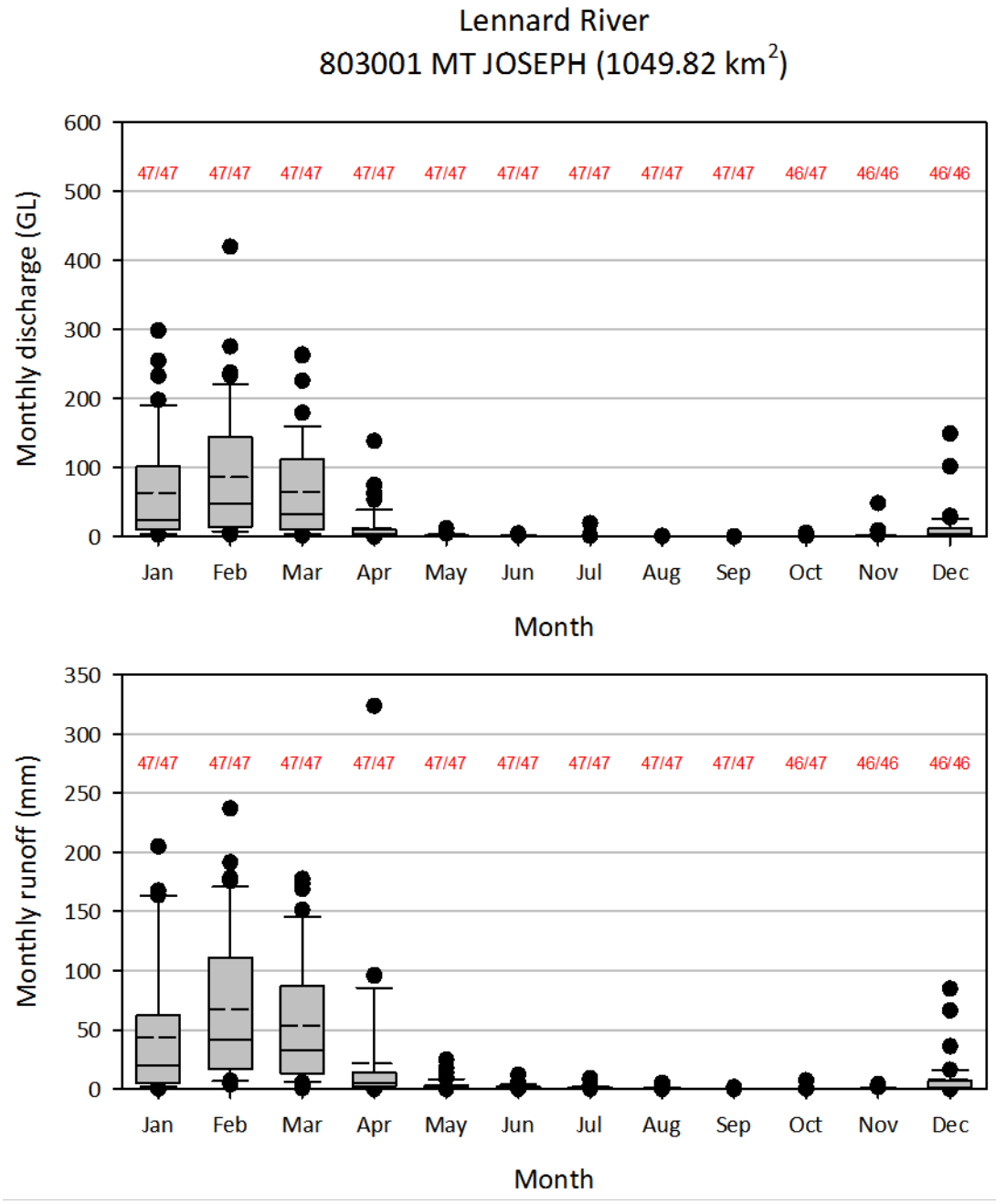

Figure 5-7. Lennard River monthly catchment discharge at station 803001 (Mt Joseph). Data only included if full monthly record available with red numbers indicating the proportion of the total months in the data record. Points represent outliers; error bars, the 10th and 90th percentiles; boxes, the 25th and 75th percentiles; solid line in box the 50th percentile and the dashed line the mean.

5.1.4 River water quality data

All available water quality data from the Kimberley streams have been collated into a database. However, apart from the Ord River these are very limited, and even the Ord has data from relatively few periods in time. The data from the Ord were considered inappropriate because of the development within the catchment which has fundamentally changed the runoff quality and character and hence is unlikely to be representative of the conditions flowing into the Walcott Inlet.

These data were analysed for emergent flow-flux relationships but the analysis showed little correlation and thus it has not been possible to develop an appropriate model for nutrient and carbon loads from catchments

under given land surface and climate conditions. The available water quality statistics are summarised in Table 5-3 and the data collection frequency summarised in Table 5-4.

Table 5-3 Summary of nutrient concentrations at the three gauging stations

	Parameter	DOC	NOx-N	N (tot kjel)	N (total)	NO2-N	NO3	P (total)
		mg/L	mg/L	mg/L	mg/L	mg/L	mg/L	mg/L
Isdell River (804001)	**Count all**	12	18	5	6	3	5	6
	Count >dl*	12	3	5	6	0	5	6
	Mean	3.65	0.013	0.227	0.212	**<0.01**	2.4	0.013
	Stdev	2.27	0.012	0.083	0.094		1.67	0.008
	Min	1.76	0.005	0.148	0.095		1	0.006
	25th percentile	2.52	0.006	0.18	0.161		1	0.007
	50th percentile	3.4	0.006	0.196	0.191		2	0.011
	75th percentile	3.78	0.016	0.252	0.26		3	0.018
	Max	10.4	0.027	0.36	0.36		5	0.024
Charnley River (804002)	**Count all**	6	8	2	2		5	2
	Count >dl*	6	2	2	2		3	2
	Mean	2.5	0.01	0.247	0.257		4	0.003
	Stdev	0.99	0.01	0.092	0.102		5.2	0.002
	Min	1.37	0.003	0.182	0.185		1	0.002
	25th percentile	1.66	0.007	0.215	0.221		1	0.0026
	50th percentile	2.48	0.01	0.247	0.257		1	0.0033
	75th percentile	3.37	0.014	0.28	0.293		5.5	0.0039
	Max	3.62	0.017	0.312	0.329		10	0.0045
Lennard River (803001)	**Count all**	7	9	3	4	2	5	4
	Count >dl*	7	2	3	4	**0**	5	4
	Mean	3.71	0.013	0.29	0.39	<0.01	2.4	0.025
	Stdev	2.2	0.006	0.2	0.25		2.6	0.034
	Min	2.03	0.009	0.14	0.15		1	0.006
	25th percentile	2.85	0.01	0.18	0.2		1	0.008
	50th percentile	3.11	0.013	0.22	0.38		1	0.009
	75th percentile	3.26	0.015	0.37	0.57		2	0.026
	Max	8.6	0.017	0.52	0.67		7	0.076

* dl = detection limit

Table 5-4. Availability of nutrient data for the three gauging stations.

No. of parameters measured on same sample	Count		
	Isdell River (804001)	**Charnley River (804002)**	**Lennard River (803001)**
1	**5**	5	5
2	**12**	6	7
3	**0**	0	0
4	**4**	2	3
5	**2**	0	1

Figure 5-8 shows the frequency distribution (blue bars) of daily runoff (x-axis), and occurrence of all measurements of the most significant water quality parameters from samples taken in the lower Fitzroy stations (AWRC gauges 802003, 802006, 802007, 802008). As also shown below (Figure 5-12) pH and dissolved oxygen (DO) are relatively stable through the full range of flow measurements.

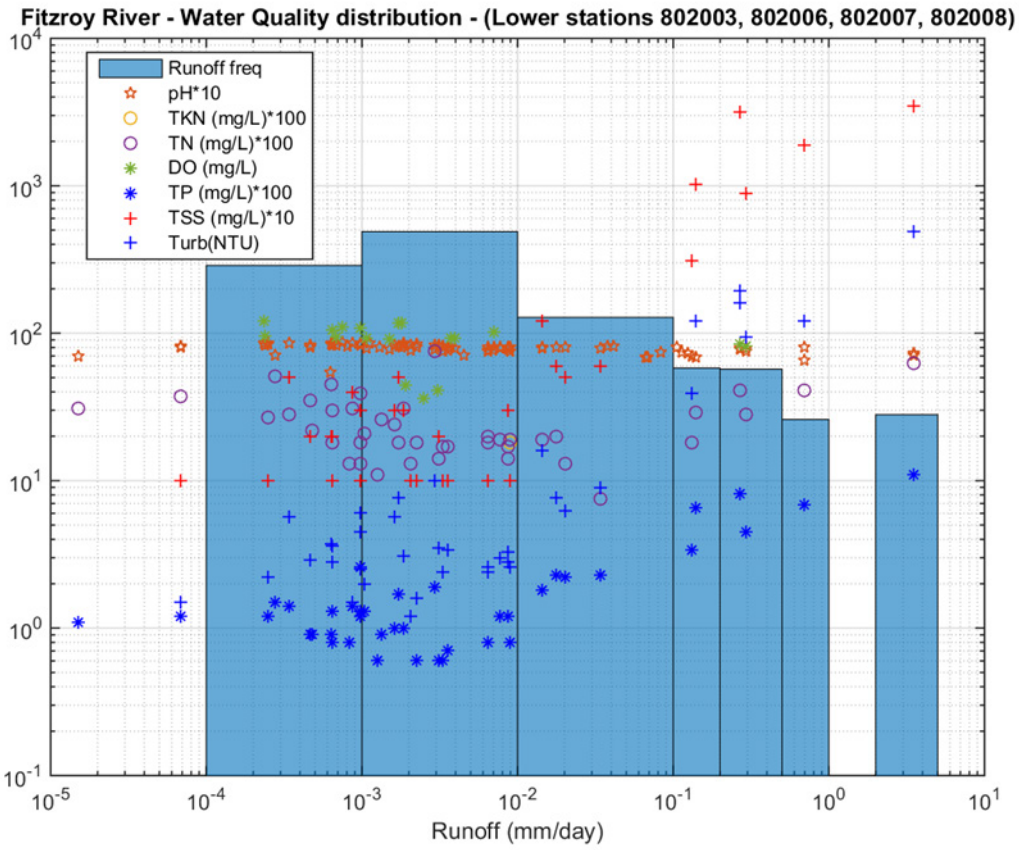

Figure 5-8. Frequency distribution of flow measurements (blue bars) at the time of water samples taken at the stream gauges of the lower Fitzroy River. Also shown are the values of the most significant water quality parameters of all samples taken at these stations, plotted against the runoff level at the time of sampling. The abscissa is the daily runoff value and the ordinate is the number of occurrences (out of a total of 1281 samples). Logarithmic scales are used to facilitate the presentation of all values on the same axes.

a)

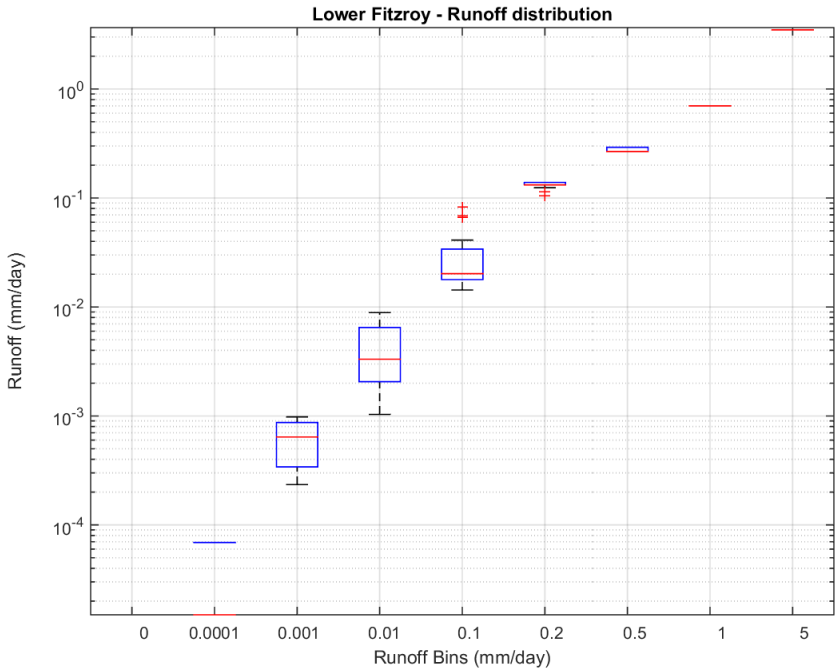

b)

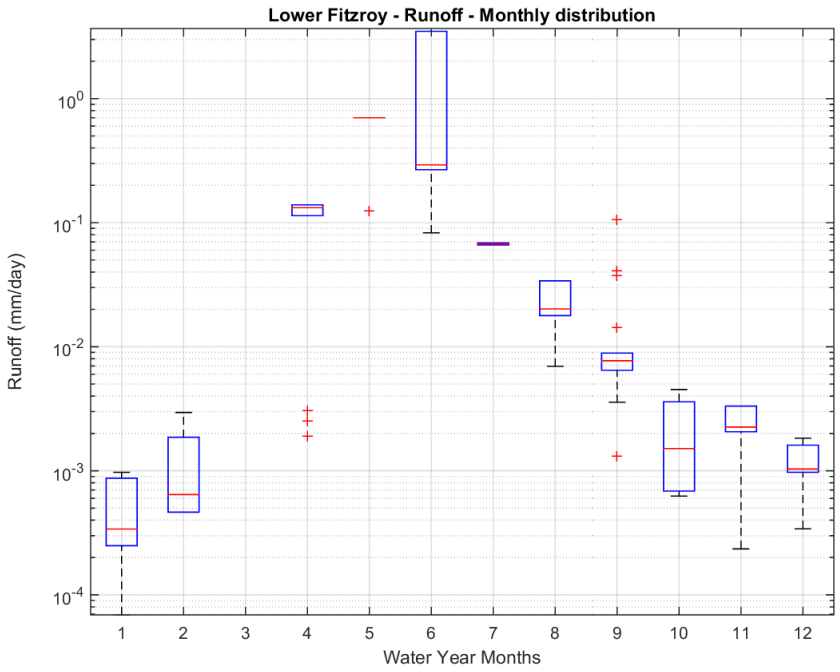

Figure 5-9. Distribution of range of a) daily runoff against runoff, and b) distribution of runoff against months from the water sample dataset at the gauges of the Lower Fitzroy River. Note that these data are taken from the times water samples were taken and thus do not represent the full distribution of flow.

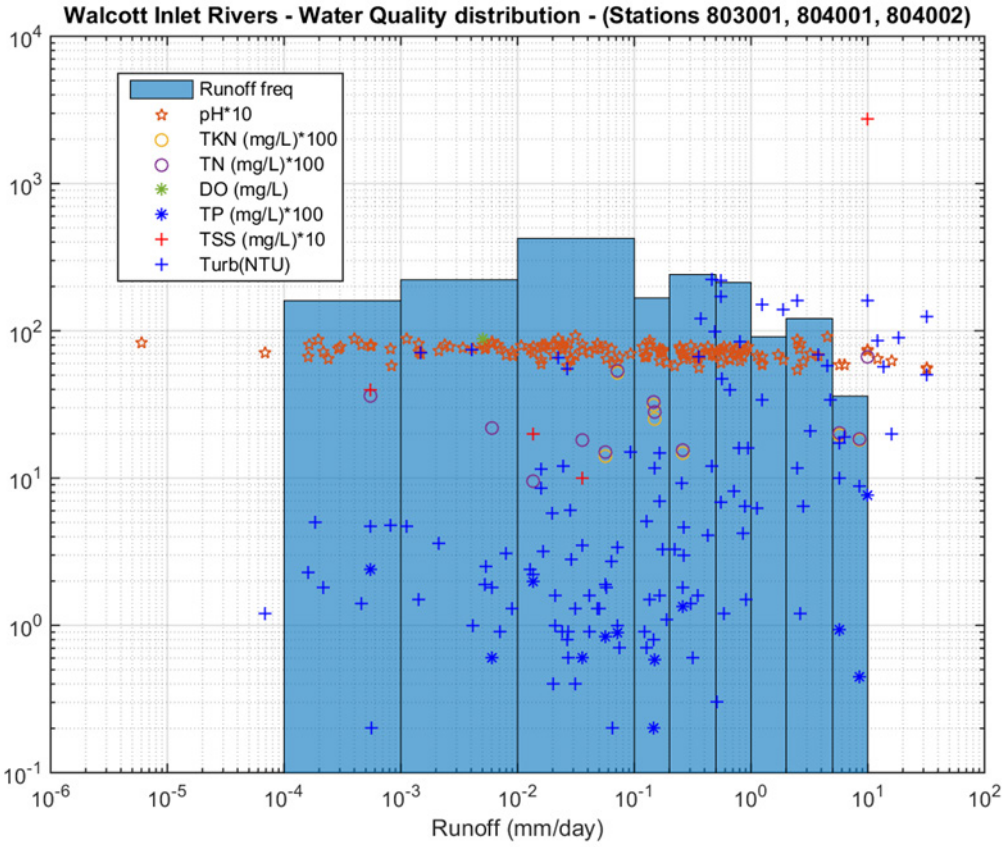

Figure 5-10. Frequency distribution of flow measurements (blue bars) at the time of water samples taken at the stream gauges on rivers flowing into the Walcott Inlet (Isdell, 804001 and Charnley, 804002), plus the Lennard (803001) River. Also shown are the values of the most significant water quality parameters of all samples taken at these stations, plotted against the runoff level at the time of sampling. The abscissa is the daily runoff value and the ordinate is the number of occurrences (out of a total of 1281 samples). Logarithmic scales are used to facilitate the presentation of all values on the same axes.

a)

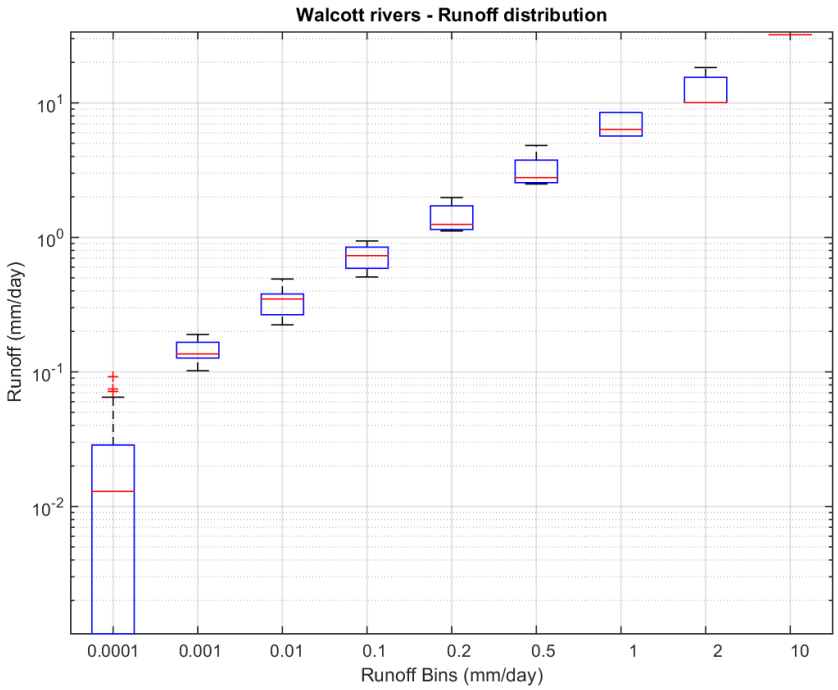

b)

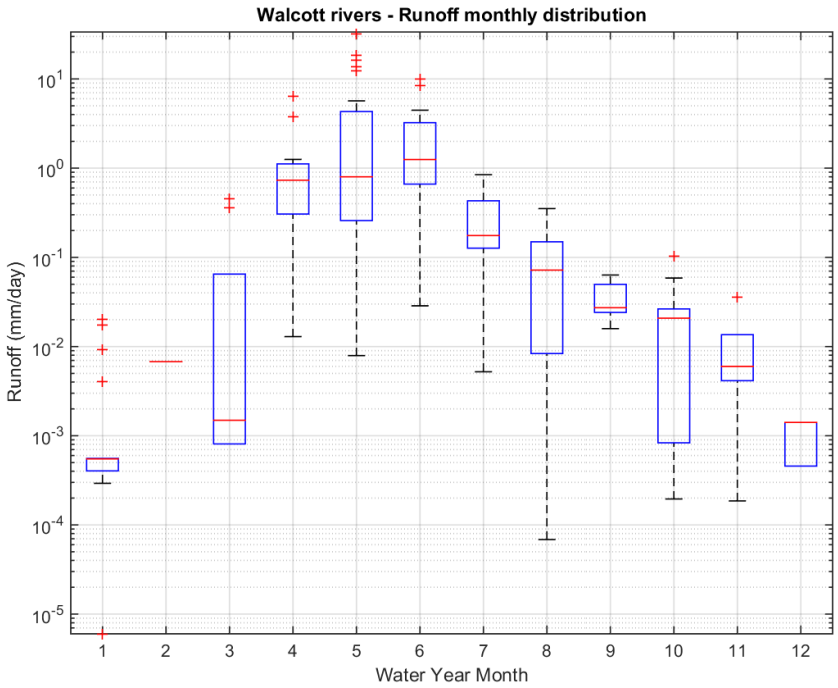

Figure 5-11. Distribution of range of a) daily runoff against runoff, and b) distribution of runoff against months from the water sample dataset for the rivers flowing to the Walcott Inlet. Note that these data are taken from the times water samples were taken and thus do not represent the full distribution of flow.

a)

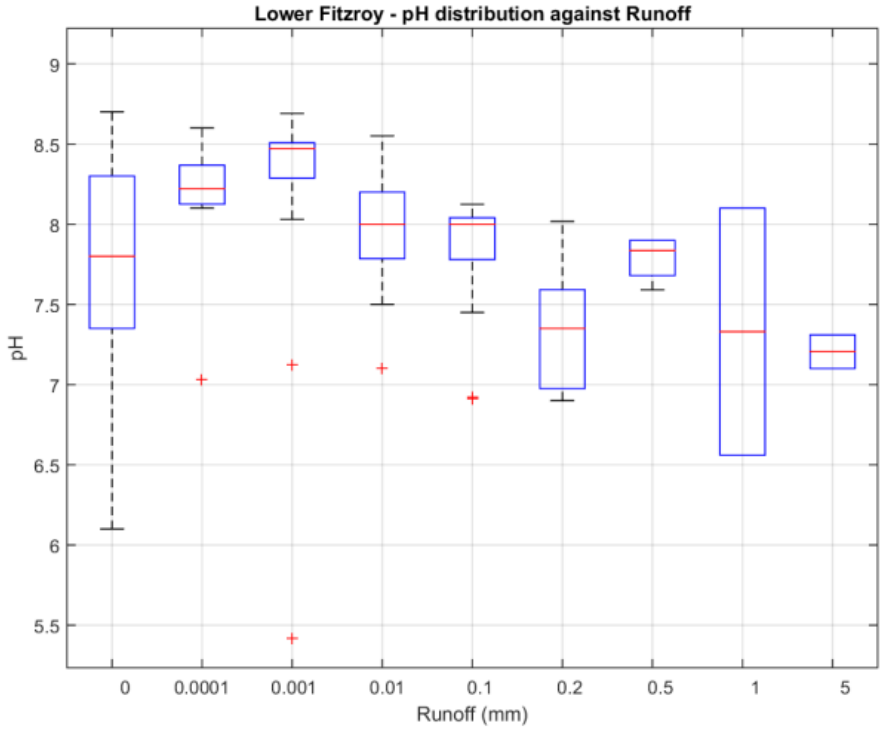
Lower Fitzroy - pH distribution against Runoff
pH
9
8.5
8
7.5
7
6.5
6
5.5
0
0.0001
0.001
0.01
0.1
0.2
0.5
1
5
Runoff (mm)

b)

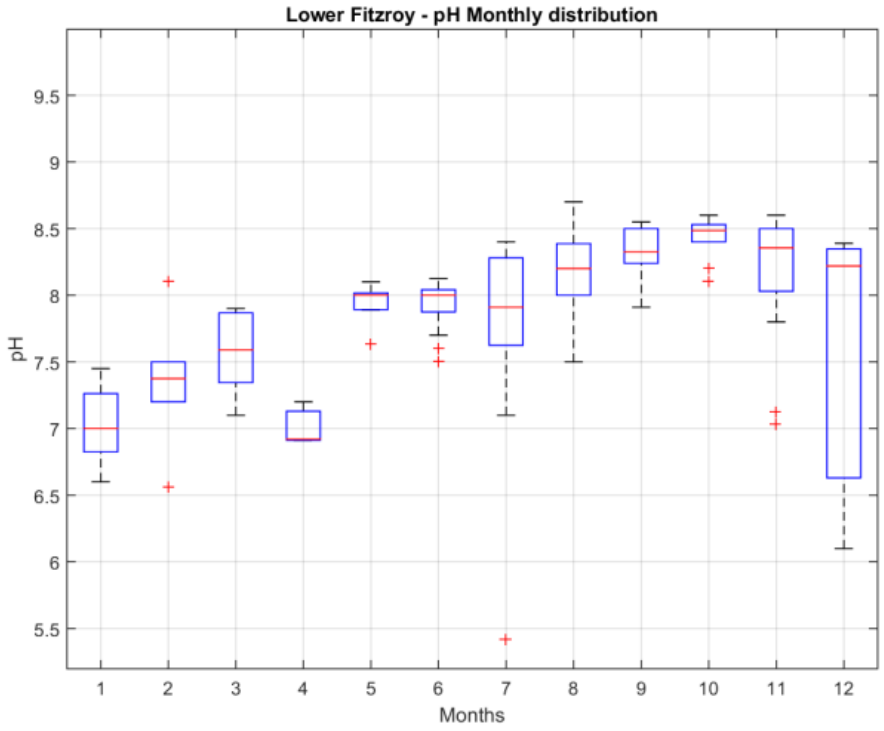
Lower Fitzroy - pH Monthly distribution
pH
9.5
9
8.5
8
7.5
7
6.5
6
5.5
1
2
3
4
5
6
7
8
9
10
11
12
Months

c)

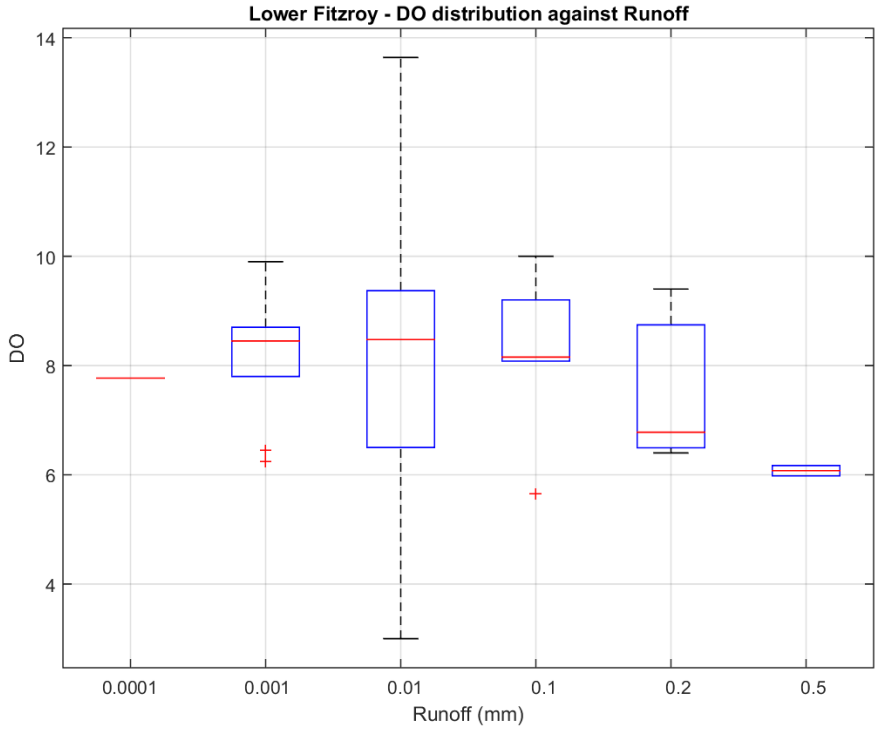

d)

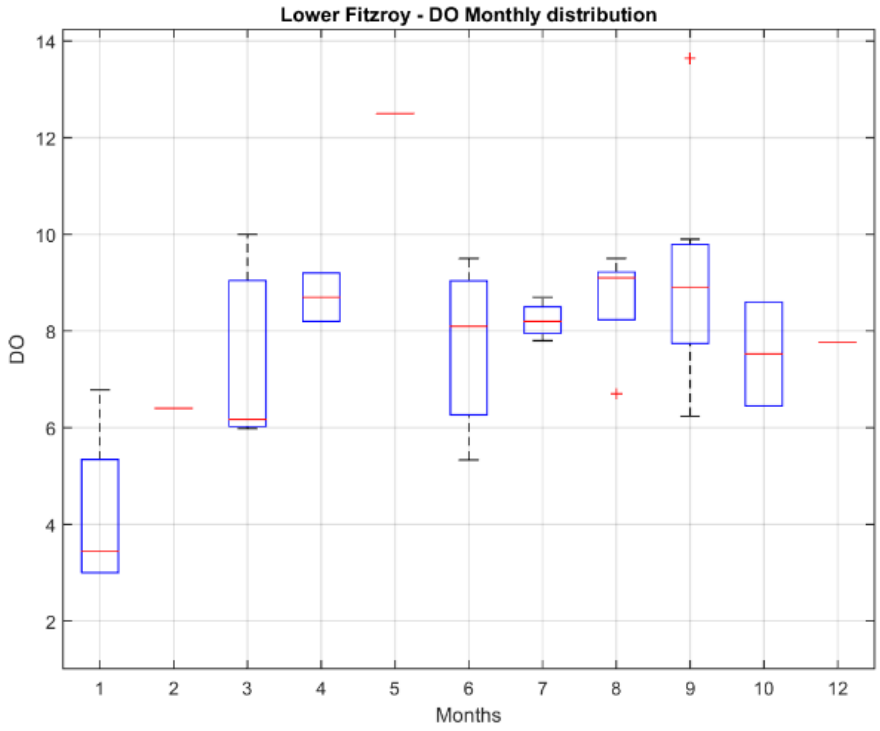

Figure 5-12. Distribution of pH by (a) runoff value and (b) by month, and dissolved oxygen (DO) against (c) runoff and (d) by month in the rivers in the Lower Fitzroy River.

a)

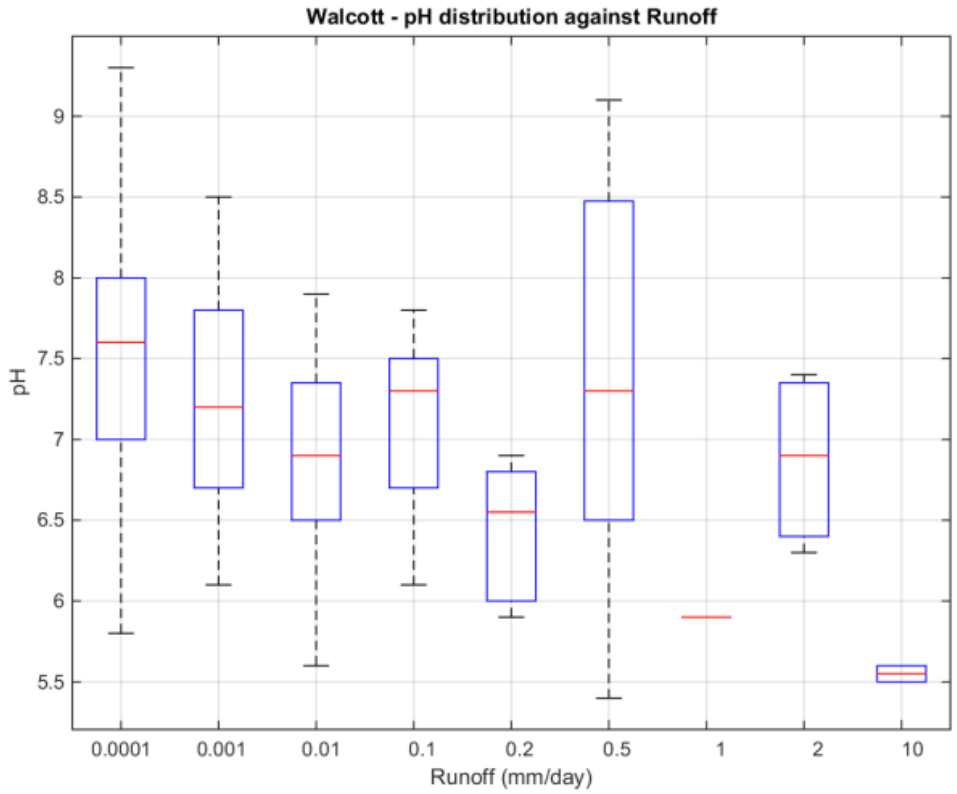
Walcott - pH distribution against Runoff
pH
9
8.5
8
7.5
7
6.5
6
5.5
0.0001
0.001
0.01
0.1
0.2
0.5
1
2
10
Runoff (mm/day)

b)

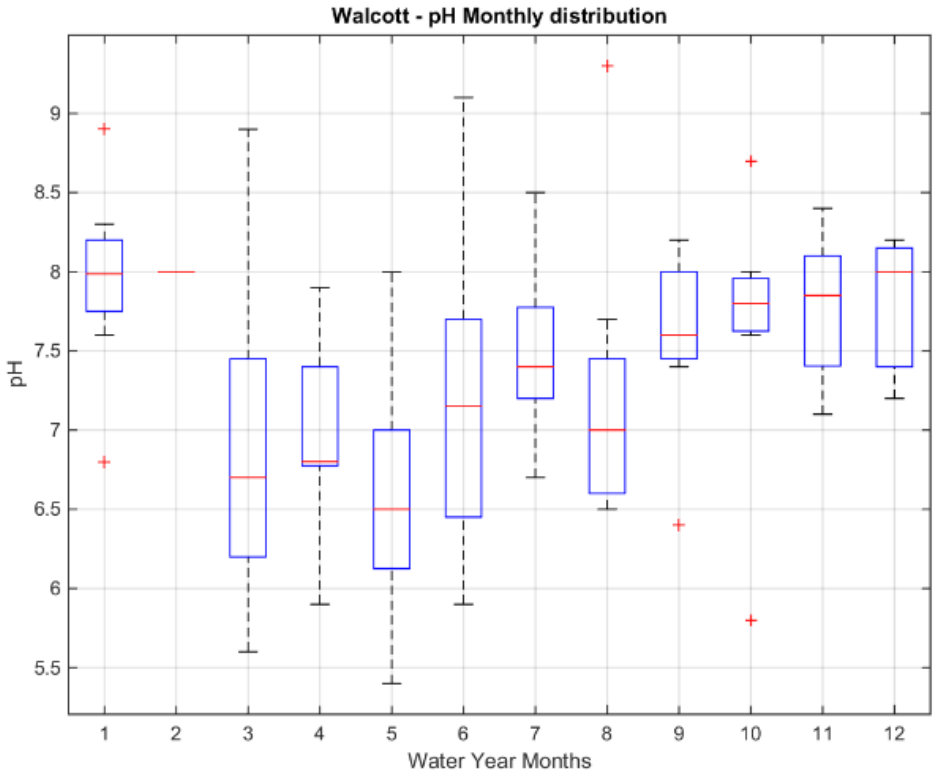
Walcott - pH Monthly distribution
pH
9
8.5
8
7.5
7
6.5
6
5.5
1
2
3
4
5
6
7
8
9
10
11
12
Water Year Months

c)

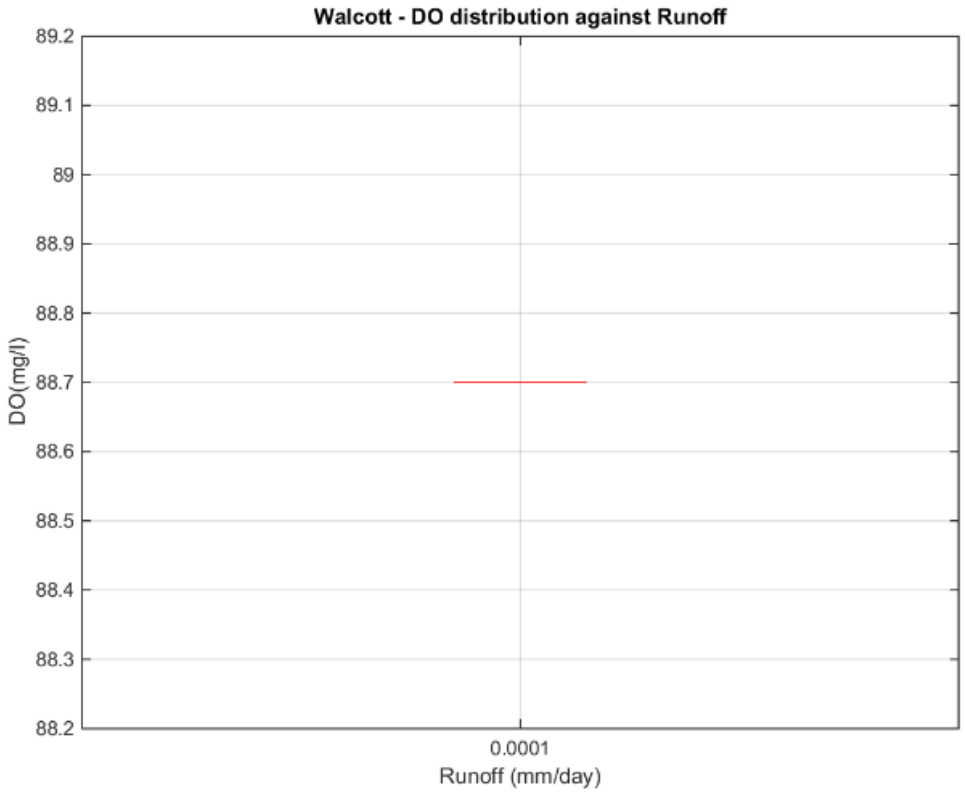

d)

Figure 5-13. Distribution of pH by (a) runoff value and (b) by month, and dissolved oxygen (DO) against (c) runoff and (d) by month in the rivers flowing to the Walcott Inlet.

a)

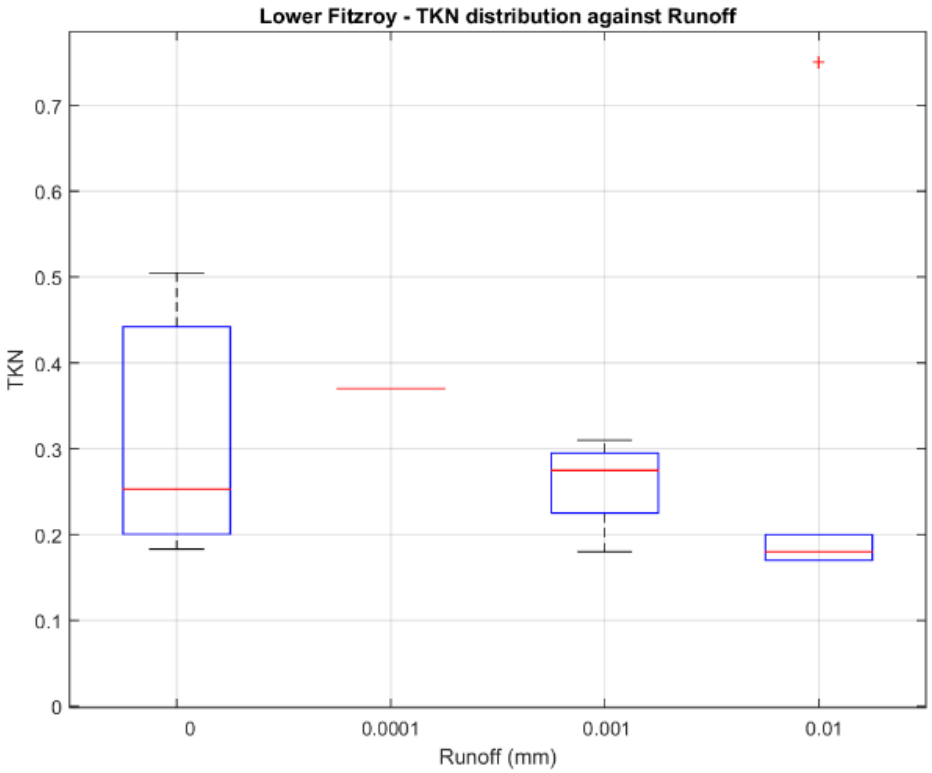
Lower Fitzroy - TKN distribution against Runoff
TKN
0
0.1
0.2
0.3
0.4
0.5
0.6
0.7
0
0.0001
0.001
0.01
Runoff (mm)

b)

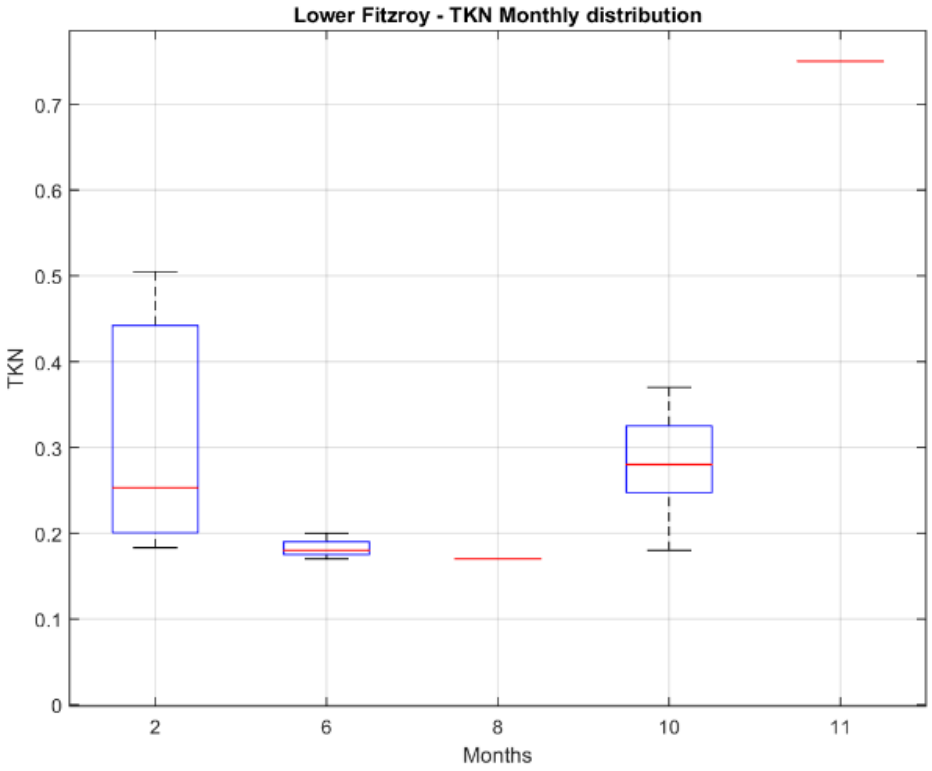
Lower Fitzroy - TKN Monthly distribution
TKN
0
0.1
0.2
0.3
0.4
0.5
0.6
0.7
2
6
8
10
11
Months

c)

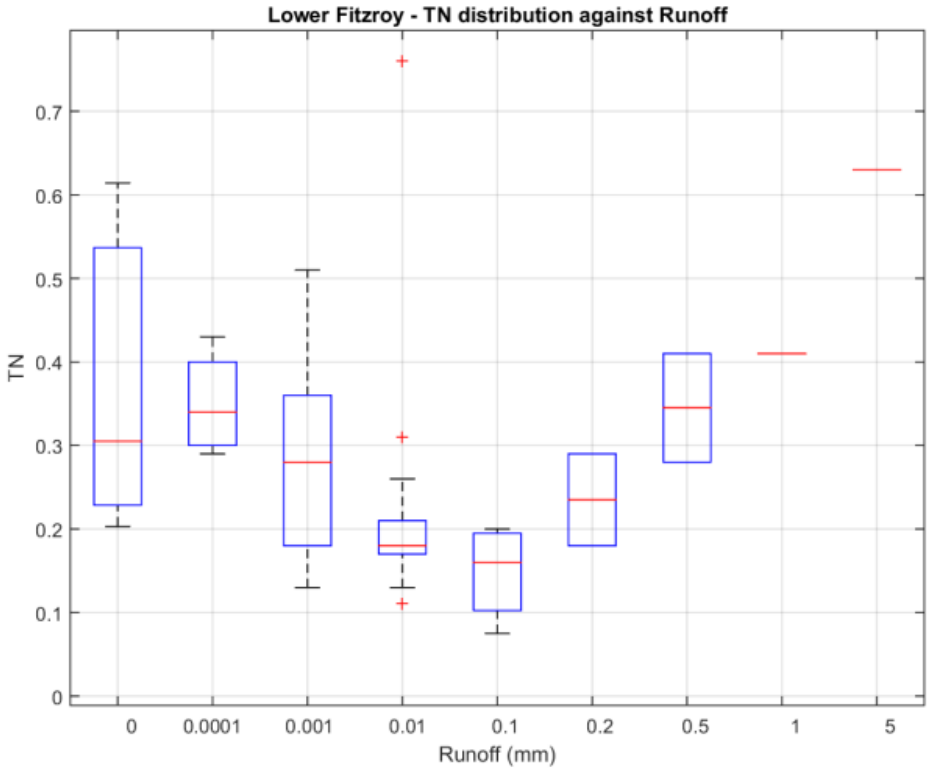
Lower Fitzroy - TN distribution against Runoff
TN
0
0.1
0.2
0.3
0.4
0.5
0.6
0.7
0
0.0001
0.001
0.01
0.1
0.2
0.5
1
5
Runoff (mm)

d)

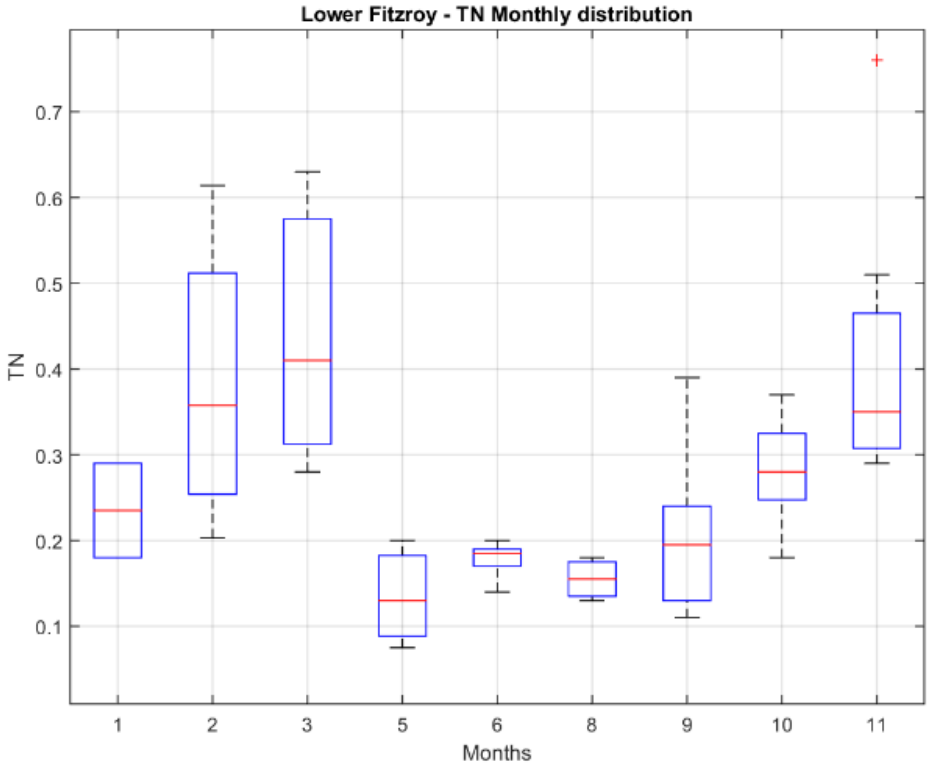
Lower Fitzroy - TN Monthly distribution
TN
0.1
0.2
0.3
0.4
0.5
0.6
0.7
1
2
3
5
6
8
9
10
11
Months

e)

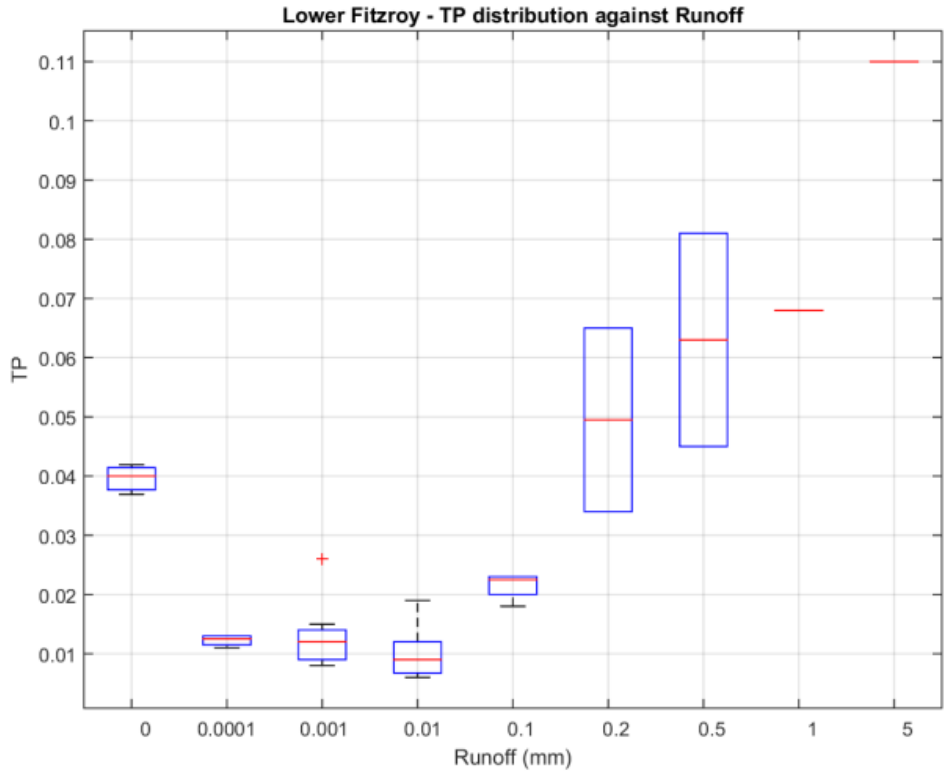

f)

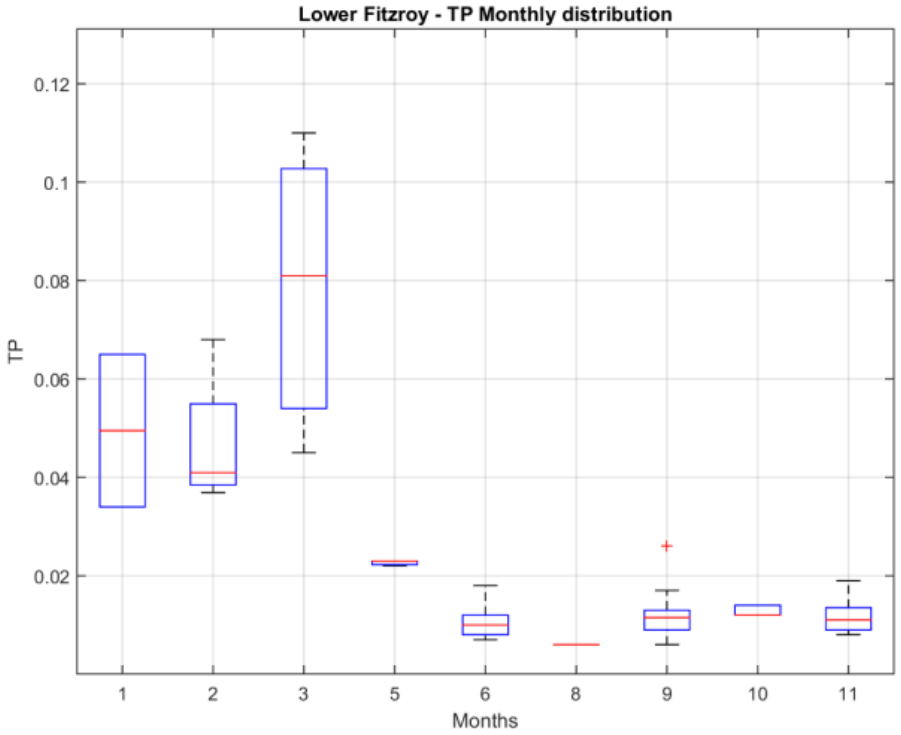

Figure 5-14. Total Kjedahl Nitrogen by (a) runoff, (b) by month, (c) total N by runoff and (d) by month, and Total P by (e) runoff and (f) by month at the gauges on the lower Fitzroy River.

a)

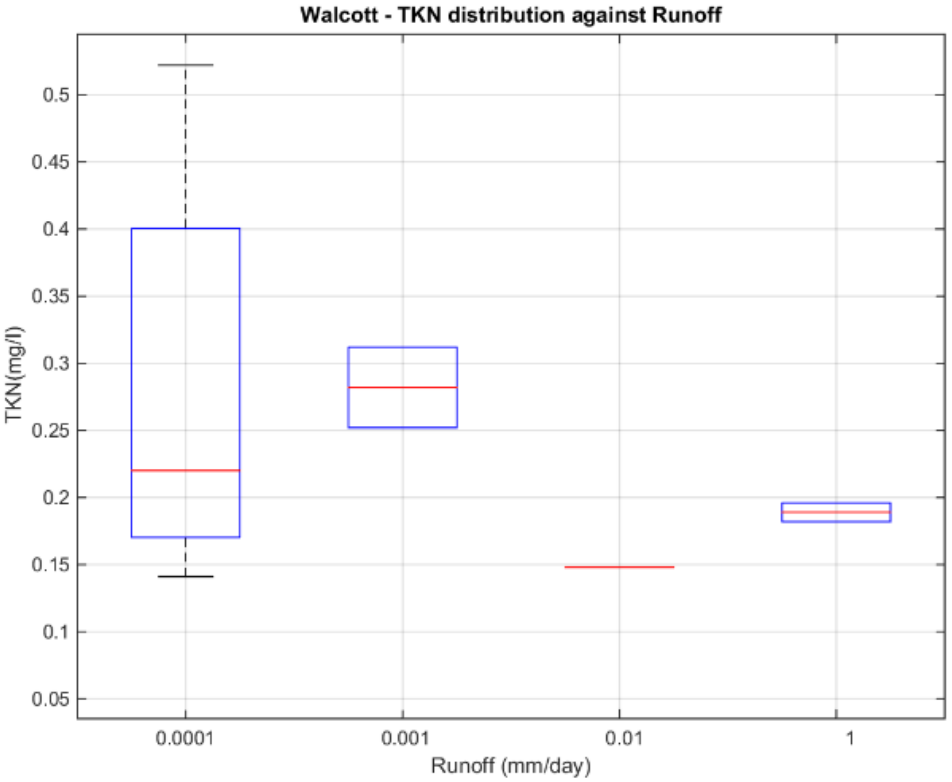
Walcott - TKN distribution against Runoff
TKN(mg/l)
0.5
0.45
0.4
0.35
0.3
0.25
0.2
0.15
0.1
0.05
0.0001
0.001
0.01
1
Runoff (mm/day)

b)

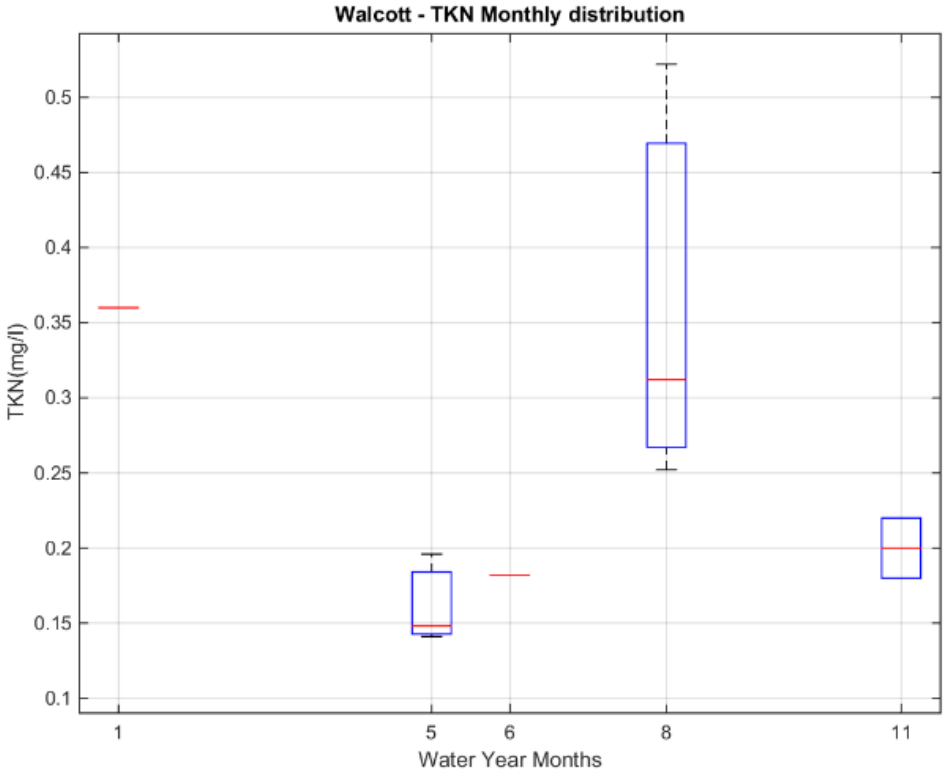
Walcott - TKN Monthly distribution
TKN(mg/l)
0.5
0.45
0.4
0.35
0.3
0.25
0.2
0.15
0.1
1
5
6
8
11
Water Year Months

c)

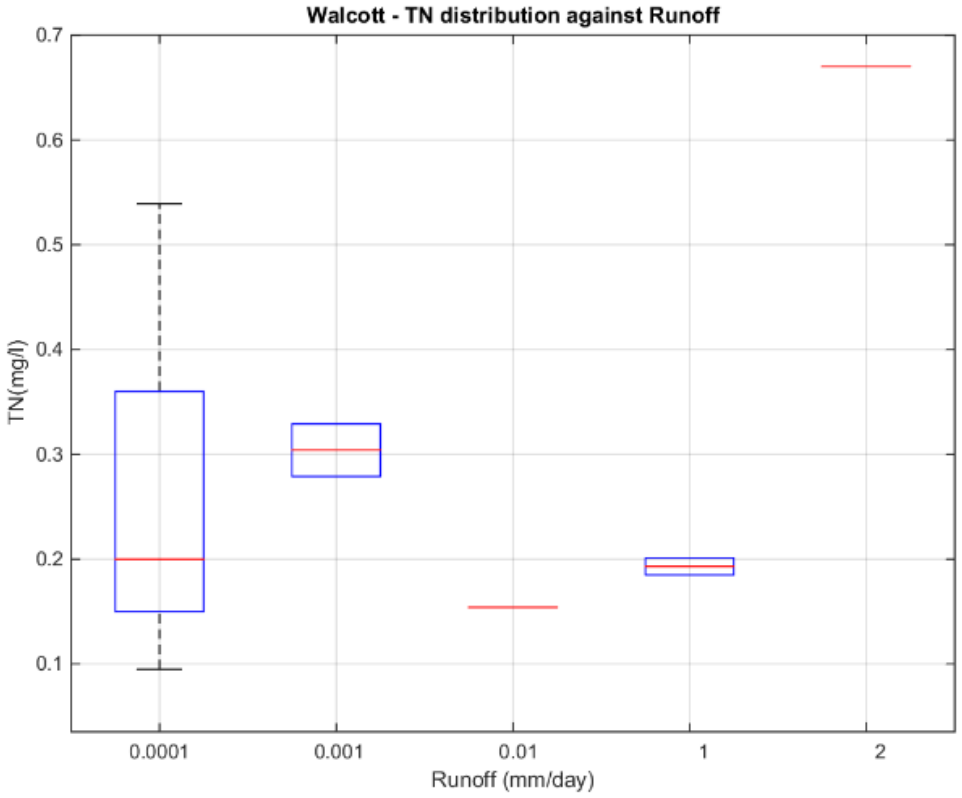
Walcott - TN distribution against Runoff
TN(mg/l)
0.7
0.6
0.5
0.4
0.3
0.2
0.1
0.0001
0.001
0.01
1
2
Runoff (mm/day)

d)

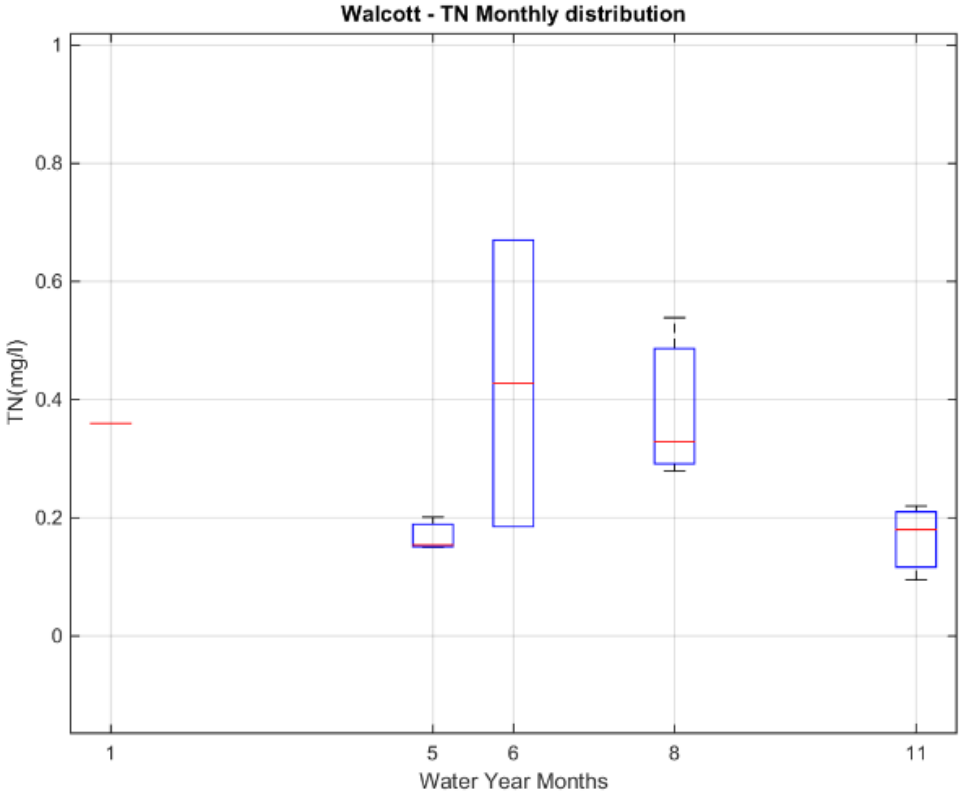
Walcott - TN Monthly distribution
TN(mg/l)
1
0.8
0.6
0.4
0.2
0
1
5
6
8
11
Water Year Months

e)

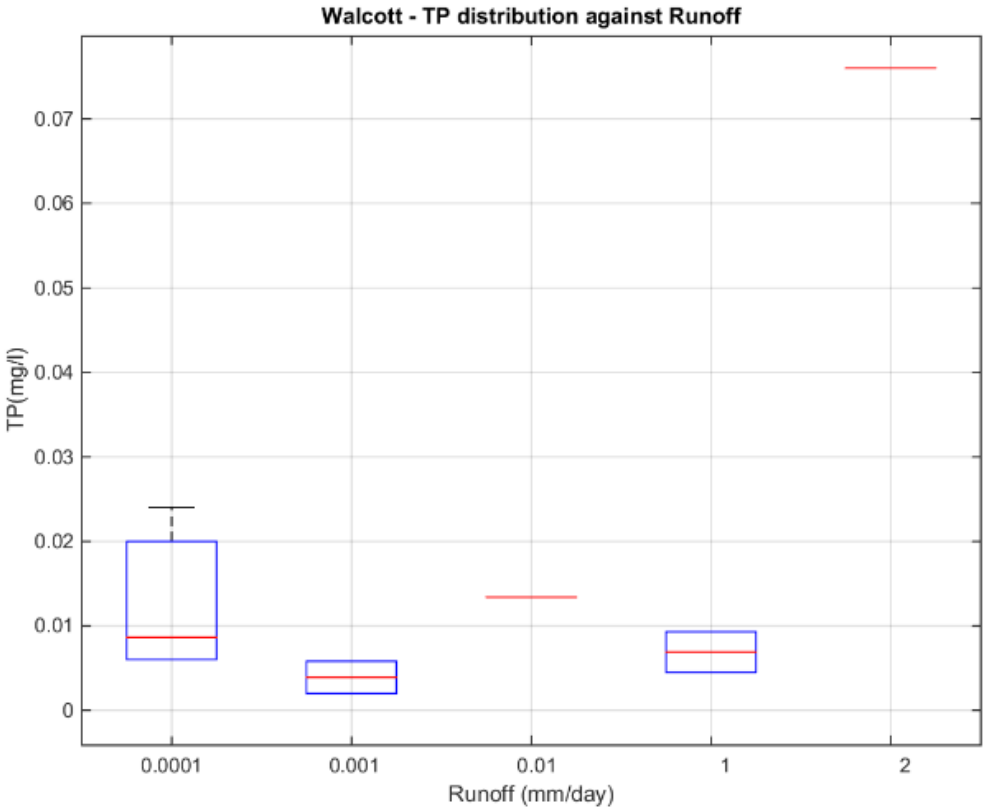

f)

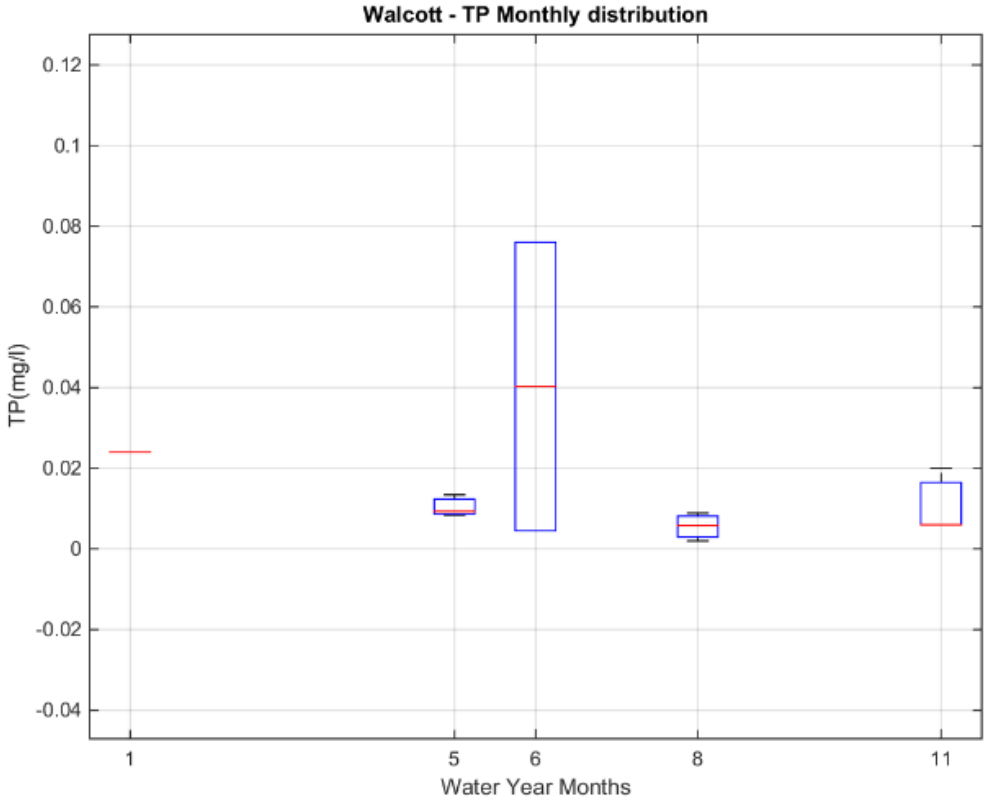

Figure 5-15. Total Kjedahl Nitrogen by (a) runoff, (b) by month, (c) total N by runoff and (d) by month, and Total P by (e) runoff and (f) by month in the rivers flowing to the Walcott Inlet.

a)

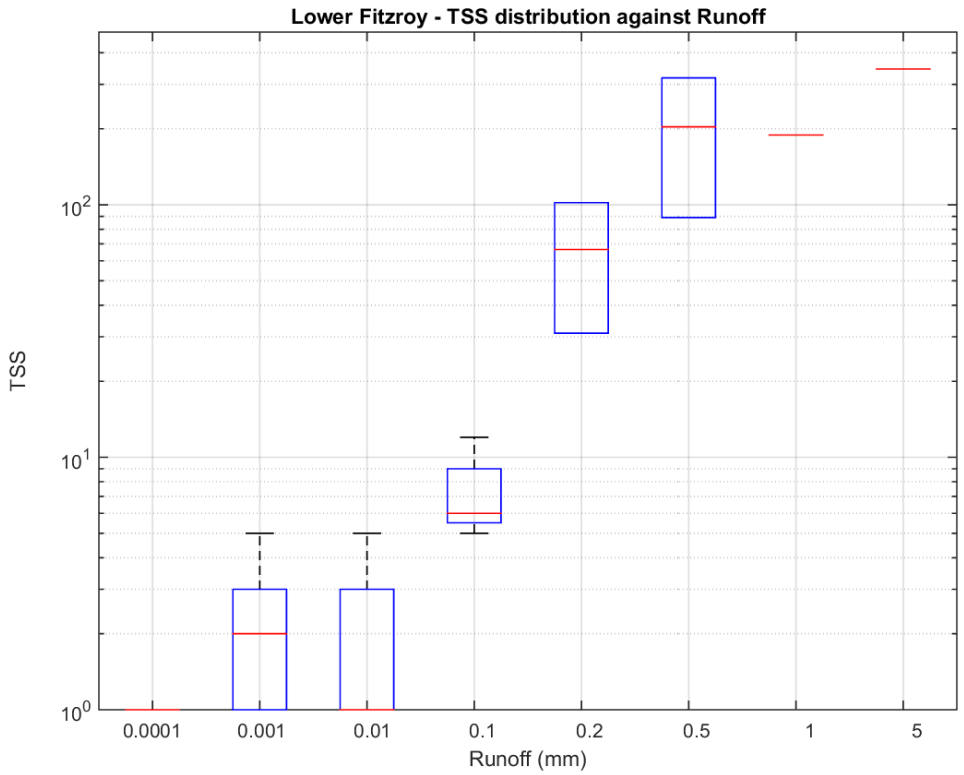
Lower Fitzroy - TSS distribution against Runoff
TSS
10^2
10^1
10^0
0.0001
0.001
0.01
0.1
0.2
0.5
1
5
Runoff (mm)

b)

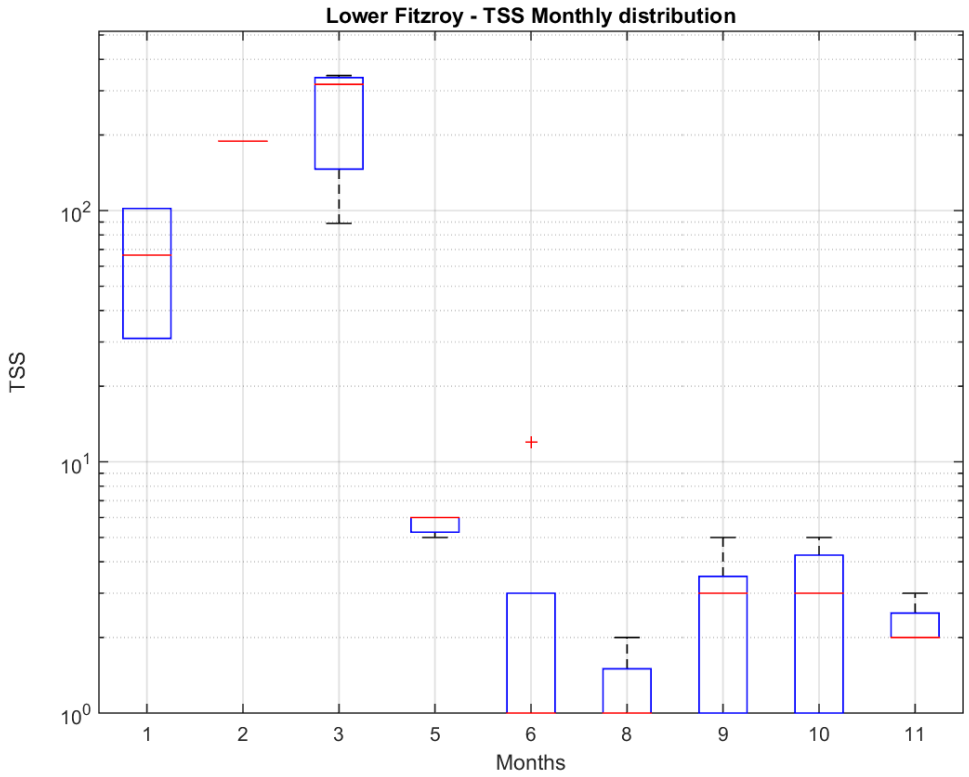
Lower Fitzroy - TSS Monthly distribution
TSS
10^2
10^1
10^0
1
2
3
5
6
8
9
10
11
Months

c)

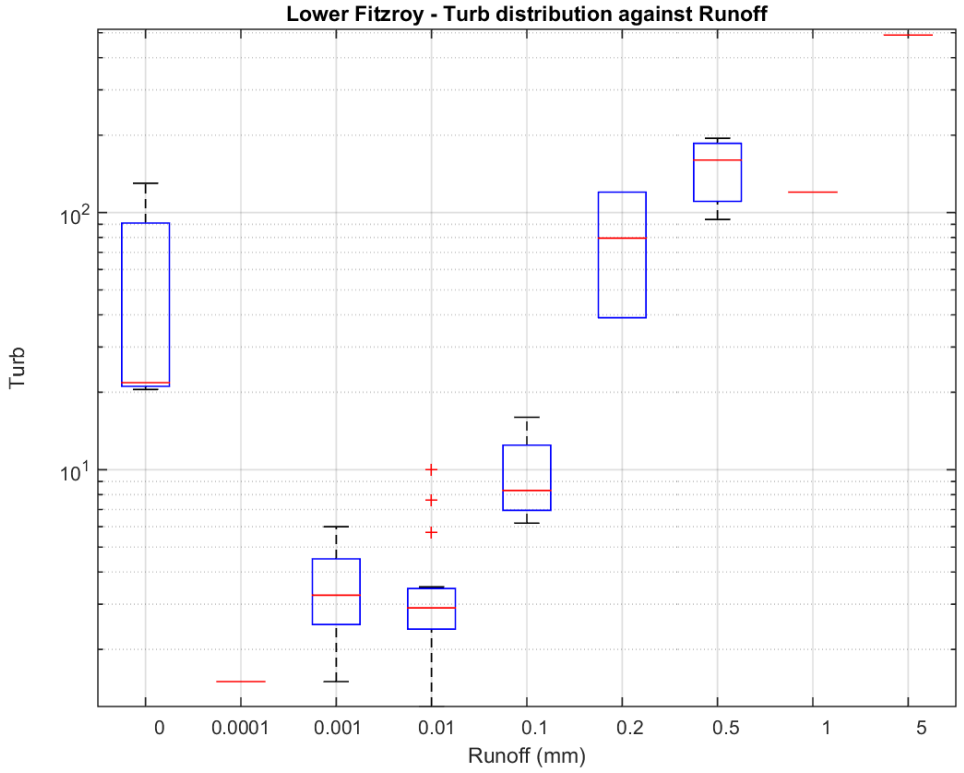

d)

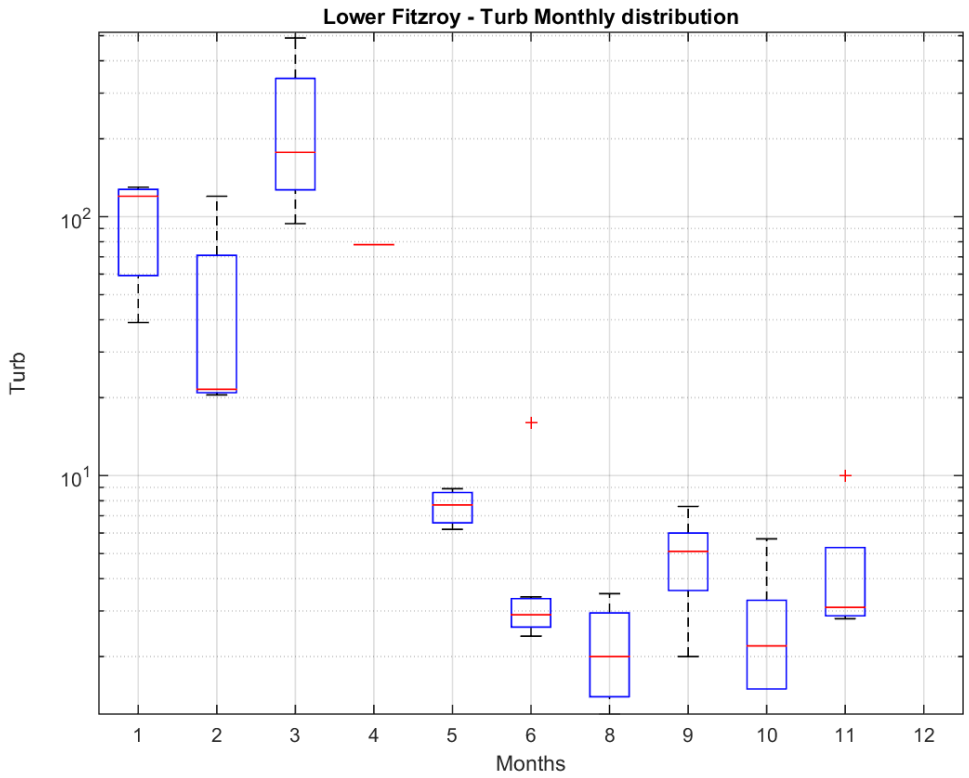

Figure 5-16. Total suspended solids against (a) runoff and (b) month, and Turbidity against (c) runoff and (d) by month in the rivers of the Lower Fitzroy River.

a)

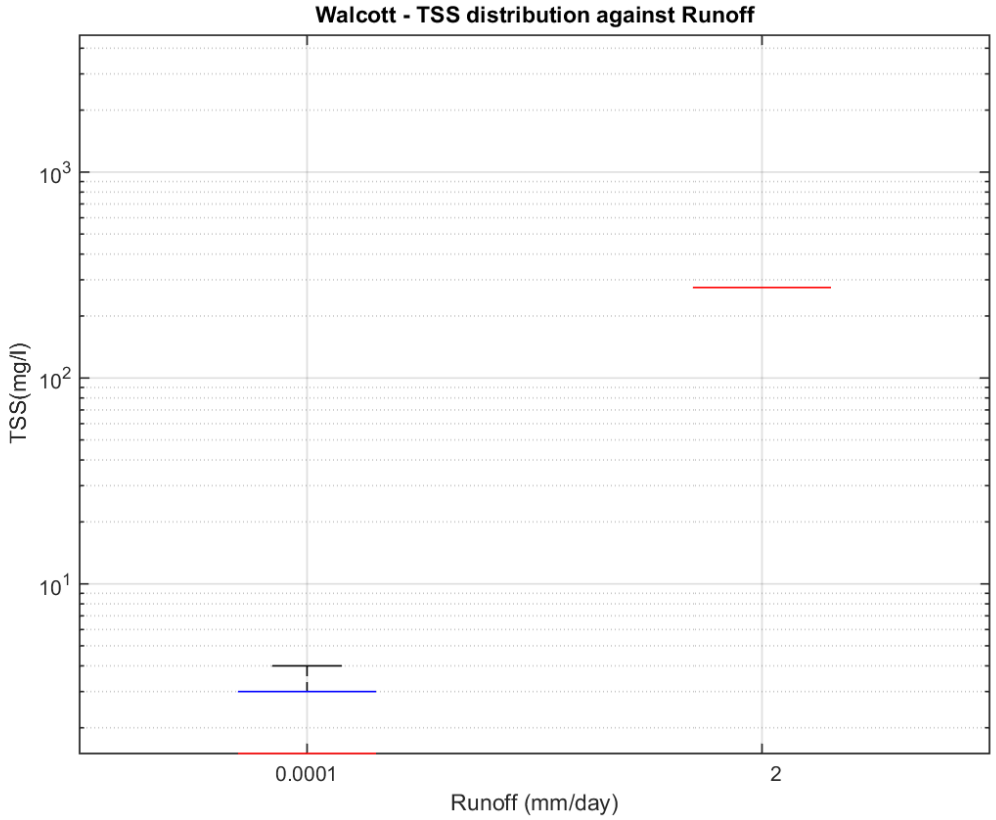
Walcott - TSS distribution against Runoff
TSS(mg/l)
10^3
10^2
10^1
0.0001
2
Runoff (mm/day)

b)

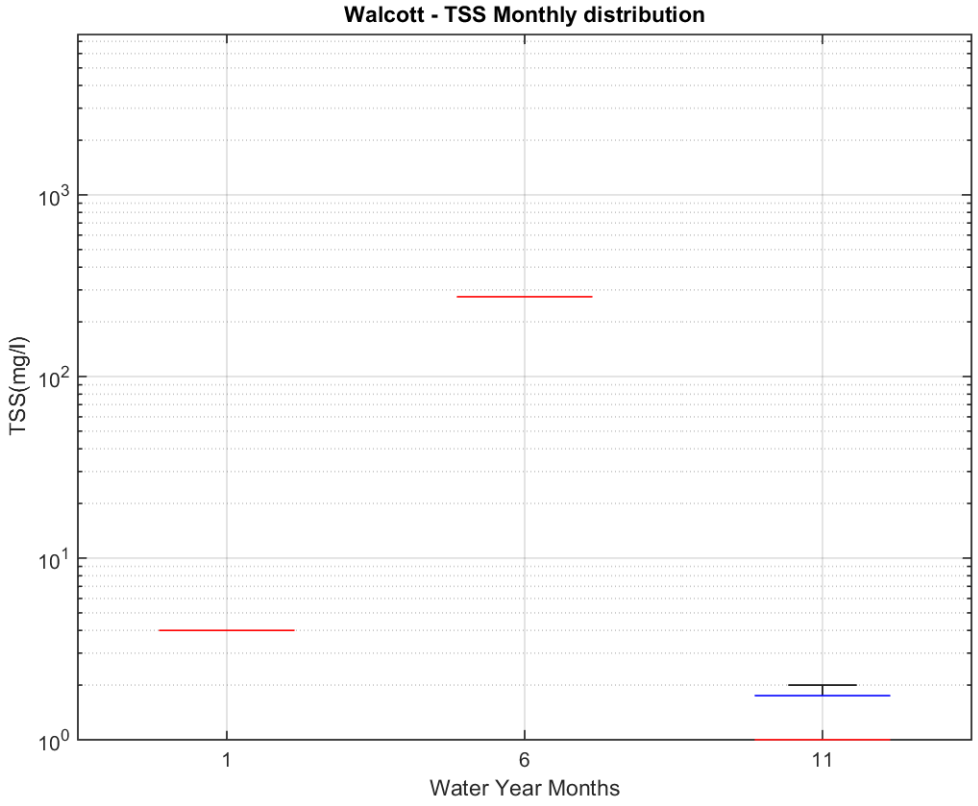
Walcott - TSS Monthly distribution
TSS(mg/l)
10^3
10^2
10^1
10^0
1
6
11
Water Year Months

c)

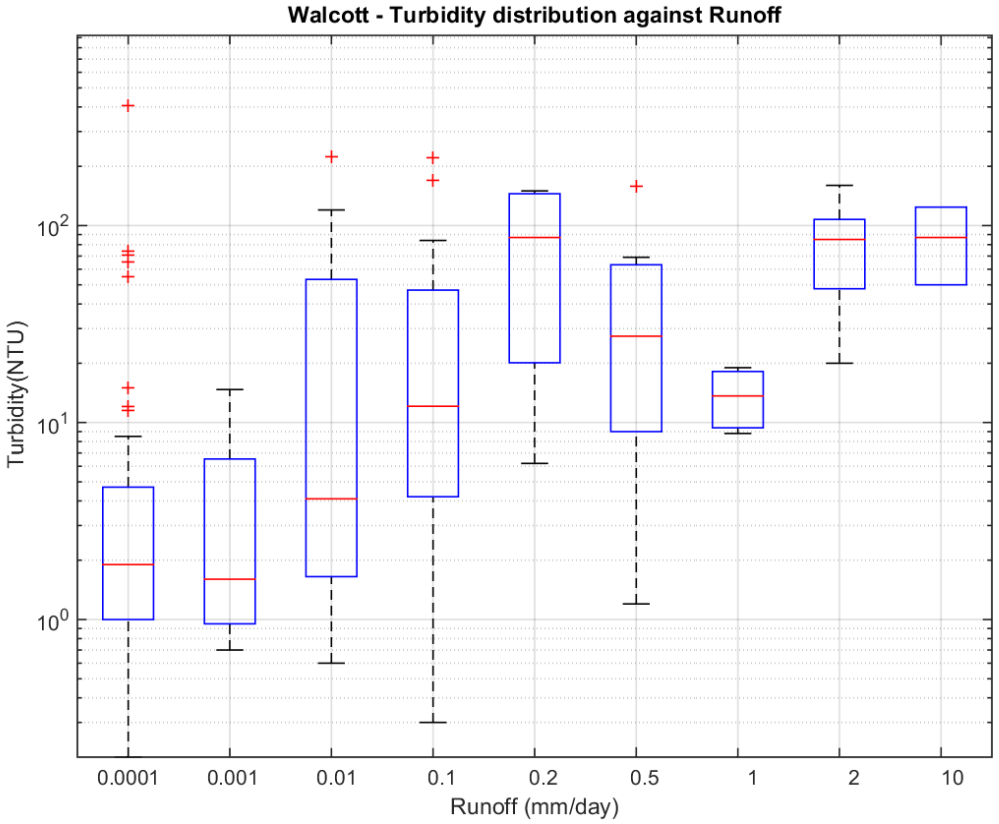

d)

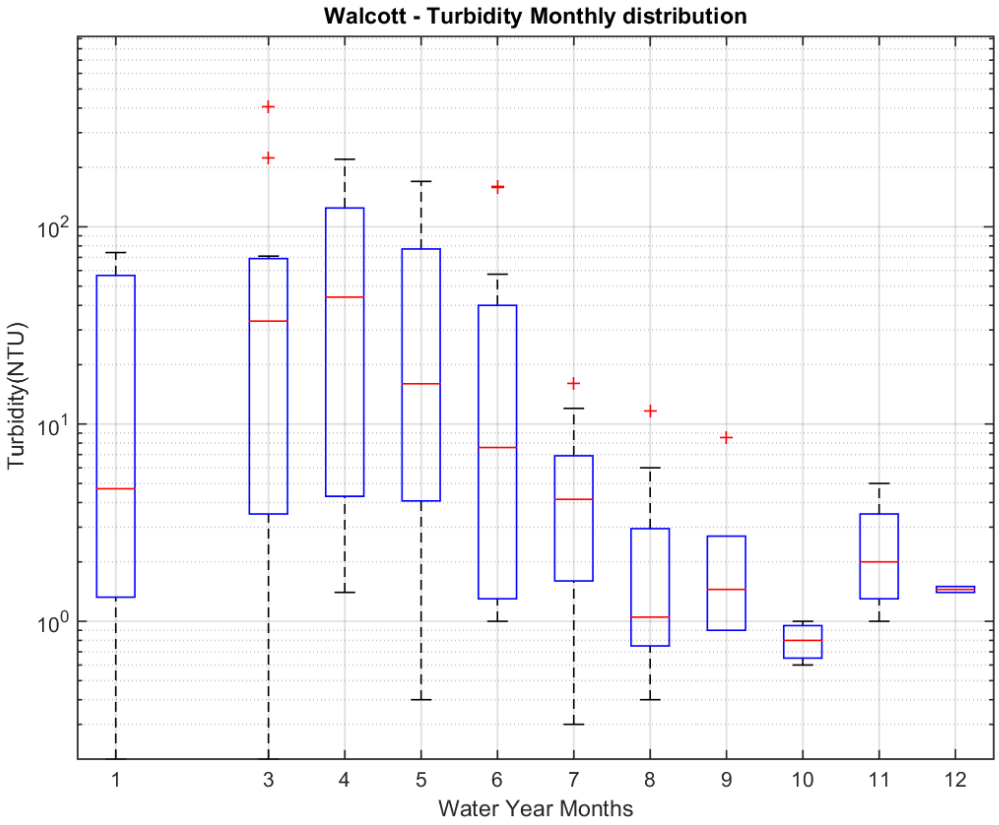

Figure 5-17. Total suspended solids against (a) runoff and (b) month, and Turbidity against (c) runoff and (d) by month in the rivers flowing to the Walcott Inlet

5.1.5 *Kimberley wide nutrients*

As part of a joint wet season WAMSI-AIMS research voyage between Darwin and Broome, nutrient data was collected for a range of Kimberley rivers and adjacent coastal waters (Figure 5-18). Interestingly this data suggests that dissolved organic nitrogen (DON) is discharged in significant quantities. Little is known about the composition of this DON component or how bio-available it might be and therefore how important it could be to coastal productivity. Currently it's not a widely measured component of routine monitoring programs.

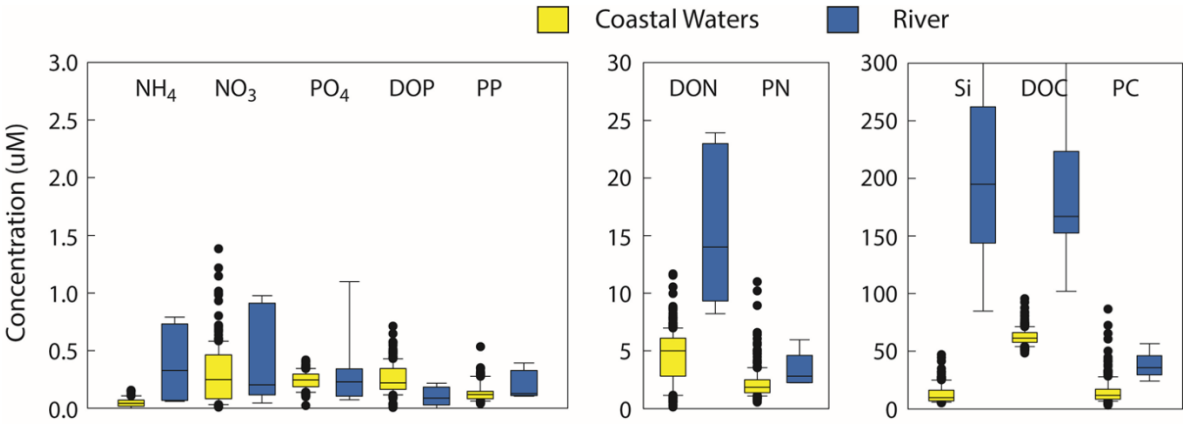

Figure 5-18 Nutrient data for a range of Kimberley rivers and adjacent coastal waters

5.1.6 *Modelling historical catchment runoff*

The annual observed and modelled hydrographs show quite a good fit for the three catchments (804001, 804002 and 803001) (Figure 5-18). The number of flow days matches reasonably well between observed and modelled results for all catchments. Observed and modelled runoff duration curves also matched well for all three gauges (only 804002, being the largest catchment representation and closest to the inlet is shown in Figure 5-19). The error and cumulative error plots show a reasonably stable error trend, with the exception of 1976, when the model significantly under estimated total flow. The slight over-estimation in the subsequent years occurs as the optimiser attempts to balance the overall simulation period.

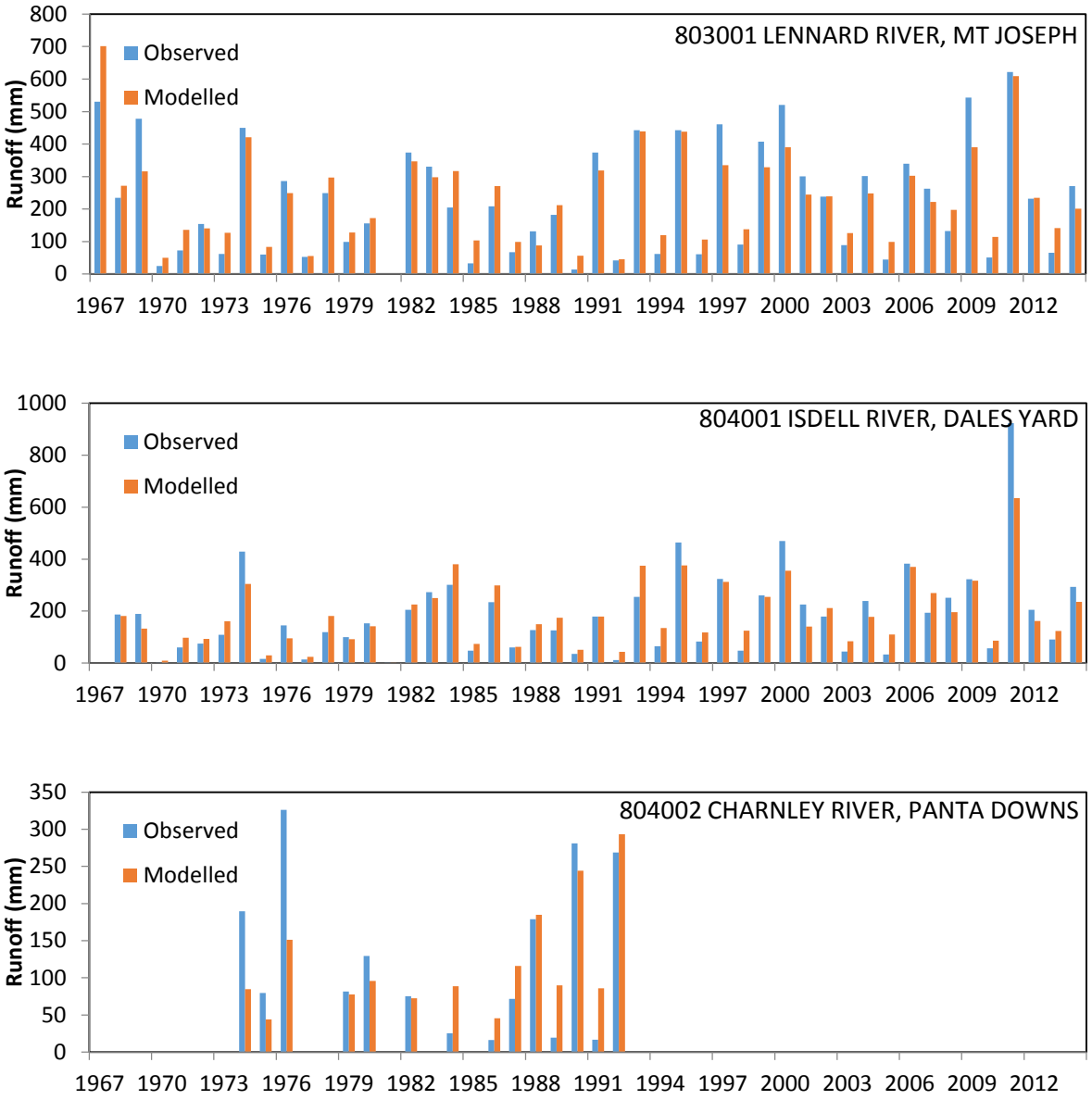

Figure 5-19. Annual observed and modelled flow for the three calibrated stations in the Walcott Inlet region.

An alternative test on the robustness of the model calibration is demonstrated by the 'double mass' plot of cumulative simulated flows against cumulative observed flows (Figure 5-21).

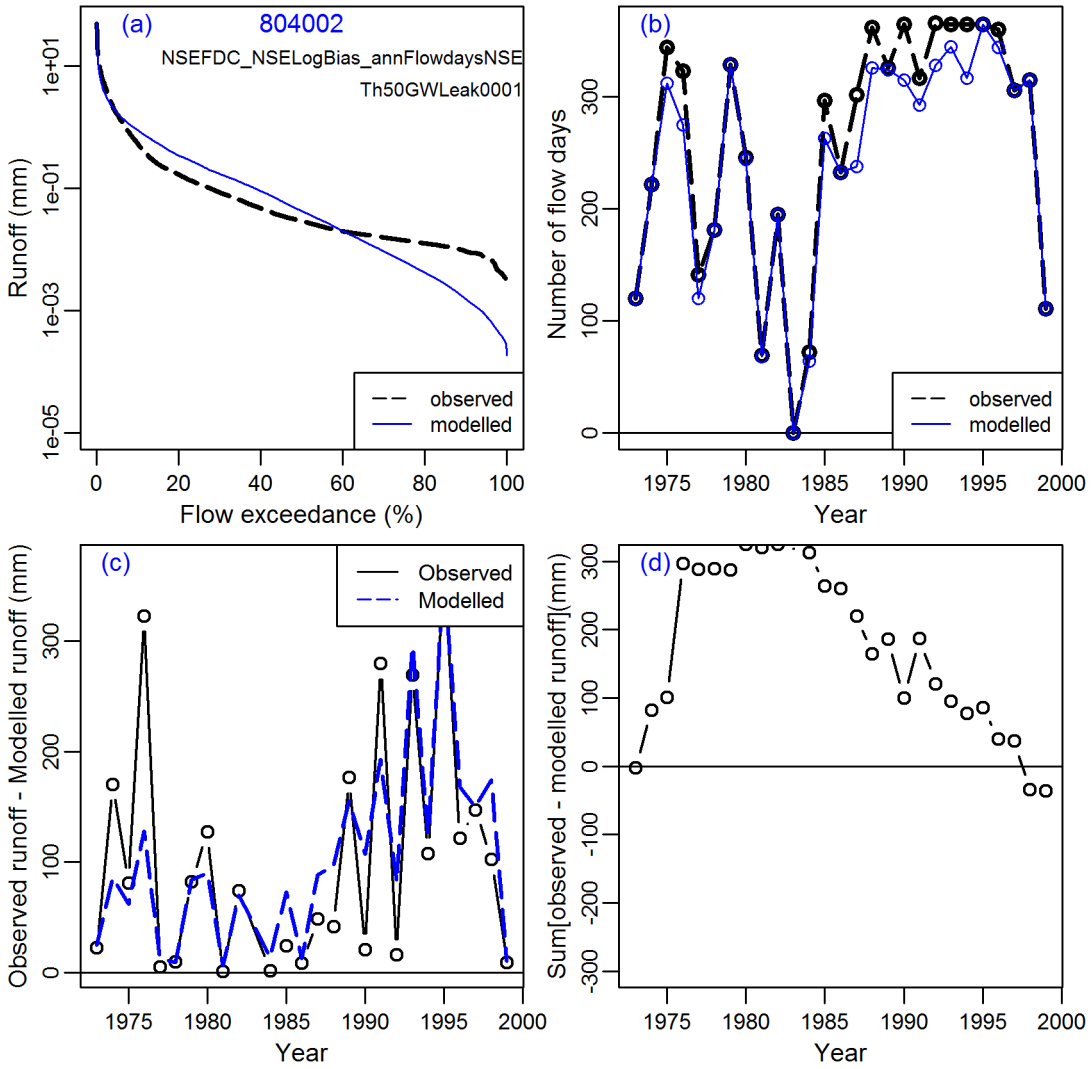

Figure 5-20. Diagnostic plot of calibration results for 804002 showing (a) flow duration curve (b) observed and modelled number of flow days (c) annual difference between observed and modelled runoff with moving average (d) cumulative error given by difference in annual observed and modelled runoff. The text in panel (a) indicates that the selected objective function was the arithmetic average of the NSE of the daily Flow Duration Curve (FDC), the daily NSE, and the NSE of annual number of days of flow, and indicates the initial parameter bounds given to the optimiser.

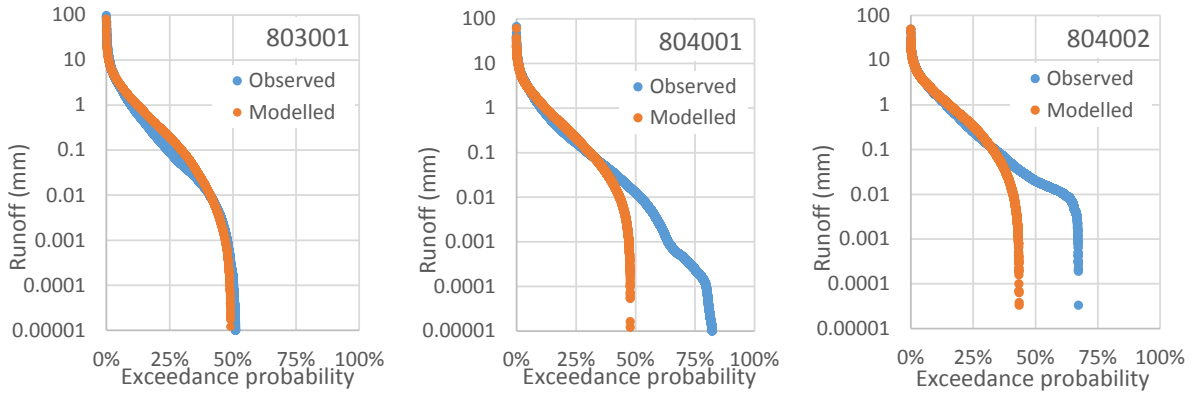

Figure 5-21. Simulated and observed daily runoff duration curves for the three gauges illustrating the good fit for the higher flow levels. Deviation for lower flows affects duration of flow but does not have a major influence on stream flow volumes

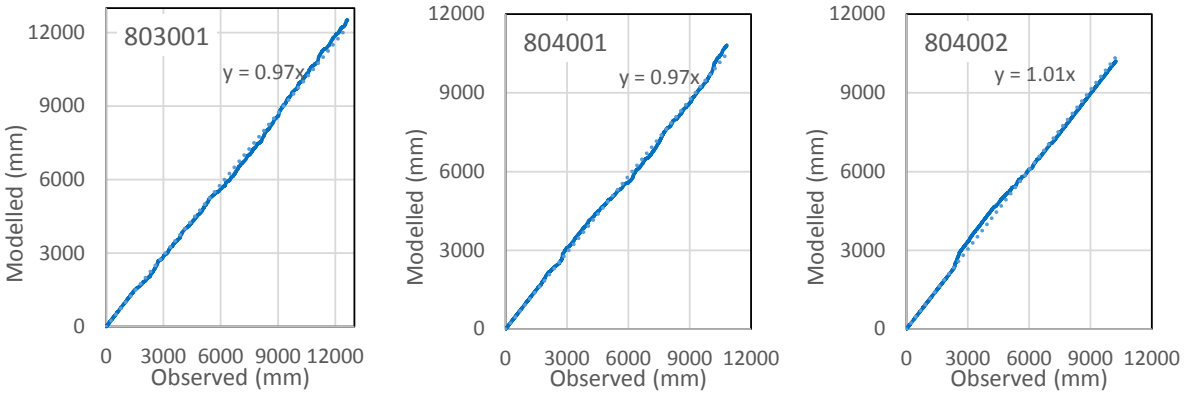

Figure 5-22. Double mass plot showing the cumulative simulated flows against the cumulative observed flows for the three catchments.

5.2 Simulated inflow to Walcott Inlet

5.2.1 Simulating the historical inflows

The calibrated model has been used to simulate river flow into the Walcott Inlet for the water years 1961 to 2014 (Figure 5-22a). This includes the period of the estuarine field surveys in October, 2013, and March, 2014 (Figure 5-22b). These daily flows are fed into both the estuarine hydrodynamic and BGC models to simulate the aquatic environment.

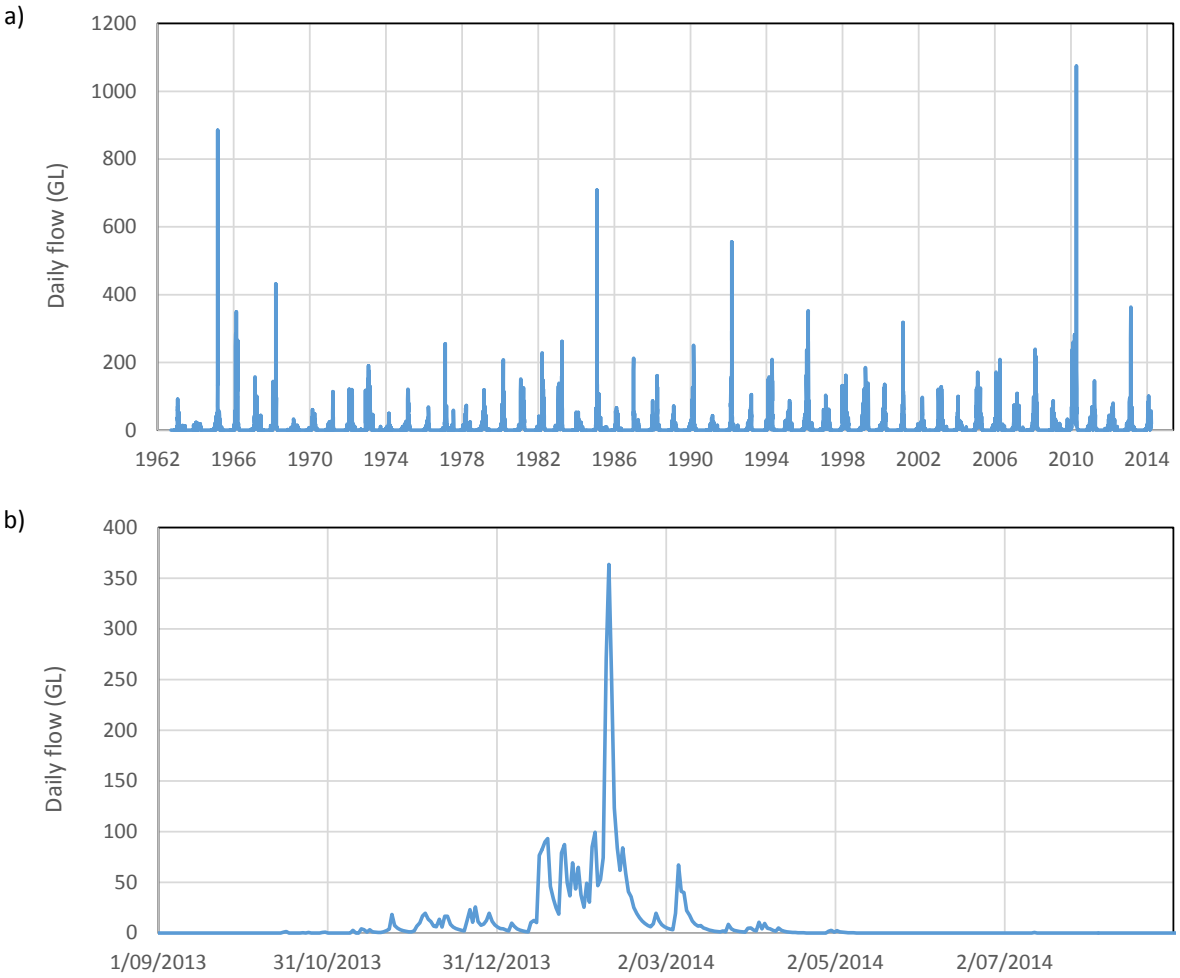

Figure 5-23. (a) Simulated streamflow into Walcott Inlet based on the calibrated SIMHYDGW model, and (b) the stream flow for the period including the estuarine field work.

5.2.2 Simulation inflow WQ sequences

To simulate water quality parameters for modelled flows, statistics extracted from the analysis above were applied to the model simulated flows, on a flow weighted basis. For each of the statistical bins analysed, presented above in Figure 5-11 to Figure 5-17, a flow—parameter relation was established and it was assumed that these relationships hold for the entire simulated flow period. Where possible relationships for the Walcott streams were used, but most data were available for the Fitzroy and hence a combination were used with contributing streams to the Fitzroy included to expand the data set. The same relationships were also used for the future climate projections presented later, as we have no evidentiary basis on which to vary them.

Table 5-5. Summary of simulated nutrient flow to Walcott Inlet.

	Flow (Annual)	**N Load (Annual)**	**P Load (Annual)**
	GL	**Tonne**	**Tonne**
Mean	**3,180**	1,163	100
Stdev	**1,778**	849	90
Min	**675**	180	9.7
10th percentile	**1,401**	395	24.0
25th percentile	**1,872**	570	40.1
Median	**2,772**	930	65.8
75th percentile	**4,088**	1,707	148.8
90th percentile	**5,287**	2,106	204.4
Max	10,613	5,041	529.3

The hydrological modelling outputs of flow and water quality parameters have been input to the estuarine hydrodynamic models as boundary condition inflows.

5.2.3 Future climate scenarios

The future climate projections developed as outlined in Section 3.1.1 have been examined and approximately one third project little or no change in rainfall over the next 50 years, one third project a reduction in rainfall and one third project an increase. To accommodate these disparate results three representative future projections were selected, namely, a low rainfall, median and high rainfall scenario, where the low and high rainfall scenarios are the second lowest and second highest rainfalls from the 18 climate sequences averaged over the Kimberley. It is important to recognise that each GCM has its own cell location and size, and that there are regional differences in the projections both between and within GCMs. As a consequence, if focus was on a particular part of the region, a different GCM sequence may be selected for any of these representations. For commonality of comparison, this assessment has been made on the climate averaged over the entire Kimberley region. The scenarios selected are given in Table 5-6 and the resulting influence on Walcott Inlet inflow is given in Table 5-7.

Table 5-6. Rainfall from the three selected GCMs used for the representative future climates and the Historical rainfall for comparison. The ratios of climate projection to the mean Historical rainfall are shown in parentheses.

Scenario	GCM	Average annual rainfall (mm)	Minimum Annual Rainfall (mm)	Maximum Annual Rainfall (mm)
Historical	-	1,031 (100%)	534 (52%)	2,058 (200%)
Dry Future	HadGEM2-ES	987 (96%)	501 (49%)	2,070 (201%)
Mid Future	CanESM2	1,045 (101%)	519 (50%)	2,199 (213%)

Wet Future	MIROC-5	1,104 (107%)	572 (55%)	2,209 (214%)

Table 5-7. Total stream flow into Walcott Inlet under the three selected GCMs used for the representative future climates. The ratios of climate projection to the mean Historical rainfall are shown in parentheses.

Scenario	GCM	Average annual inflow (GL)	Minimum Annual Inflow (GL)	Maximum Annual Inflow (GL)
Historical	-	3,206 (100%)	675 (21%)	10,316 (322%)
Dry Future	HadGEM2-ES	2,931 (91%)	589 (18%)	10,603 (331%)
Mid Future	CanESM2	3,357 (105%)	623 (19%)	12,105 (378%)
Wet Future	MIROC-5	3,584 (112%)	770 (24%)	11,742 (366%)

5.3 Characterising Estuary and Bay Hydrodynamics

Here we determine how water exchange and mass transport occurs between the shallower inshore water in Collier Bay and the deeper offshore water occurs through three channels separated by islands and reefs using the ROMS circulation model (Figure 3-33).

5.3.1 Model evaluation

ROMS was validated against sea surface height (SSH), temperature (T) and salinity data collected by the three moorings shown in Figure 2-5. ROMS captured the variations of SSH (data at the middle mooring has not been presented as the pressure sensor failed), temperature and salinity very well (Figure 5-24 and Figure 5-25). In particular, ROMS simulated the sharp drop of salinity (from about 34.5 psu to 29.8 psu) at the inner mooring due to the peak freshwater inflow into the bay, which matched well with the measurement (dropped from about 34. 8 psu to 29.1 psu). The statistics in Table 5-8 also confirmed that the temperature and salinity simulated by ROMS agreed well with the mooring measurements.

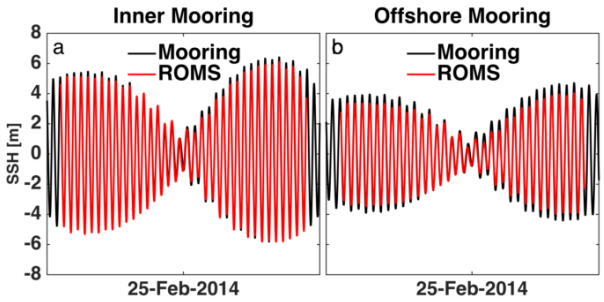

Figure 5-24. Sea surface heights simulated by ROMS (black) compared with measurements (red) during a wet season spring-neap cycle at (a) inner mooring and (b) offshore mooring.

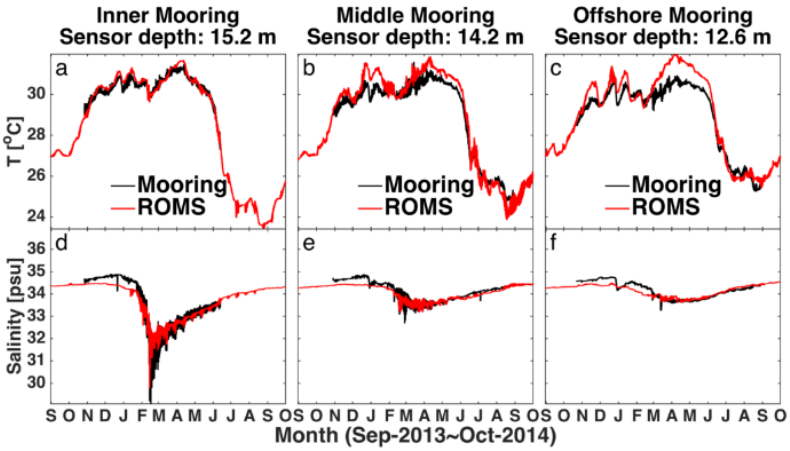

Figure 5-25. Temperature (upper panel) and salinity (lower panel) simulated by ROMS (black) compared with measurements (red) at the inner mooring (a & d), middle mooring (b & e) and offshore mooring (c & f).

Table 5-8. Model data agreement with field measurements at the three moorings, indicated by the centred Root Mean Square difference (E) and the correlation coefficient (R).

		Inner	Middle	Offshore
Temperature	Centred RMS difference (E, ℃)	0.201	0.421	0.466
	Correlation coefficient (R)	0.966	0.991	0.979
Salinity	centred RMS difference (E, psu)	0.305	0.154	0.174
	Correlation coefficient (R)	0.980	0.957	0.891

ROMS was also validated with shipboard thermosalino-graph data (temperature and salinity) sampled at 2.8 m below the sea surface during a dry season cruise in October 2013 and a wet season cruise in March 2014 (not shown here), demonstrating that ROMS was able to reproduce the density field in both the dry and wet seasons, and in particular the salinity field in the wet season.

5.3.2 Results and Discussion

The Eulerian decomposition reveals that the mechanisms driving the salt flux differed between North Channel and Walcott Inlet. At North Channel the advective salt flux was the dominant component and the other two Eulerian salt flux components were negligible (Figure 5-26, notice the different scales in the panels). In contrast, at Walcott Inlet the advective salt flux was the same order as the other two salt fluxes (Figure 5-27). Results of the isohaline decomposition (Figure 5-28 and Figure 5-29) shows that at North Channel and Walcott Inlet, the variation of both the upgradient salt flux and downgradient salt flux was largely influenced by the freshwater inflow. At North Channel, the upgradient flux-weighted salinity varied at the same rate as the downgradient flux-weighted salinity, indicating a well-mixed condition in the channel. At Walcott Inlet, the upgradient flux-weighted salinity dropped much more dramatically than the downgradient flux-weighted salinity, indicating that the buoyancy introduced by the peak freshwater inflow was sufficient to maintain a strong vertically stratified condition at the estuary for that short period of time. The salinity at the cross section for the upgradient fluxes show lower salinity because these fluxes are directed from the interior of the bay towards the open ocean.

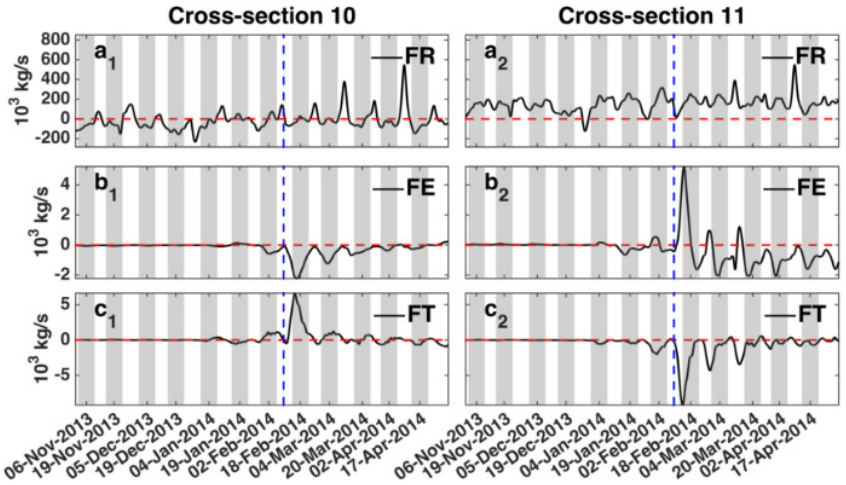

Figure 5-26. Eulerian salt flux components across cross-section 10 (left column) and 11 (right column) at North Channel. $a_{1,2}$: Advective salt flux (FR). $b_{1,2}$: Steady shear dispersion salt flux (FE). $c_{1,2}$: Tidal oscillatory salt flux (FT). Red dashed line indicates zero salt flux; blue dashed line indicates the date of the peak total river runoff (10-Feb-2014) as shown in Figure 3-34. Shaded panels (7 days in width) indicate spring tides.

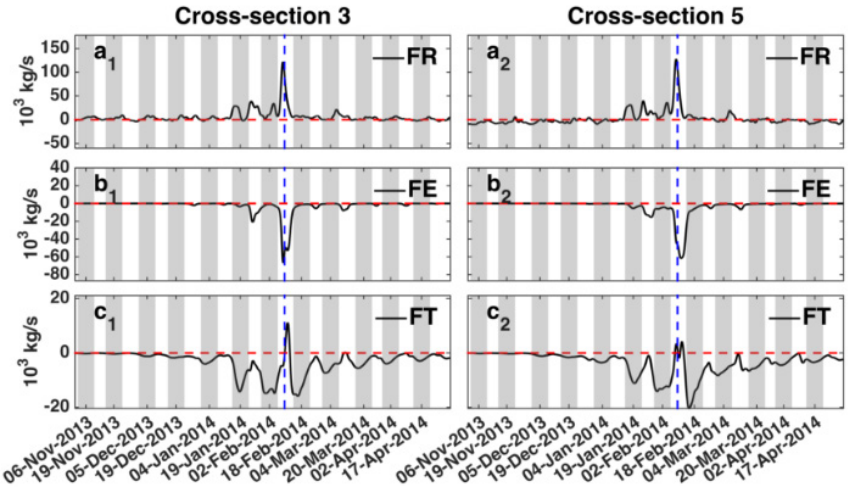

Figure 5-27. Eulerian salt flux components across cross-section 3 (left column) and 5 (right column) at Walcott Inlet (notations as in Figure 5-26).

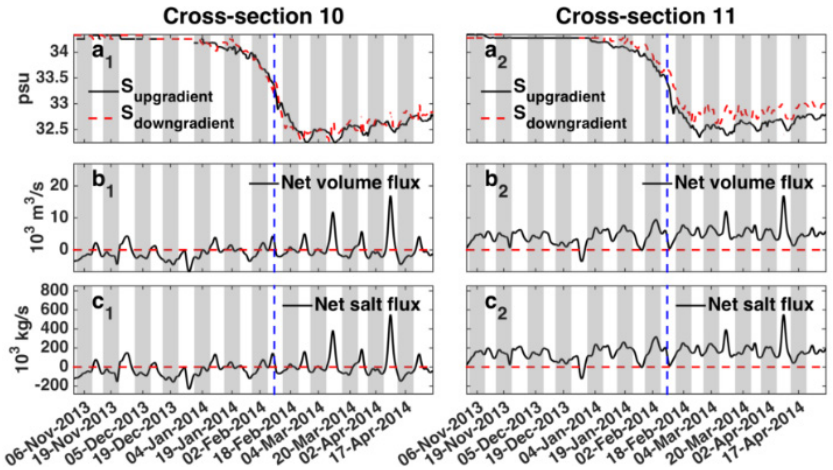

Figure 5-28. Isohaline salt flux components across cross-section 10 (left column) and 11 (right column) at North Channel. $a_{1,2}$: Flux-weighted salinity ($s_{up/downgradient}$). $b_{1,2}$: Net volume fluxes ($Q_{upgradient} - Q_{downgradient}$); $c_{1,2}$: Net salt fluxes ($F_{upgradient} - F_{downgradient}$). Blue dashed line indicates the date of the peak total river runoff (10-Feb-2014) as shown in Figure 3-34. Shaded panels (7 days in width) indicate spring tides.

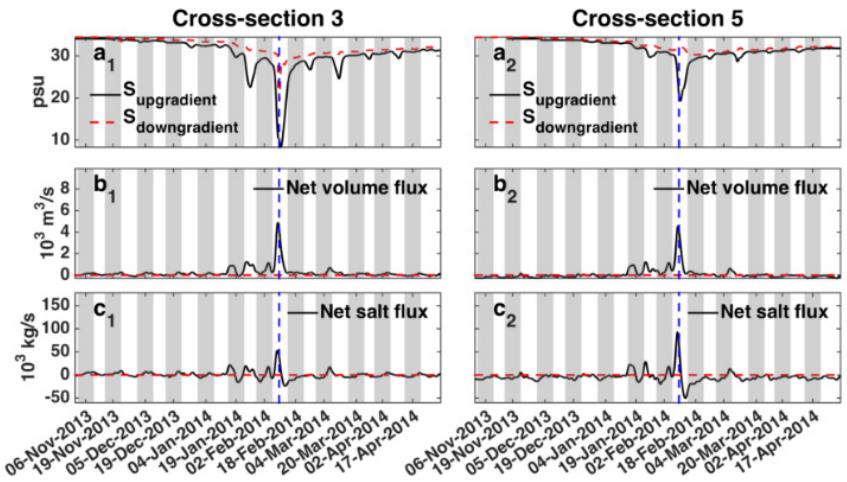

Figure 5-29. Isohaline salt flux components across cross-section 3 (left column) and 5 (right column) at Walcott Inlet (notations as in Figure 5-28).

North Channel is bordered by Montgomery Reef. To study the influence of this shallow region on exchange through North Channel we compared the salt flux across the deep part of the channel (cross-section 10, Figure 5-26) to a cross-section that extends further to include a shallow section over Montgomery Reef (cross-section 11, Figure 5-26). Firstly, Eulerian decomposition results at North Channel (Figure 5-28) show that the dominant advective salt flux at cross-section 10 (deep part of channel) fluctuated between upgradient (positive) and downgradient (negative); while the advective salt flux at cross-section 11 (including Montgomery Reef section) was generally upgradient throughout the entire wet season. The net salt fluxes derived from the isohaline decomposition concurred (Figure 5-28c). Secondly, directions of steady shear dispersion salt flux and tidal oscillatory salt flux at cross-section 10 were downgradient and upgradient, respectively, the reverse was observed at cross-section 11. Thirdly, although North Channel was well-mixed, as indicated by the upgradient and downgradient flux-weighted salinity at both cross-sections ($a_{1,2}$ in Figure 5-28), the difference between the upgradient and downgradient flux-weighted salinity at cross-section 11 was more evident than that at cross-section 10. In summary, freshwater and ocean water was not as well mixed in the shallow part of North Channel over Montgomery Reef, contributing to the upgradient net salt flux at North Channel.

In Walcott Inlet, the topography varies in the longitudinal direction, differing from that in North Channel. The Eulerian salt fluxes at the shallower cross-section 3 behaved similarly to those at the deeper cross-section 5 (Figure 5-27), but very differently from those at North Channel. As mentioned above, the advective salt flux at Walcott Inlet was not a dominant component, but it was the major upgradient component. In contrast, both the steady shear dispersion salt flux and the tidal oscillatory salt flux were downgradient, with the exception that the latter reversed quickly during peak river runoff. The isohaline decomposition results show that periodic vertical stratification was established in Walcott Inlet as the upgradient flux-weighted salinity dropped more dramatically than the downgradient flux-weighted salinity ($a_{1,2}$ in Figure 3-38), especially when the estuary was flooded by the peak freshwater inflow. The net volume flux and net salt flux ($b_{1,2}$ and $c_{1,2}$ in Figure 5-27) indicated a general balance through the entire wet season, with only a sharp fluctuation towards upgradient fluxes due to the peak freshwater inflow. The stratification then weakened dramatically and the salt balance was quickly restored to a similar level prior to the peak freshwater inflow as the upgradient flux-weighted salinity started to increase immediately after the river inflow decreased.

Figure 5-30 compares the differential isohaline volume fluxes parameterized by Eq. 6 along the longitudinal-axis of Walcott Inlet on a spring tide and a neap tide after the peak freshwater inflow when the flow rate had greatly declined, representative of the majority of the wet season. On the spring tide, the differential volume flux with salinity below 28 was mostly trapped in Walcott Inlet, especially in the shallow part between cross-section 1 and 3 (Figure 5-30a). On the neap tide, there was a stronger upgradient volume flux from upstream of Walcott Inlet into Collier Bay, of which the salinity range varied between 22~26 and 29~31.5, indicating continuous mixing with ocean water along the path (Figure 5-30b). Figure 530a). On the neap tide, there was a

stronger upgradient volume flux from upstream of Walcott Inlet into Collier Bay, of which the salinity range varied between 22~26 and 29~31.5, indicating continuous mixing with ocean water along the path (b). Figure 530a). On the neap tide, there was a stronger upgradient volume flux from upstream of Walcott Inlet into Collier Bay, of which the salinity range varied between 22~26 and 29~31.5, indicating continuous mixing with ocean water along the path (b). Figure 530a). On the neap tide, there was a stronger upgradient volume flux from upstream of Walcott Inlet into Collier Bay, of which the salinity range varied between 22~26 and 29~31.5, indicating continuous mixing with ocean water along the path (b).

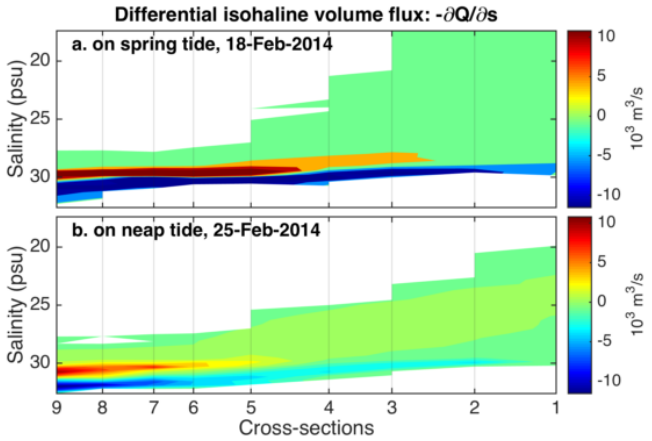

Figure 5-30. Differential isohaline volume fluxes ($-\frac{\partial Q}{\partial s}$) at Walcott Inlet tide after the peak inflow on (a) a spring tide and (b) a neap tide.

5.3.3 Summary

The net salt flux was different at each of the three channels connecting Collier Bay to the surrounding ocean (not shown). The net salt flux through the southern channel was downgradient, while the net salt flux through the other two channels was upgradient. The upgradient flux was stronger at North Channel than at the middle channel. Thus, Collier Bay received salt from the ocean through the southern channel while being diluted through the middle and North Channels. Note that the southern channel is the deepest among the three channels (Figure 3-4). This understanding of the salt fluxes, reveals the patterns of scalar transport within the Bay/ Estuary system which aids our interpretation of the more complex reactive components in the BGC model described in the following section.

5.4 Characterising Estuary and Bay Biogeochemistry

5.4.1 Model assessment

General spatial patterns along the gradient from Walcott Inlet and the other embayments to outer Collier Bay are depicted in Figure 5-31 and Figure 5-32 for the dry season and wet season, respectively. Limited flow in the dry season has only a minor influence within the eastern limit of Walcott Inlet. In contrast, the wet season flows are able to significantly influence Walcott Inlet, Secure Bay and Doubtful Bay, bringing them below 25psu during flow peaks, and diluting Inner Collier Bay to ~30 psu. The results are consistent with those of the ROMS simulations reported in section 5.3 and report for KMRP Project 2.2.1 for the main Collier Bay region, and in addition provide a clear indication of salinity variation in the upstream estuarine portion of Walcott Inlet, Secure Bay and Doubtful Bay, due to high-resolution of the domain in these regions.

The pattern predicted for suspended solids is somewhat different to that of salinity, due to the relatively high levels of resuspension. The high tidal range drives large current velocities that exceed the threshold bed critical shear stress for resuspension of particulates within several regions of the domain. This is in addition to the relatively high loads of turbidity entering from the river inputs. Since the river inputs are higher in the wet season there is a relatively higher concentration of suspended material during this season (exceeding 30 mg/L).

Comparing cross section plots through Walcott Inlet into the main embayment for the wet and dry season demonstrate the changing extent of salinity, suspended solids, and also nutrients, due to riverine inputs (Figure 5-33). In the dry season horizontal gradients in salinity are largely absent however notable variation is seen in the water quality attributes including the suspended solids, DON, NO_3 and Chl-a. In the wet season, the salinity variation becomes notable, however, it is predicted to have a surprisingly limited effect on the gradients in nutrients. In the upstream portion of Walcott Inlet, suspended solids increased during the flow period, and the dilution and light limitation had a corresponding negative impact on the chlorophyll biomass. See: http://www.wamsi.org.au/news/kimberley-coastal-system-links-land-deep-sea for animations of the system.

Despite the limited data available for model setup and assessment, the model overall performed reasonably well in resolving salinity, turbidity and nutrients when compared against the two cruise datasets. In general, the mean concentrations, horizontal variation away from the coast, and seasonal differences (where relevant) were reproduced in all of the measured variables (S, SS, PO_4, NO_3, NH_4, DON, DOP, DOC, POC, Chl-a), as shown in Figure 5-34 - Figure 5-37 and Table 5-7. The model tended to under-predict the POC concentrations, and didn't fully capture the sharp transition in SS from the inner to outer bay (at -20 km chainage), as is reflected in the relatively high bias (PRE) and other metrics for these variables. These errors are likely due to inadequate parametrisation of the resuspension and sedimentation rates for these particulate variables, and lack of any spatial resolution of benthic sediment distribution within the model. Other attributes such as the inorganic and organic nutrients showed some errors that were most likely attributable to uncertainty in either the ocean and/or river inflow boundary condition value that was assigned, rather than a fundamental short-coming with the biogeochemical cycling within the model. Uncertainty in the assigned sediment flux rates may also have led to some of the error seen in the NO_3 prediction, given these have not been studied extensively in the region.

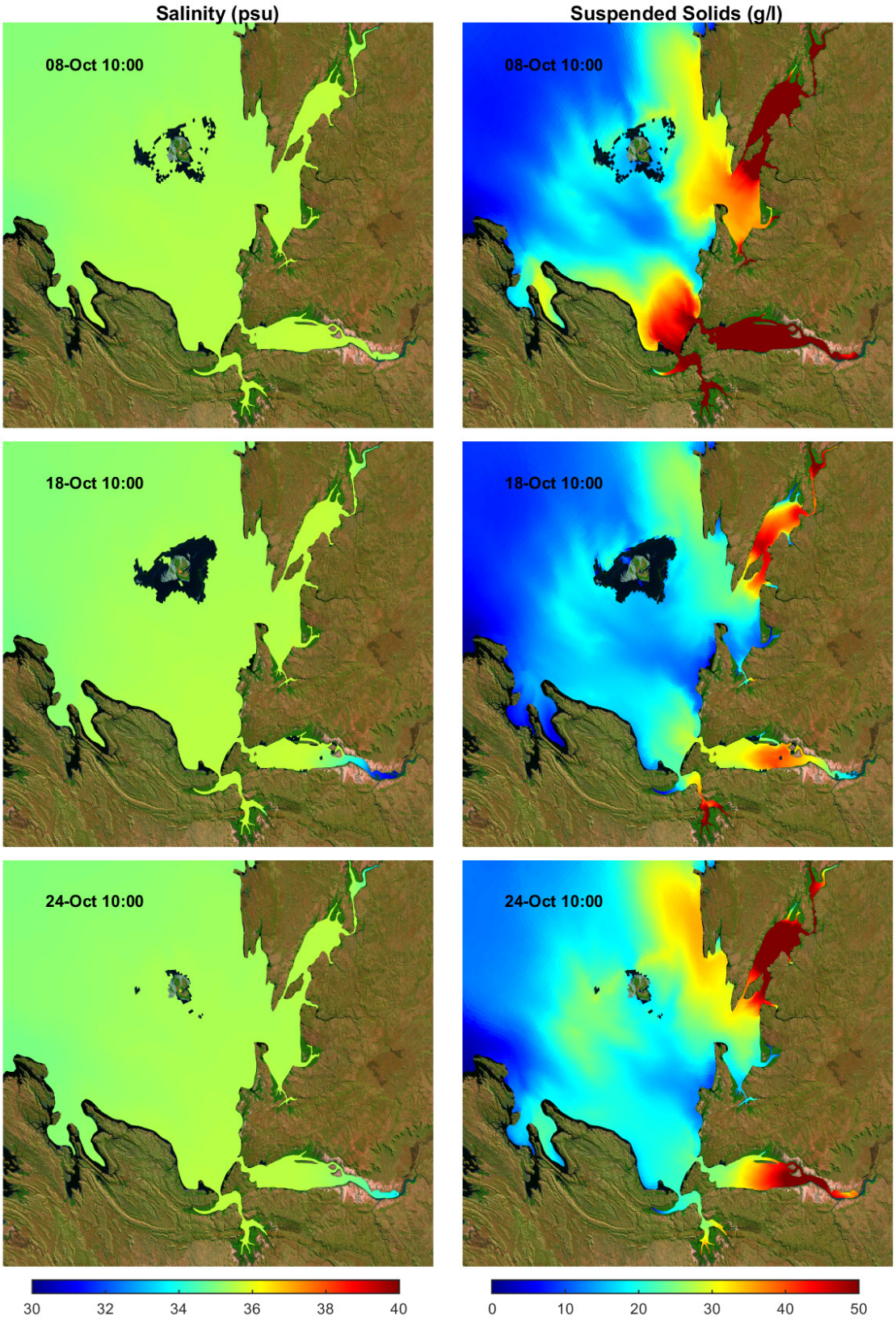

Figure 5-31. Plan view output from the FV-AED model for three dates in October 2013 (dry season), highlighting spatial variation in salinity (left) and suspended solids (right).

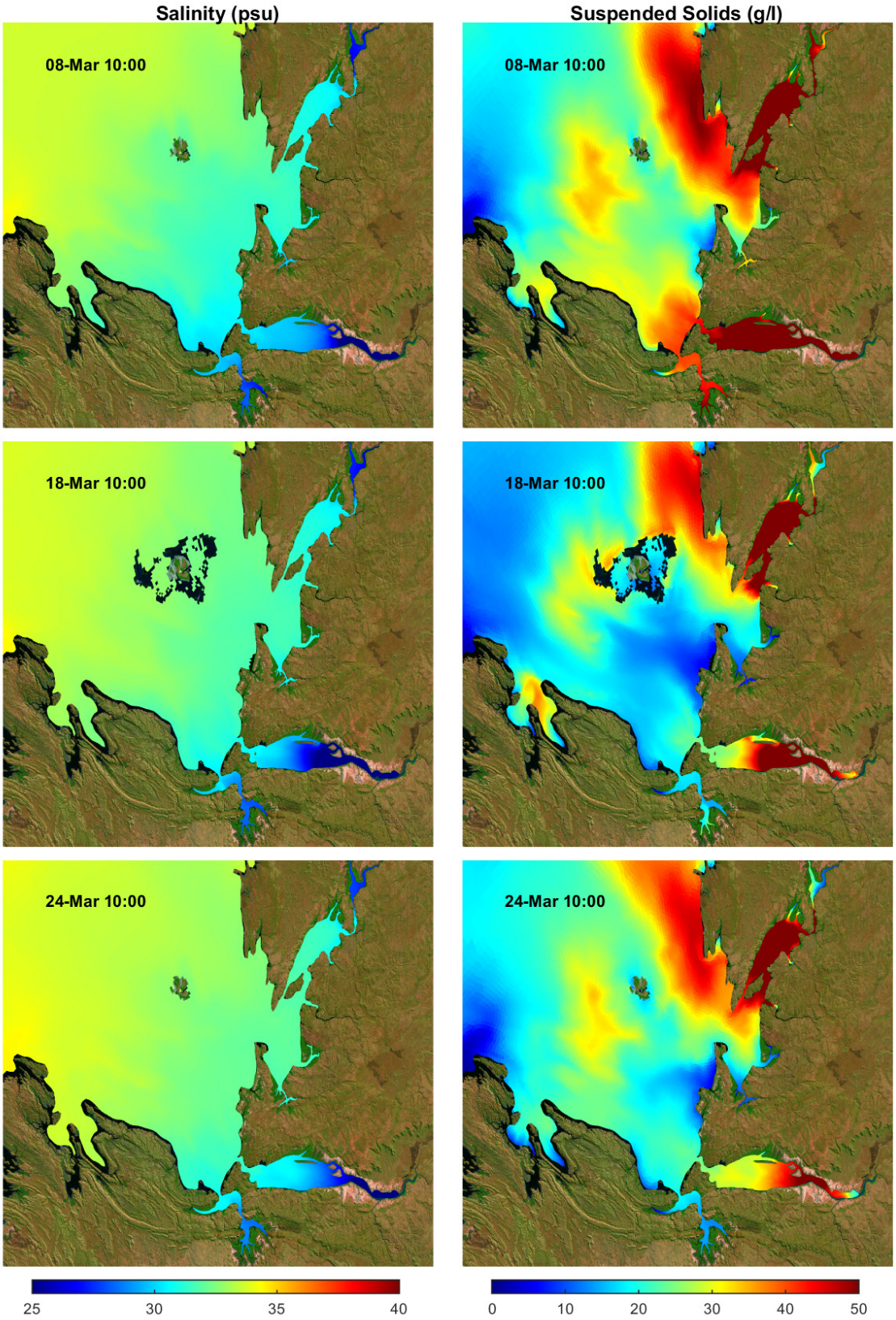

Figure 5-32. Plan view output from the FV-AED model for three dates in March 2014 (wet season), highlighting spatial variation in salinity (left) and suspended solids (right).

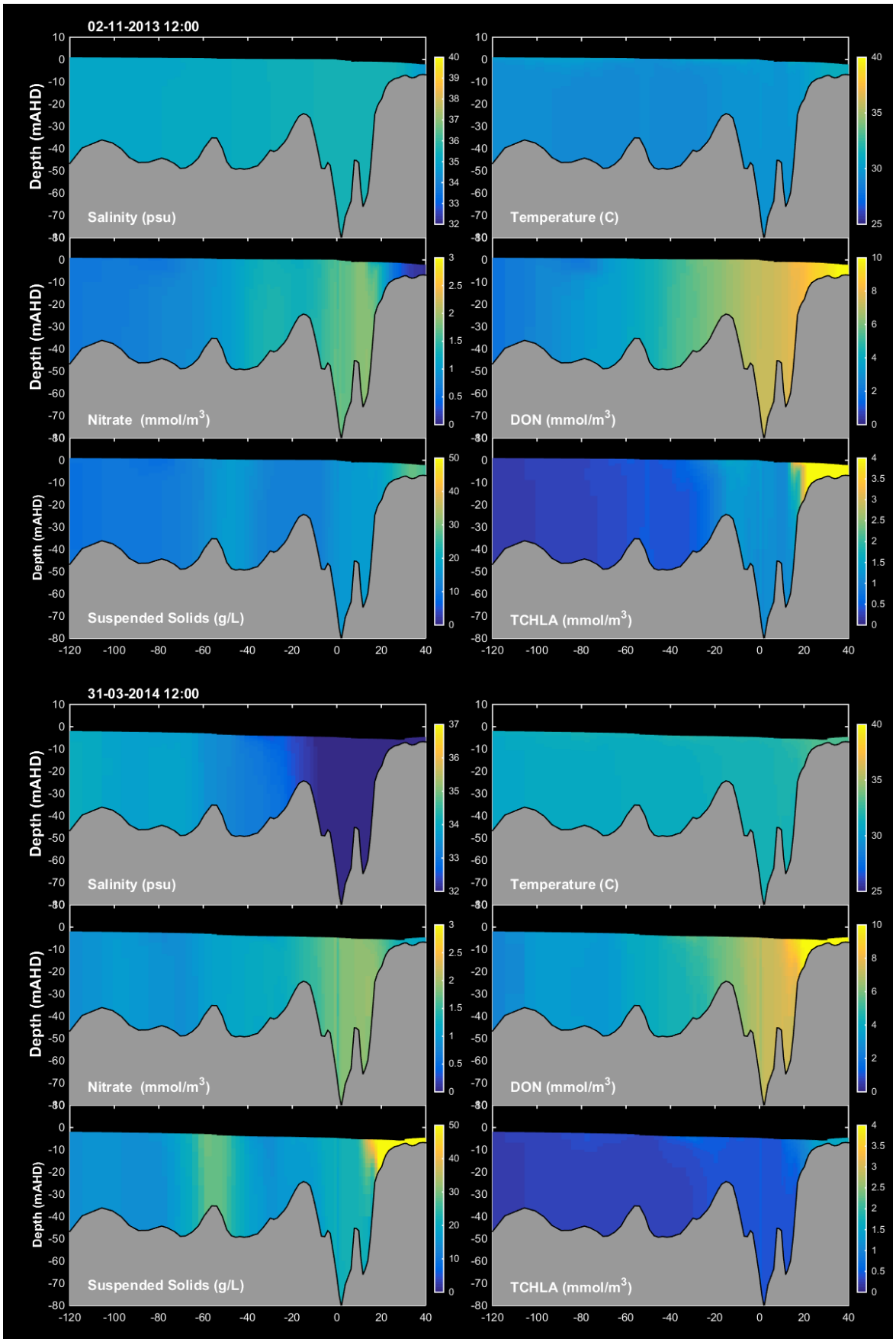

Figure 5-33. Cross section from within Walcott Inlet (right) to outer Collier Bay (left) for six main simulated variables (S, T, NO3, DON, SS, Chl-a), comparing typical dry season (top) and wet season (bottom) conditions. On the x axis 0 is the mouth

of Walcott Inlet and positive values (kms) are extending into Walcott Inlet, whist negative values (kms) extend into Collier Bay.

a)

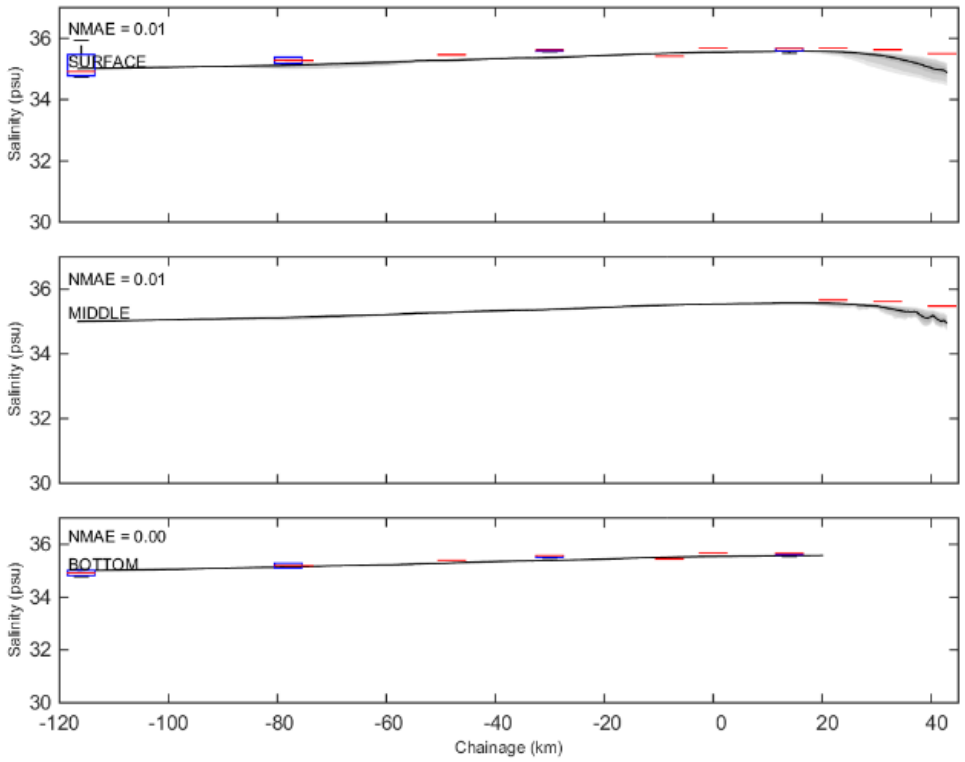

b)

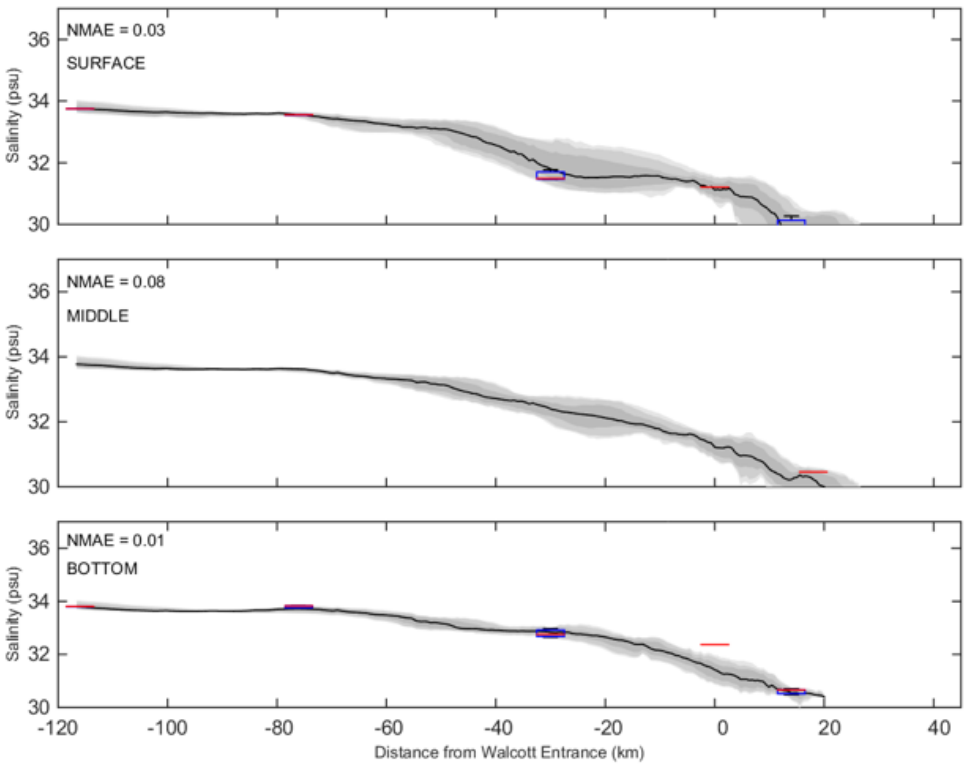

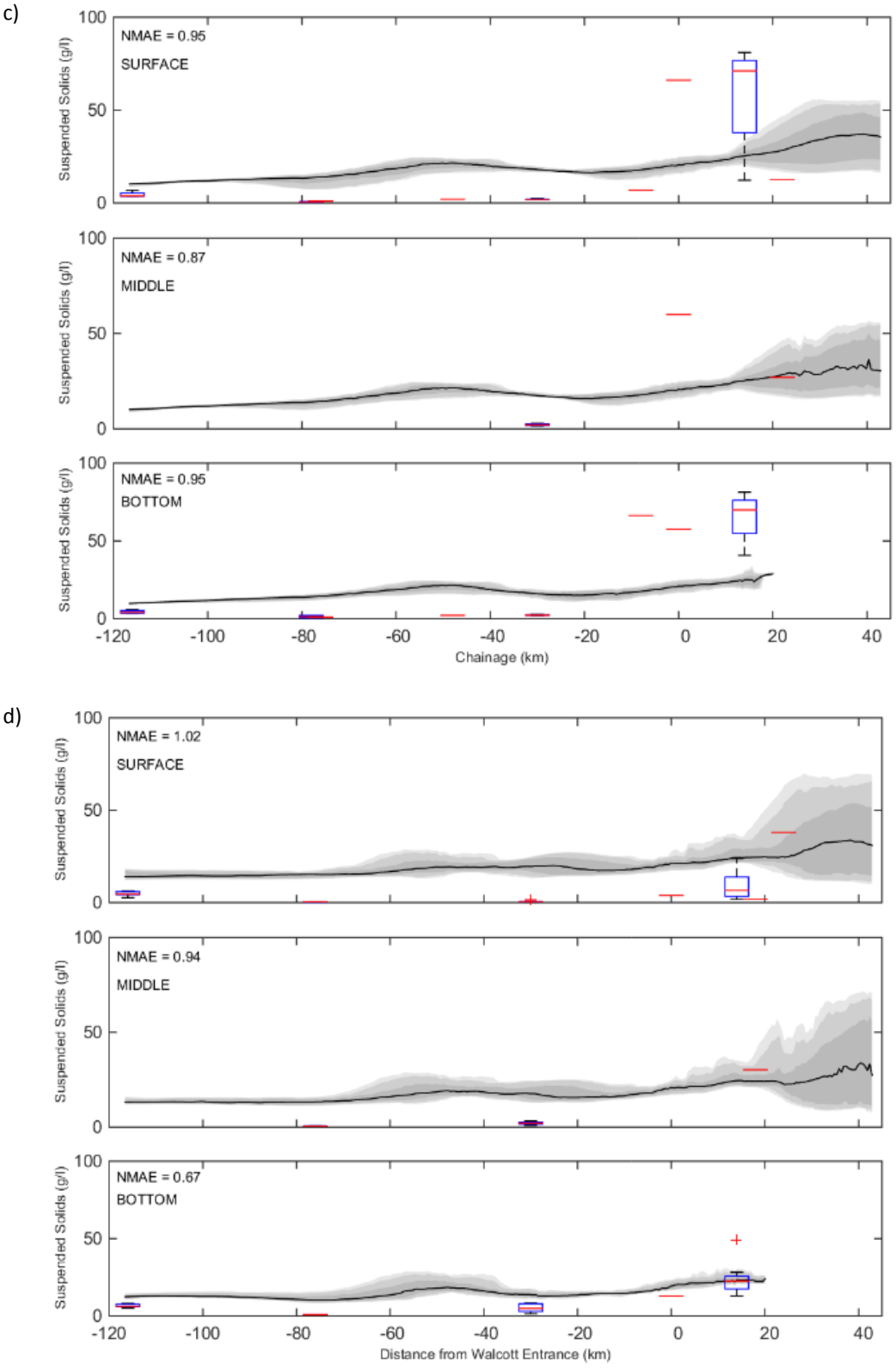

Figure 5-34. Comparison of model results of salinity (a,b) and suspended solids (c,d) against the October 2013 dry season (a,c) cruise data (KM5887) and the March 2014 wet season (b,d) cruise data (KM5938). Field data are represented as box plots (centred around the median, red dash is the mean, edges 25% and 75% percentiles, whiskers extend to the most extreme non outlier data points and outliers are represented as red crosses). Distance is measured as chainage (originating from the Walcott Inlet entrance). Grey shading around the model prediction (black) reflects the range of concentrations experienced at the model station over the relevant cruise/sampling period.

a)

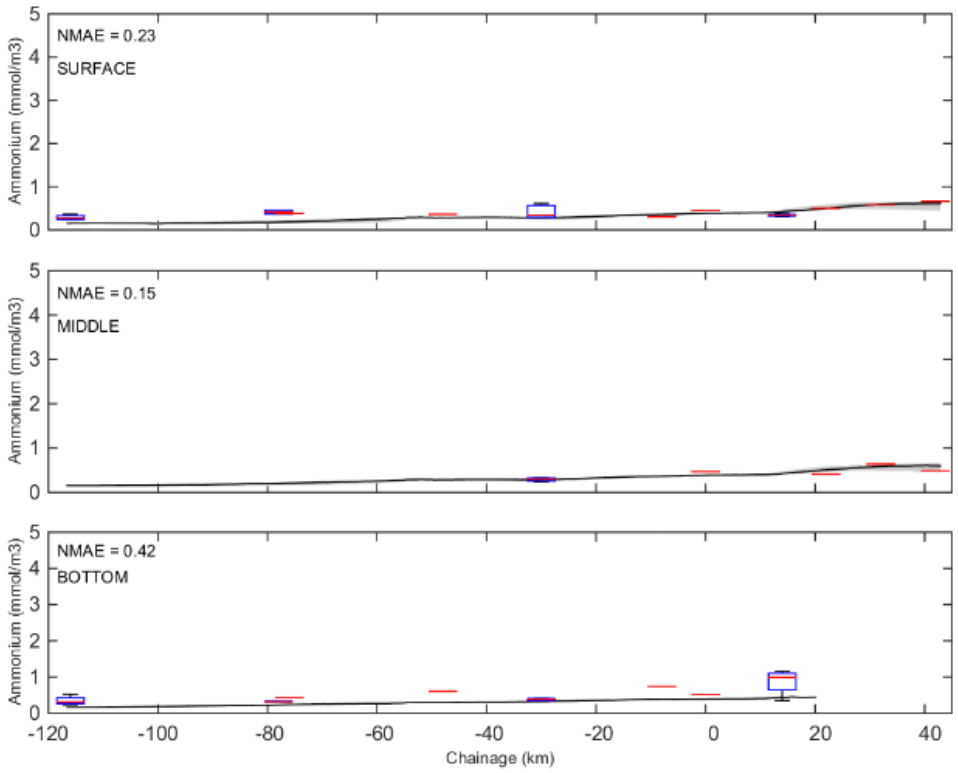
NMAE = 0.23
SURFACE
NMAE = 0.15
MIDDLE
NMAE = 0.42
BOTTOM
Ammonium (mmol/m3)
Chainage (km)

b)

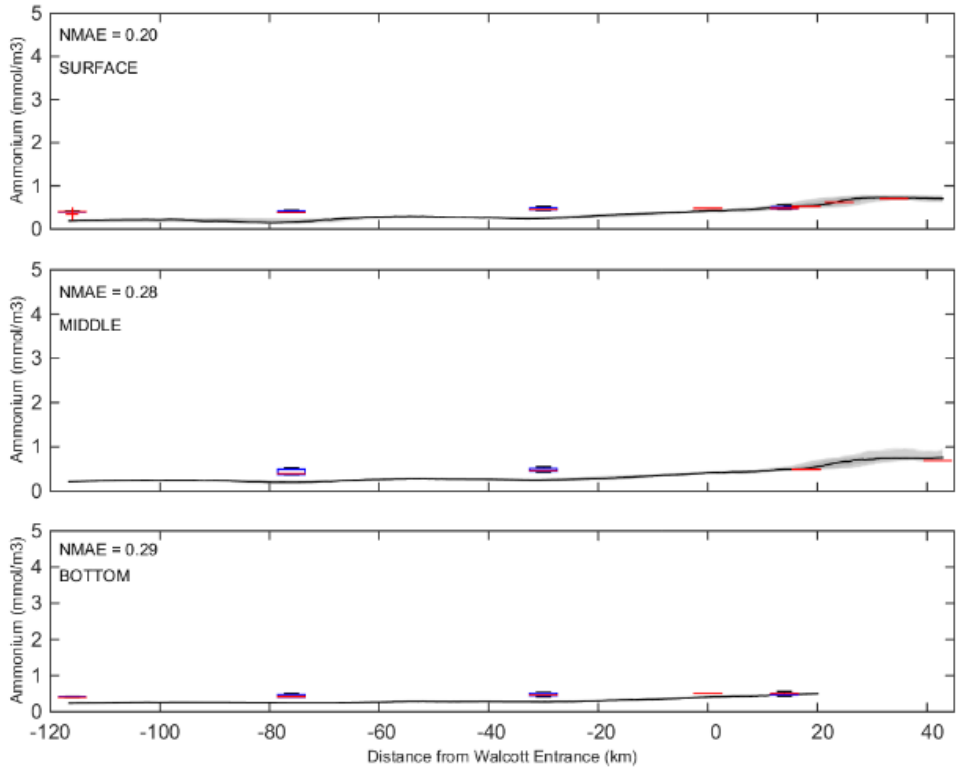
NMAE = 0.20
SURFACE
NMAE = 0.28
MIDDLE
NMAE = 0.29
BOTTOM
Ammonium (mmol/m3)
Distance from Walcott Entrance (km)

c)

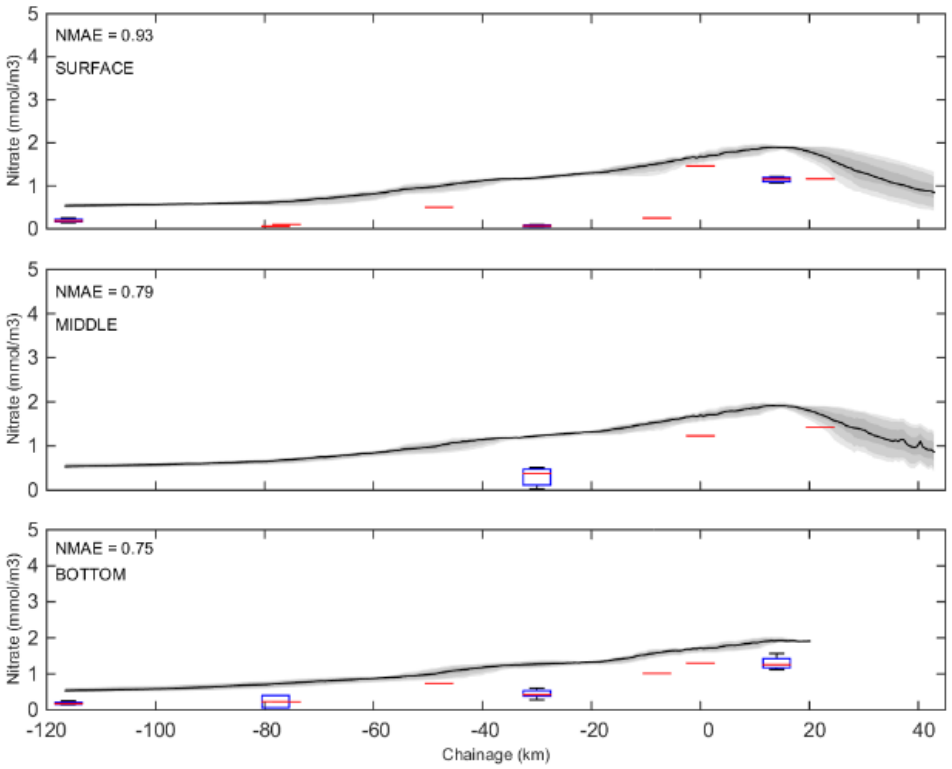
NMAE = 0.93
SURFACE
NMAE = 0.79
MIDDLE
NMAE = 0.75
BOTTOM
Nitrate (mmol/m3)
Chainage (km)

d)

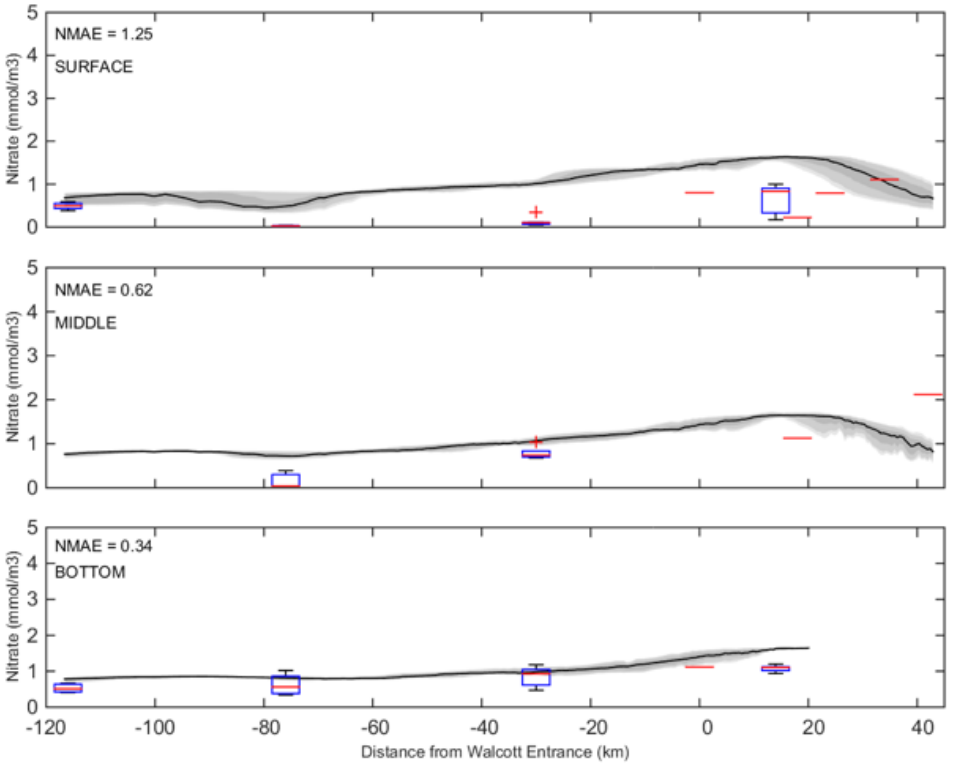
NMAE = 1.25
SURFACE
NMAE = 0.62
MIDDLE
NMAE = 0.34
BOTTOM
Nitrate (mmol/m3)
Distance from Walcott Entrance (km)

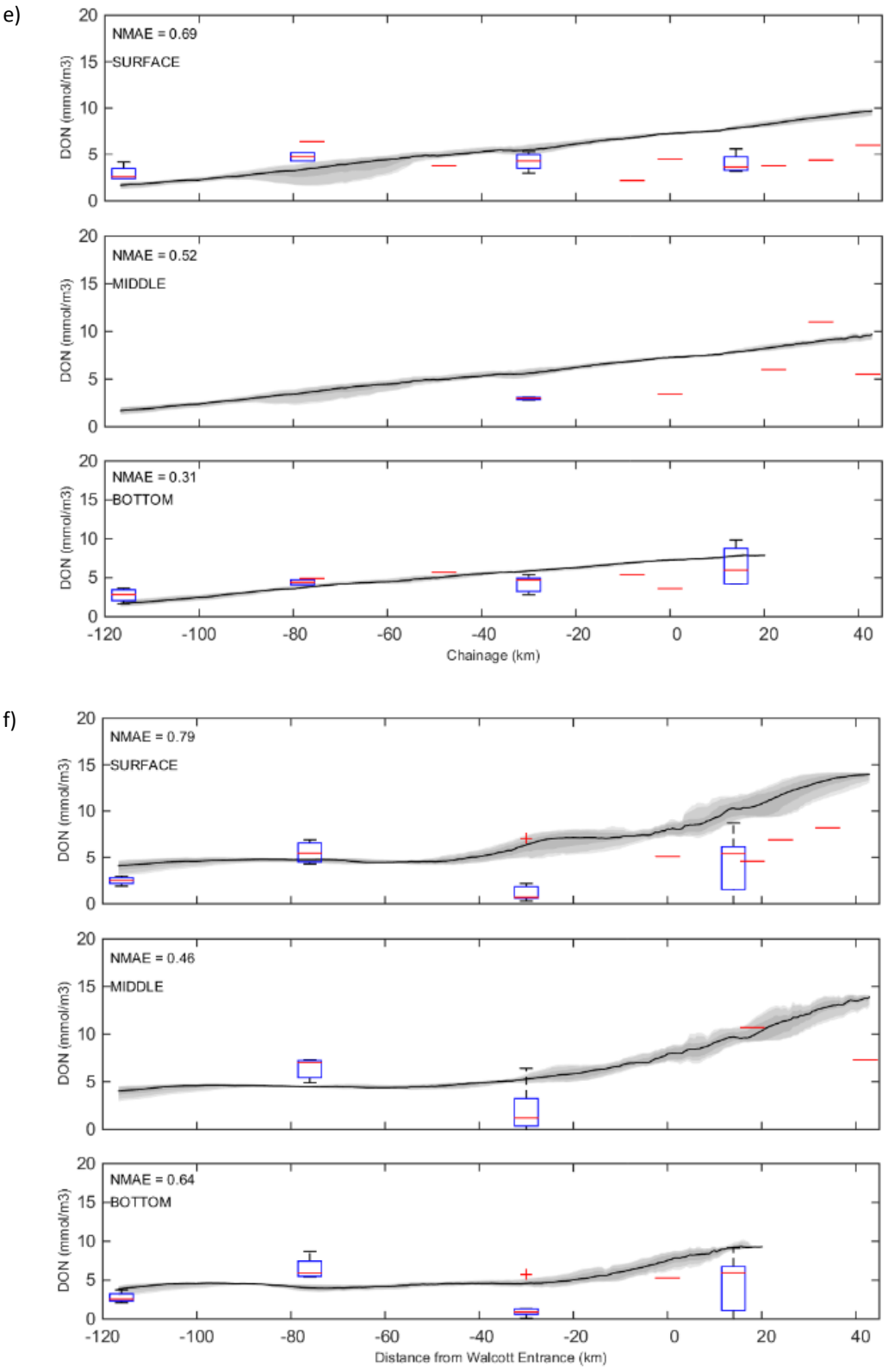

Figure 5-35. Comparison of model results of NH_4 (a,b), NO_3 (c,d) and DON (e,f) against the October 2013 dry season (a,c,e) cruise data (KM5887) and the March 2014 wet season (b,d,f) cruise data (KM5938). Field data are represented as box plots (centred around the median, red dash is the mean, edges 25% and 75% percentiles, whiskers extend to the most extreme non outlier data points and outliers are represented as red crosses). Distance is measured as chainage (originating from the Walcott Inlet entrance). Grey shading around the model prediction (black) reflects the range of concentrations experienced at the model station over the relevant cruise/sampling period.

a)

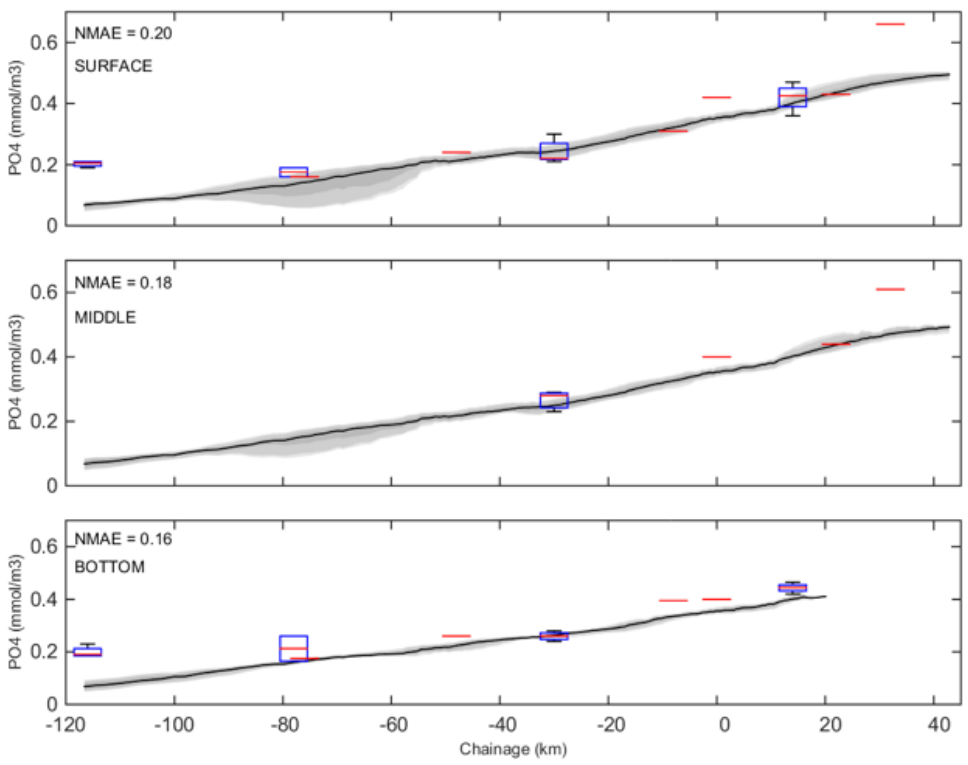
NMAE = 0.20
SURFACE
NMAE = 0.18
MIDDLE
NMAE = 0.16
BOTTOM
PO4 (mmol/m3)
0
0.2
0.4
0.6
-120
-100
-80
-60
-40
-20
0
20
40
Chainage (km)

b)

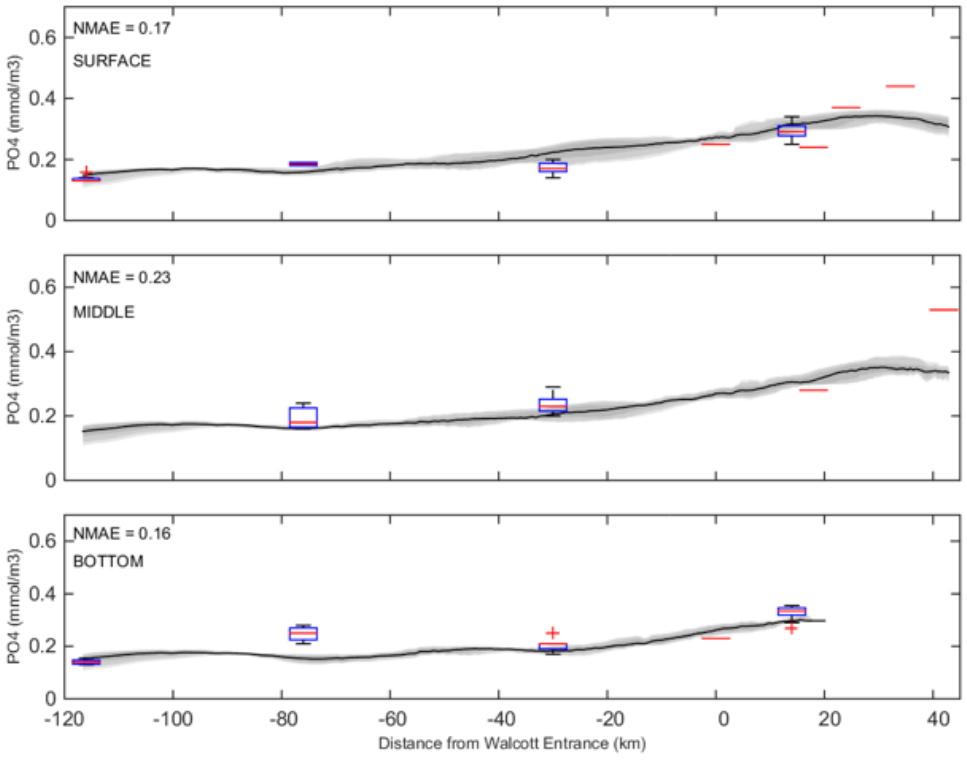
NMAE = 0.17
SURFACE
NMAE = 0.23
MIDDLE
NMAE = 0.16
BOTTOM
PO4 (mmol/m3)
0
0.2
0.4
0.6
-120
-100
-80
-60
-40
-20
0
20
40
Distance from Walcott Entrance (km)

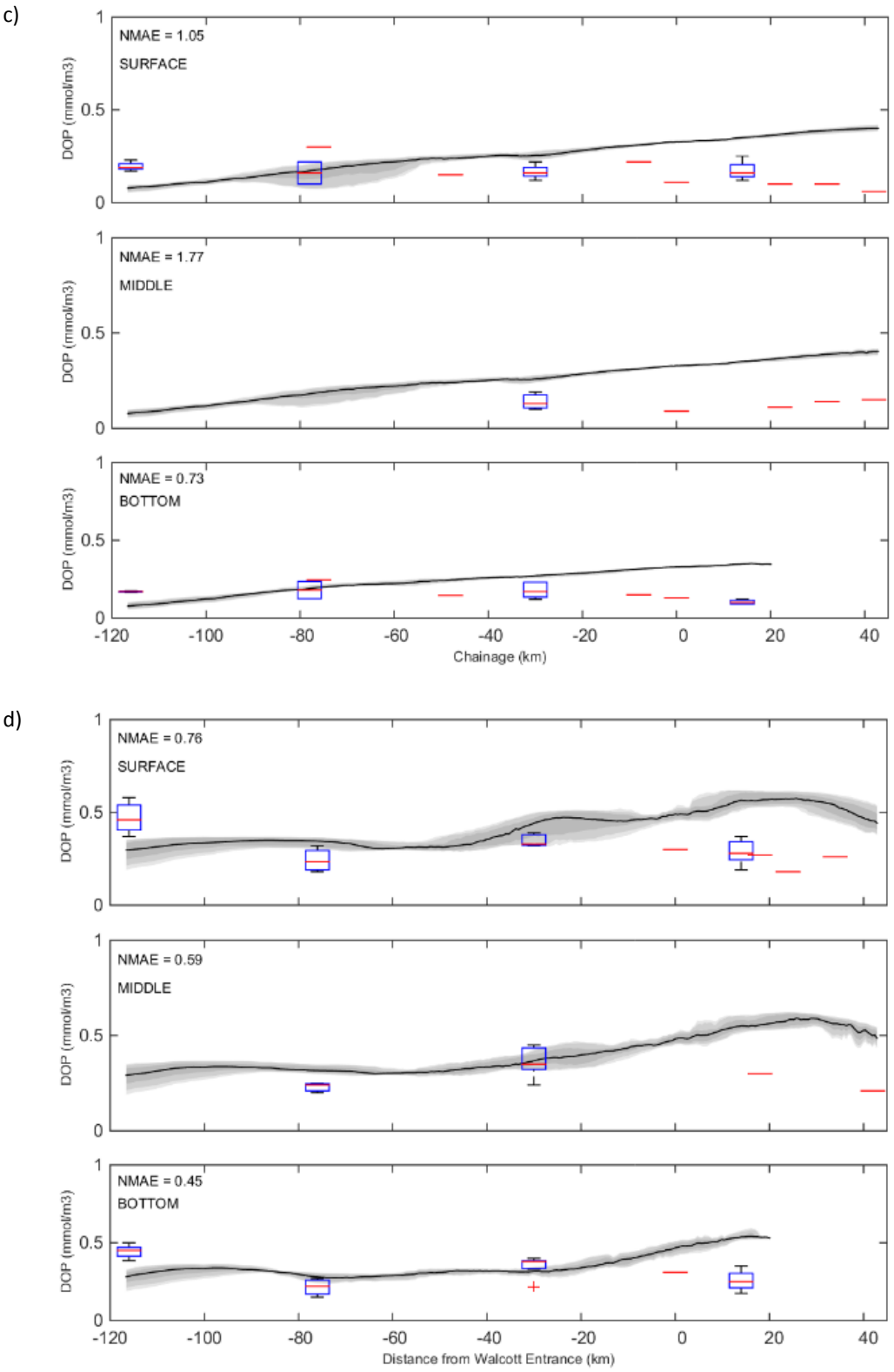

Figure 5-36. Comparison of model results of PO_4 (a,b) and DOP (c,d) against the October 2013 dry season (a,c) cruise data (KM5887) and the March 2014 wet season (b,d) cruise data (KM5938). Field data are represented as box plots (centred around the median, red dash is the mean, edges 25% and 75% percentiles, whiskers extend to the most extreme non outlier data points and outliers are represented as red crosses). Distance is measured as chainage (originating from the Walcott Inlet entrance). Grey shading around the model prediction (black) reflects the range of concentrations experienced at the model station over the relevant cruise/sampling period.

a)

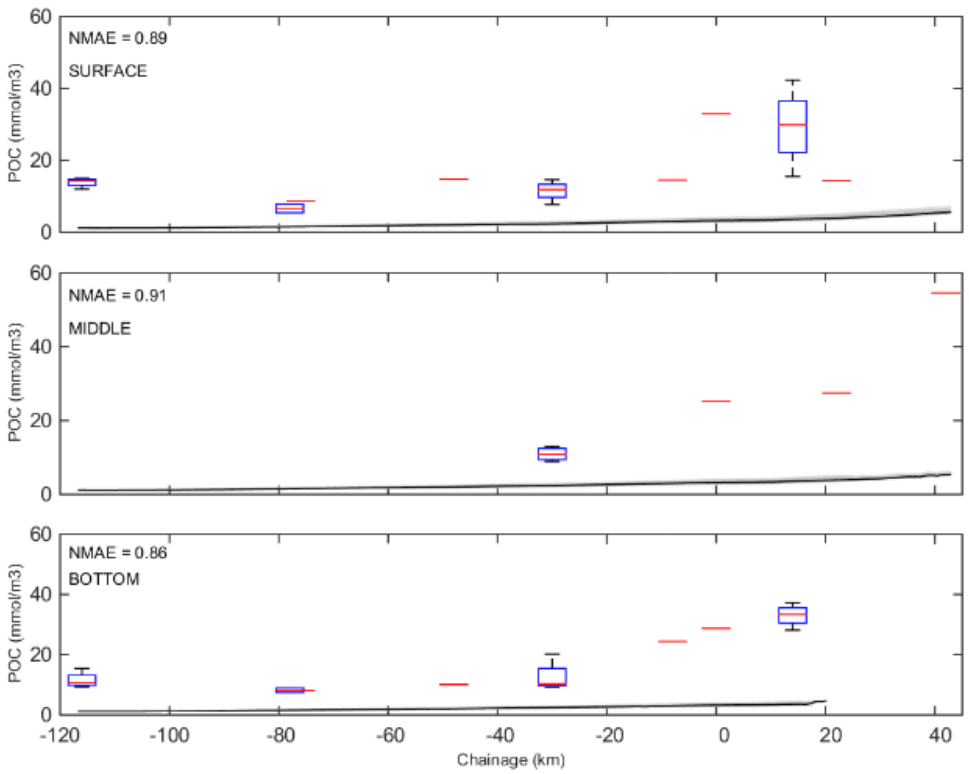
NMAE = 0.89
SURFACE
NMAE = 0.91
MIDDLE
NMAE = 0.86
BOTTOM
POC (mmol/m3)
Chainage (km)

b)

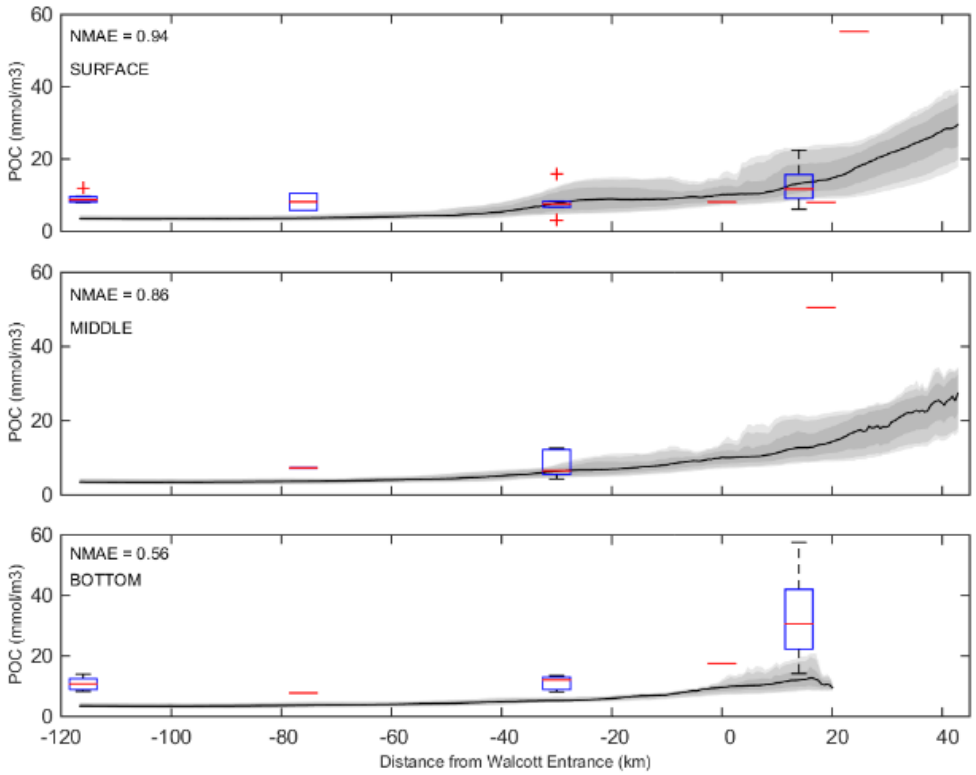
NMAE = 0.94
SURFACE
NMAE = 0.86
MIDDLE
NMAE = 0.56
BOTTOM
POC (mmol/m3)
Distance from Walcott Entrance (km)

c)

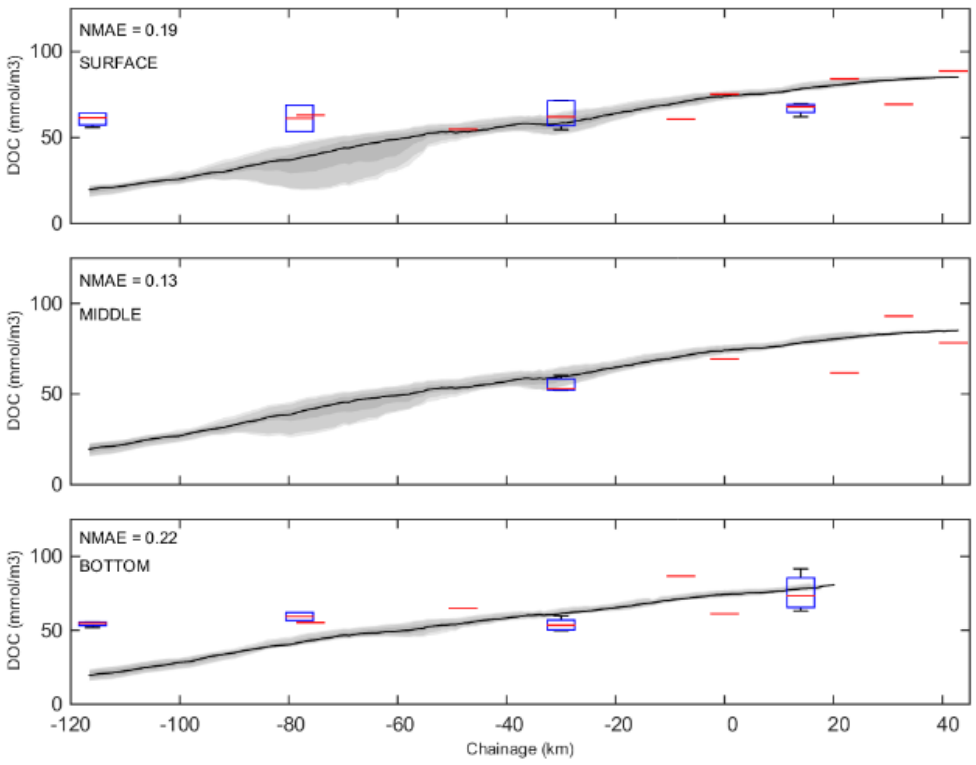
NMAE = 0.19
SURFACE
NMAE = 0.13
MIDDLE
NMAE = 0.22
BOTTOM
DOC (mmol/m3)
0
50
100
-120
-100
-80
-60
-40
-20
0
20
40
Chainage (km)

d)

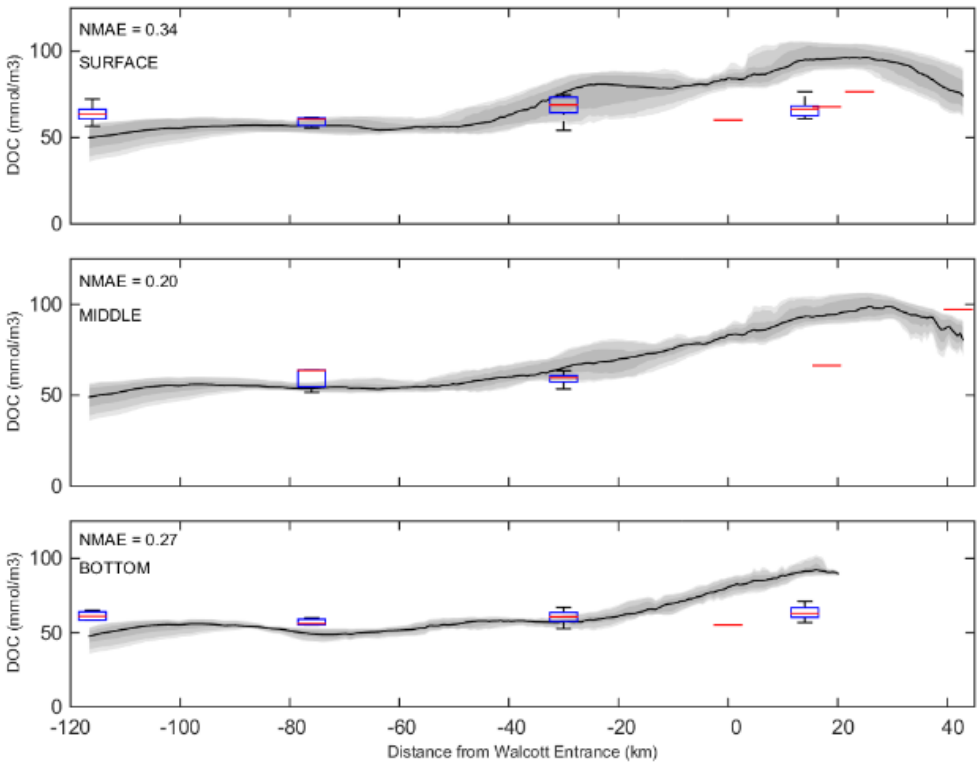
NMAE = 0.34
SURFACE
NMAE = 0.20
MIDDLE
NMAE = 0.27
BOTTOM
DOC (mmol/m3)
0
50
100
-120
-100
-80
-60
-40
-20
0
20
40
Distance from Walcott Entrance (km)

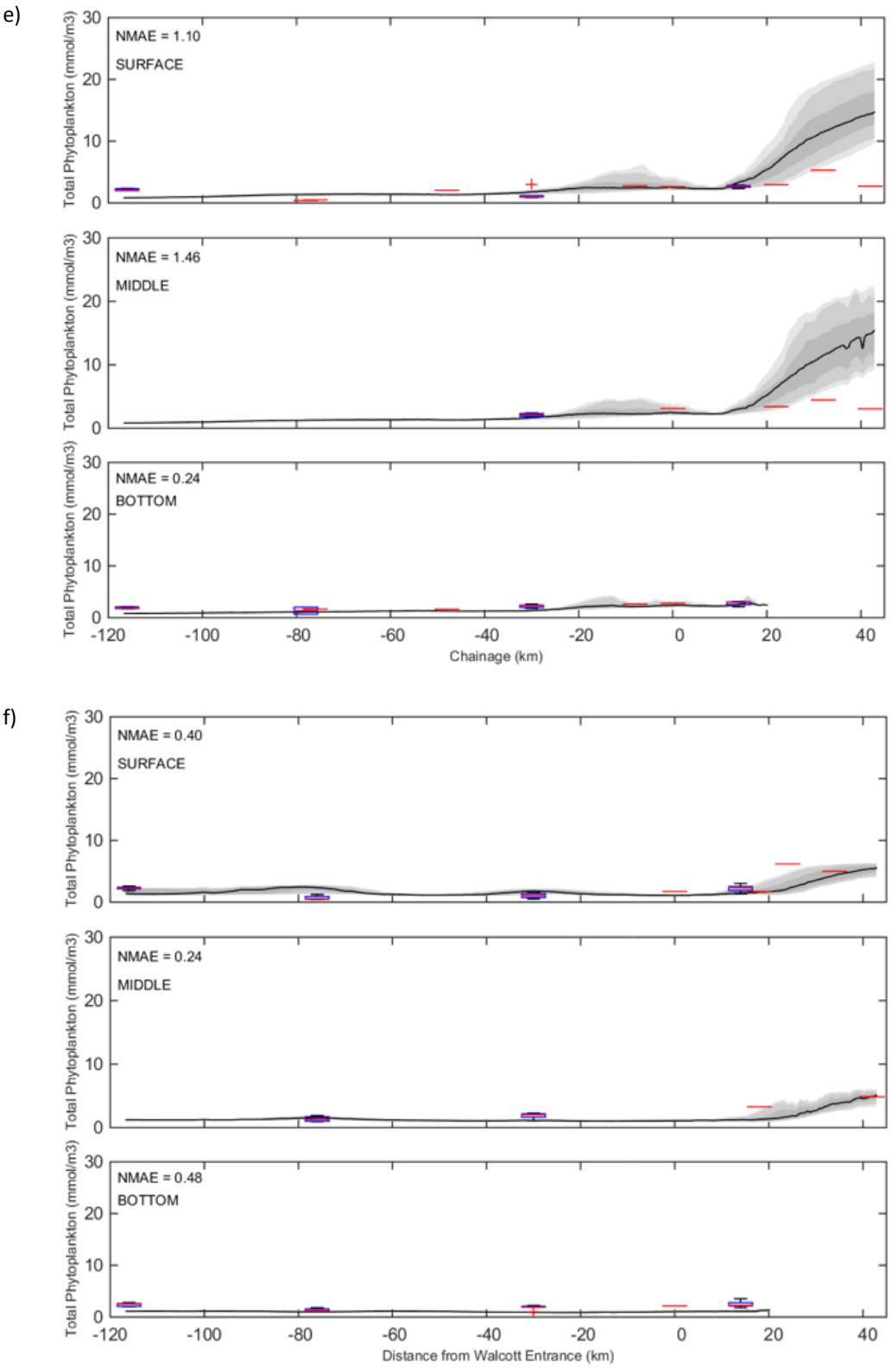

Figure 5-37. Comparison of model results of POC (a,b), DOC (c,d) and Chl-a (e,f) against the October 2013 dry season (a,c,e) cruise data (KM5887) and the March 2014 wet season (b,d,f) cruise data (KM5938). Field data are represented as box plots (centred around the median, red dash is the mean, edges 25% and 75% percentiles, whiskers extend to the most extreme non outlier data points and outliers are represented as red crosses). Distance is measured as chainage (originating from the Walcott Inlet entrance). Grey shading around the model prediction (black) reflects the range of concentrations experienced at the model station over the relevant cruise/sampling period.

Table 5-9. Model fit metrics assessed against the dry season (KIM5887) and wet season cruise (KIM5938) observed data, showing: number of samples (N), field data mean (mean), field data standard deviation (std), normalised mean absolute error (NMAE), root mean square error (RMSE), model efficiency (MEF), model skill score (MSS), correlation coefficient (r2) and percent relative error (PRE).

Variable	season	N	mean	std	NMAE	RMSE	MEFF	MSS	r2	PRE
Salinity	dry	22	35.48	0.18	0.01	0.34	-13.90	0.54	0.73	-0.7
	wet	15	30.21	2.68	0.05	1.86	0.34	0.90	0.95	-4.0
Suspended Solids	dry	24	94.38	133.69	0.92	139.13	-0.20	0.44	0.78	-65
	wet	17	95.23	210.98	0.80	205.78	0.10	0.54	0.69	-48
Ammonium	dry	24	0.47	0.15	0.27	0.15	-0.19	0.74	0.80	-21
	wet	17	0.50	0.09	0.26	0.16	-6.65	0.61	0.87	-26
Nitrate	dry	24	1.91	2.22	0.73	2.29	-0.11	0.52	0.22	-14
	wet	17	0.81	0.49	0.72	0.59	-1.26	0.52	0.39	47
Phosphate	dry	24	0.38	0.16	0.20	0.10	0.50	0.84	0.94	-20
	wet	17	0.27	0.11	0.22	0.08	0.26	0.74	0.70	-13
DON	dry	24	4.91	1.87	0.42	2.31	-1.81	0.55	0.44	29
	wet	17	5.21	2.56	0.64	3.49	-1.70	0.53	0.47	42
DOP	dry	24	0.15	0.04	1.03	0.17	-33.23	0.18	-0.45	98
	wet	17	0.30	0.08	0.55	0.20	-7.00	0.27	-0.12	49
DOC	dry	24	67.78	12.34	0.13	10.47	0.12	0.79	0.71	-3.2
	wet	17	69.97	20.36	0.26	24.27	-11.21	0.42	0.29	1.4
POC	dry	24	29.47	23.97	0.87	33.49	-1.49	0.47	0.86	-87
	wet	17	88.08	183.56	0.79	180.79	-0.26	0.48	0.87	-78
Total Phytoplankton	dry	24	2.56	0.91	0.69	2.72	-12.22	0.50	0.66	38
	wet	17	2.50	1.32	0.39	1.14	-1.73	0.71	0.63	-22

5.4.2 Computing the realm of influence

A time series of L_1 and L_{50} was compared against Walcott Inlet inflow, Q_f (Figure 5-38). The length scales representing both the outer extent of terrestrially derived nitrogen (L_1) as well as the point where autochthonous and allocthonous nitrogen sources are in equal measure (L_{50}) demonstrate the strong tidal signal, but superimposed on this is the effect of the flow rate into Walcott Inlet (and to a lesser extent Secure Bay and Doubtful Bay), where there is a positive correlation between inflow rate and extent of terrestrial nitrogen influence with a 3-5 day time lag (Figure 5-40). We can see that in the absence of any freshwater inflow that the terrestrially derived nitrogen (L_1) was depleted within Walcott Inlet and that it is not until the end of December, after some modest freshwater inflow, that any terrestrially derived nitrogen made it into Collier Bay. In fact, even following the peak freshwater inflow, 50% of the terrestrially derived nitrogen only just exited Walcott Inlet.

L_1 and L_{50} are dependent on antecedent conditions, as well as influenced by the changes in the nature of the tidal movements in the model domain, and the complex circulation within the bay (see also Section 5.3), thereby it is difficult to develop a simple relationship between flow and position of the terrestrial nutrient plume. However, to provide a simple "rule of thumb" for the system, a 14-day moving average smoothing function was applied to dL_1/dt for surface waters and also to the inflow (Figure 5-39). We then correlated the smoothed dL_1/dt and inflow rate, applied with a 12-day time lag (Figure 5-40). The resulting correlation was high (r^2 =0.85), demonstrating that the freshwater flow played a large role in increasing the realm of influence of the terrestrially derived nitrogen.

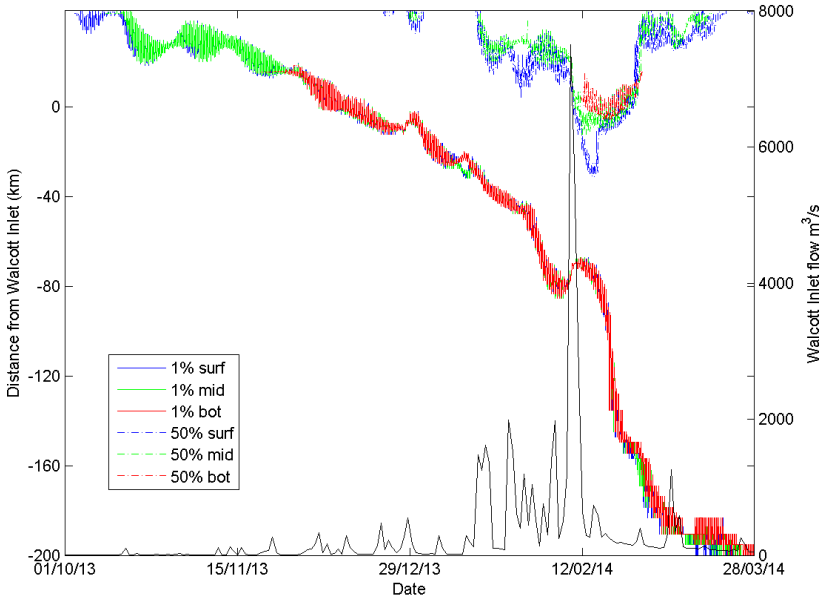

Figure 5-38. Predicted horizontal extent of the terrestrial nutrient influence for 1% and 50% contribution (L1 and L50 respectively), over the simulation period, compared against flow rate (right axis).

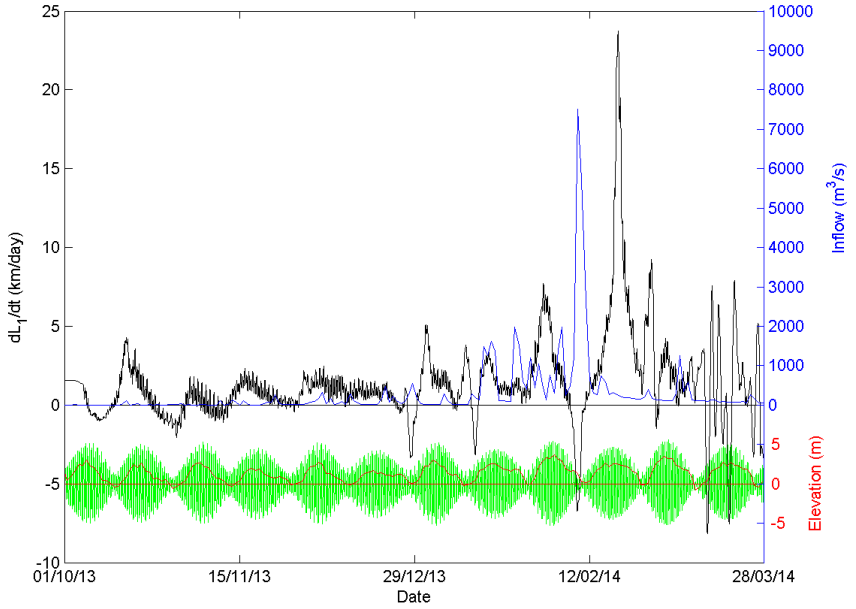

Figure 5-39. Rate of change of the terrestrial nutrient influence (based on L1) over the model domain to dissect the influence of inflow alone, a 14-day moving average smoothing function was applied to dL_1/dt for surface waters and a 14-day moving average was also applied to the inflow volume.

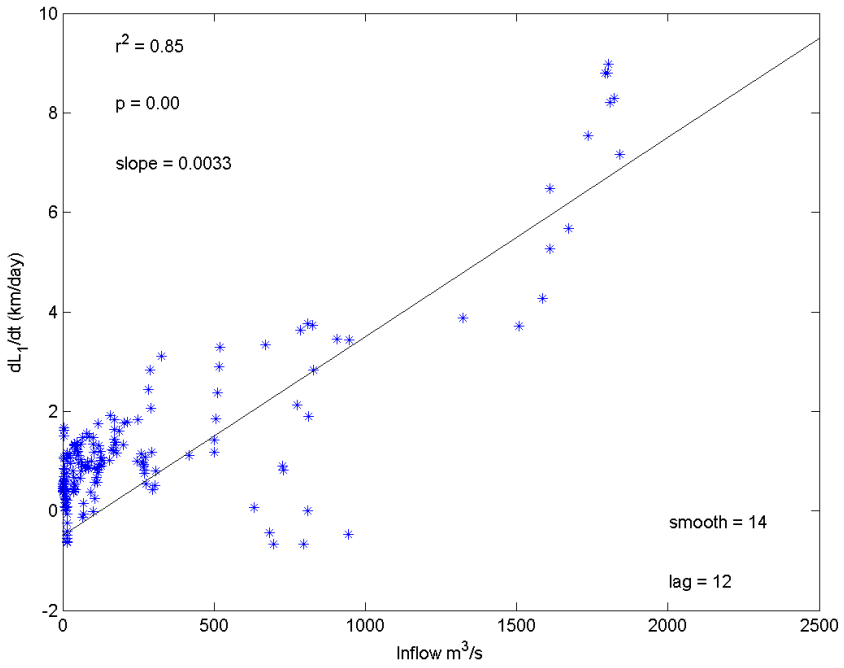

Figure 5-40. Scatter plot of rate of change of terrestrial nutrient influence (L_1) with 14-day moving average applied vs inflow with 14-day moving average and 12-day time lag applied.

In order to develop a simple relationship between the extent of terrestrial influence of nitrogen relative to flow, the domain was partitioned into four zones spanning from the coastal zone to outside of the embayment Figure 5-41). We computed the percentage of terrestrial nitrogen for each zone as a function of time. This was fitted to a simple function as indicated in Figure 5-41. The percentage of terrestrial nitrogen was unsurprisingly highest within Walcott Inlet for all flow conditions; with up to 80% terrestrial nitrogen in Walcott for the strongest inflow. The percentage of terrestrial nitrogen generally increased with increasing inflow for all zones,

with the exception of zone 2. Zone 2 had a decreasing trend for the lowest flows indicating that biogeochemical transformation of nitrogen was dominating the balance in this zone during low flow rates.

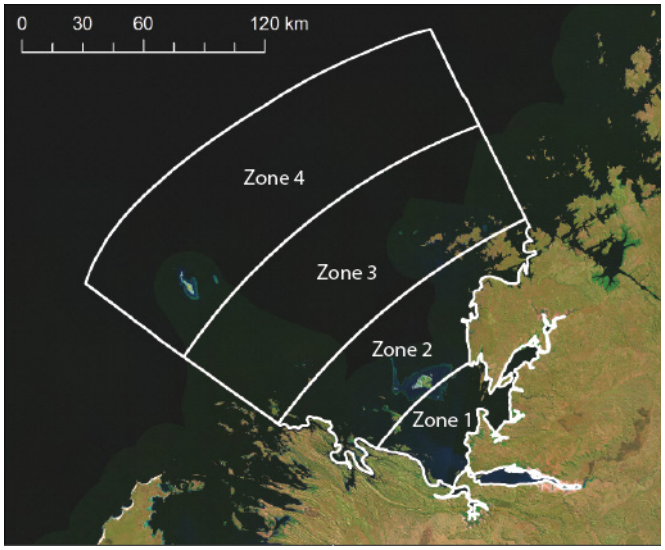

Figure 5-41. Zones used to estimate % of terrestrial N for different flow rates in Figure 5-42.

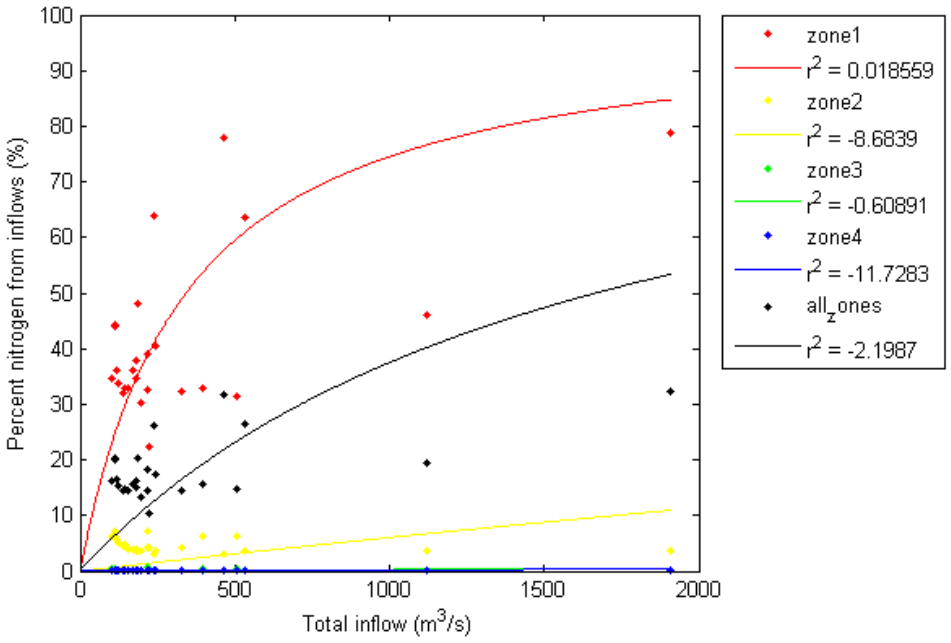

Figure 5-42. Percent terrestrial nitrogen (N%) within the overall domain (black) and 4 discrete zones plotted against total inflow for each day in March 2014. The solid line represents empirical fit to a function of the form:
$N\% = a\ Q/[K_q+Q]$.

5.4.3 Nutrient budget

The nitrogen budget for the Walcott Inlet and Inner region of Collier Bay is shown in Figure 5-43 for the month of March, following the peak inflow. Here we show the pools, transport fluxes, and the biogeochemical fluxes of nitrogen. The pools of N decreased over the month-long period, indicating that without the freshwater inflow the system uses up the N. The inner nitrogen (IN) and particulate organic nitrogen (PON) were the 2 largest pools of nitrogen in both Walcott Inlet and the Inner Bay. The inner nitrogen (IN) is that incorporated

into living phytoplankton. The fact that IN was the largest pool indicates that free N was quickly taken up by the primary producers. All of the N pools cycle up and down at the tidal frequency, indicating that water of different concentration was advected toward and away from the region of interest. Not surprisingly, the material transport fluxes were very large and followed the tidal cycle. The variation in the material transport fluxes eclipsed the biogeochemical cycling fluxes, by 2 orders of magnitude. However, if the advection by the tides is removed (low pass filtered) then the material transport fluxes were of similar magnitude to the biogeochemical cycling fluxes.

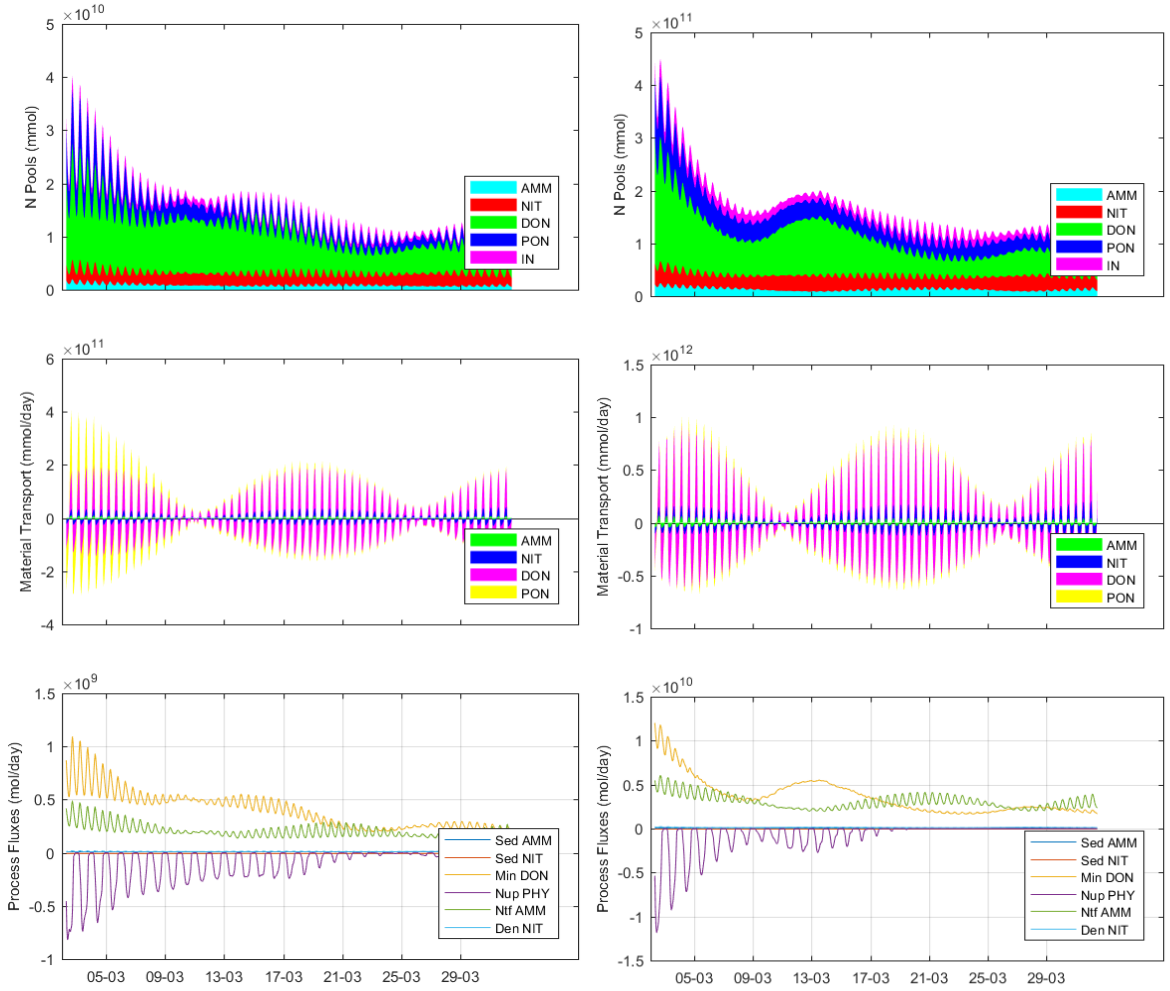

Figure 5-43. Overview of the nitrogen budget for two sub-regions of the simulation domain: Walcott Inlet (left) and The Inner Bay (right). The top panel indicates mass of N in the different forms, the middle panel indicates the transport flux into and out of the domain, and the bottom panel indicates the biogeochemical fluxes.

By tracking the distribution of a passive tracer released in the upper reaches of Walcott Inlet we can quantify the portion of "new" terrestrially sourced N that supports gross primary production (GPP) compared with recycled sources of N. A 140 km transect that extended from the upper reaches of Walcott Inlet into Camden Sound demonstrates that GPP was much larger in Walcott Inlet, compared with the semi-enclosed embayment and Camden Sound (Figure 5-43). The GPP was higher in the dry season and beginning of the wet season compared with the GPP at the end of the wet season. Over the 140 km transect studied, recycled N was the most significant source of N stimulating primary productivity in both the dry and wet season. In both the dry and wet season terrestrial N was only important to GPP within Walcott Inlet. Within Walcott Inlet, in the wet season (11/03/14) the relative portion of the terrestrially derived N was much higher than in the dry season

(28/10/2013).

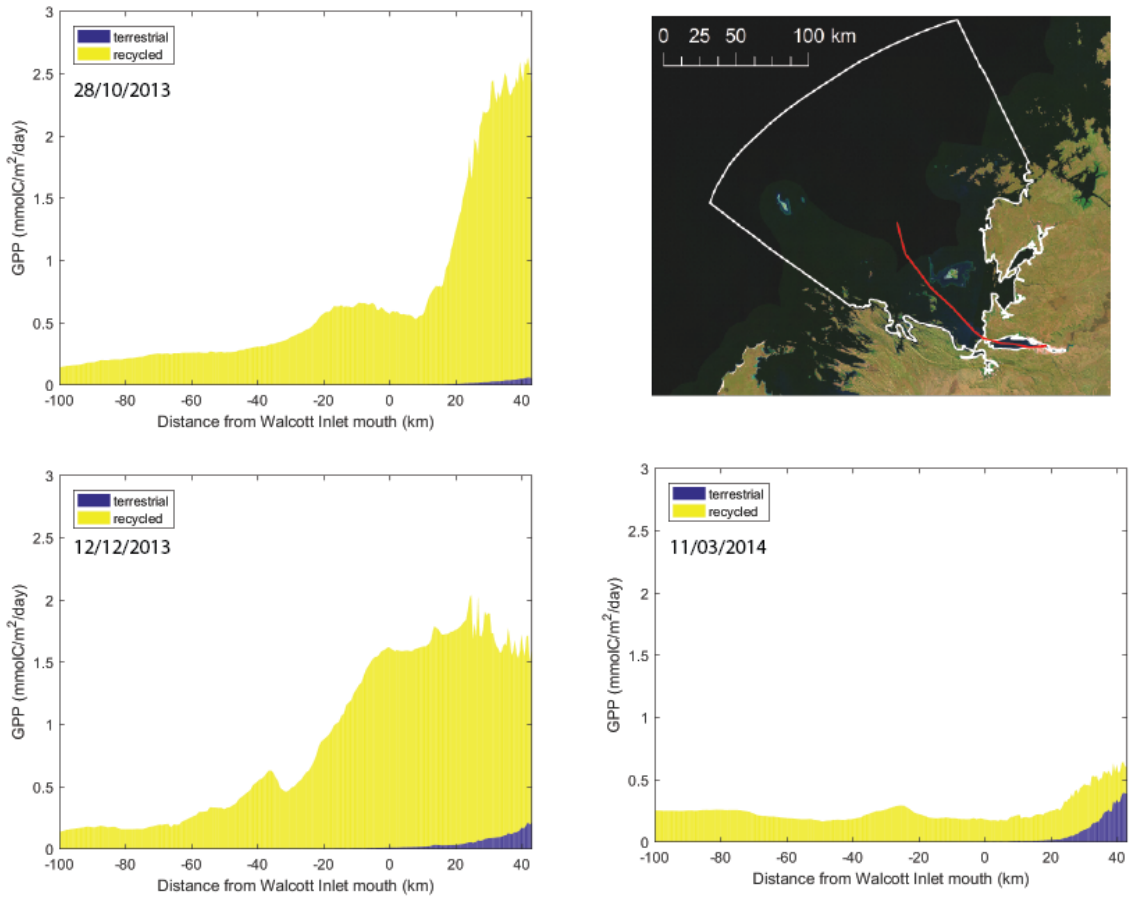

Figure 5-44. Gross primary production resulting from terrestrial/ shelf and recycled nutrients along transect from Walcott Inlet on right hand side (0 is at Inlet mouth) to offshore during three representative times. All examples were from noon during neap-tides.

5.4.4 Climate change scenario assessment

Using the fitted relationships derived from the above analyses (i.e., Figure 5-41), it is possible to predict an indicative change in the extent of terrestrial influence on primary productivity via nutrient input (i.e., a change to L1) under projected climate change scenarios, using the predicted flows from the catchment hydrology model (described in Section 5.2.3 and Table 5-7). The projected wet scenario predicts only 14% greater river inflow and thereby the analysis shows that the rate of terrestrial input (km/day) would increase by about 15% for an average wet season flow rate of 1000 m^3/s. This would be similar for the median climate change projections, but almost no difference would result under the dry future projection for this region. In conclusion, because the terrestrial inputs on an annual basis are quite small in the system the impact of small increases/ decreases in rainfall in any one year are minimal. However, we do not have the computational power to run the model for decades to measure the cumulative impact, which would eventually affect the recycled component available for GPP and could ultimately lead to shifts in the biogeochemistry.

6 Discussion and Conclusions

From the biogeochemical data Walcott Inlet appears to be a carbon poor environment where any labile carbon from algae is rapidly re-mineralised by bacteria. There is visual evidence that large amounts of more recalcitrant terrestrial material may be transported into the inlet during high flow events, but from the lipid marker results there is little evidence that this becomes incorporated into sediments suggesting it is most likely transported through the inlet.

The hydrological simulations were the first serious attempts to generate flows and loads in the Kimberley for coastal modelling. The simulations were necessarily highly simplified, because of the limited data availability. We have confidence the flow volumes provide reasonable estimates of real flows, but without measured data during the period of estuarine field programme we remain cautious of over-interpretation of the findings, particularly of the connections between river flows and estuarine conditions. The catchments were represented as a set of grid cells and the model was forced by a single daily climate file for each catchment. As such, spatial variability within the catchments is not represented but experience, with a previous project in the Pilbara, has demonstrated that, within the constraints of available data, such an approach yields result with little difference in catchment outlet from a more spatially distributed approach. Since we are primarily interested in the export to the estuary this approach is satisfactory. However, there were no stream flow gauges close to the Walcott Inlet and the closest gauge is no longer operational. While our calibrations attained very good representations of the stream flows, as measured by our Objective Function, the lack of measurements for the whole catchment necessarily limits our confidence in the overall result.

Some of the biophysical and chemical processes within the estuary occur on much shorter time scales than daily and this is also a limitation on the hydrological interpretation. An assessment could be undertaken to determine to what extent the simulated daily inflows limit the estuarine simulations.

In particular, as referred to above, the water quality data are severely limited, with most parameters having only a handful of samples at best. The range of flow conditions during sampling is very limited and it was not possible to derive any discharge-quality relationships. This is not to say that such relationships would necessarily be easily determined even with more data, as the catchments are highly variable and the nature of runoff generation, particularly annual and seasonal variability, may result in such relationships not emerging in the way they often do in more temperate streams. However, it is a clear recommendation from our work that a comprehensive water quality sampling along with stream flow gauging should be undertaken as part of any further work in the region.

There are some interesting features of the flow generated by the GCMs. Table 5-6 and Table 5-7 show that firstly, there is not a great difference in mean rainfall or flows between the three future climates and the Historical sequence. The projections for all future climates, even the driest one, are for an increase in mean annual rainfall and flow. Furthermore, the projections are also for a greater inter-annual variability, so that while the average flows may increase, there will be a greater range between wet and dry years and low flow years will be more severe. Because of the limitations in the historical water quality data we are cautious about drawing strong conclusions on the future trends of water quality parameters.

A ROMS simulation was first applied to explore the nature of the salt fluxes through Collier Bay in the wet season. The model was found to perform well considering the unique context of the complex coastline shape, bathymetry and macro-tidal forcing. Salt (a tracer) was to trace the cross-shore exchange of water within the estuary/bay system. Identifying the important patterns of exchange flows with the open ocean. Salt flux components driven by different mechanisms (advection, steady shear dispersion and tidal oscillation) were obtained with an Eulerian salt flux decomposition method and complemented with information about the upgradient and downgradient salt fluxes using the isohaline salt flux decomposition method. Through the comparison of the dynamics at North Channel and Walcott Inlet, it is clear that bathymetric variation in different directions (lateral or longitudinal) has different impacts on the interaction between tides and freshwater inflow in shaping salt fluxes and thus the horizontal mass exchange. At the North Channel, shallow

flow in the lateral direction plays a significant role in the net salt flux. The longitudinal bathymetric variation had less impact on the Eulerian salt fluxes and the net salt flux, but had a significant impact on both the upgradient and downgradient components as shown for Walcott Inlet. This detailed hydrodynamic understanding of the nature of the bay and estuarine hydrodynamics provided an important foundation for the more complex assessment of carbon and nutrient fate and transport.

To investigate the physical-biogeochemical interactions in this region, a second model simulation was setup using a high-resolution finite volume approach with the FV-AED platform. This model was first setup to also simulate the hydrodynamics with focus on the coastal margin, inter-tidal dynamics and the estuarine reaches, and then additionally configured to simulate turbidity (including particle resuspension), and inorganic and organic carbon and nutrients. This model was run in a continuous 6 month simulation that spanned the dry and wet season, and its performance was evaluated by comparing predictions against all available data from the October 2013 and March 2014 R.V. *Solander* cruises. Whilst the model configuration was relatively simple with many assumed parameters, the simulations reasonably captured the mean concentrations within the region, concentration changes along the estuary portion of the domain, and differences between wet and dry conditions. The validated model was then interrogated to assess the "realm of influence" of terrestrial nutrients (i.e., the area of the embayment whose nitrogen had come from either >1% or >50% from the river inflow), and how this varied with flow magnitude, or within different areas of the system. Flows greater than 300 m^3/s were shown to dominate nutrient loads within Walcott Inlet itself (>50%) and significantly contribute to the inner reaches of Collier Bay (>15%). The hydrological modelling was all undertaken with daily timesteps, and hence direct comparison of instantaneous flows with daily averages should be done with caution. A flow rate of 300 m^3s^{-1} is equivalent to a daily flow rate of 26 GL. On the scale of the Walcott Inlet this has a probability of daily exceedance of about 7%. In conclusion, because the terrestrial inputs on an annual basis are quite small in the system the impact of small increases/ decreases in rainfall in any one year are minimal.

The analysis has elucidated key aspects biogeochemical dynamics of this system, however, uncertainty remains in several aspects of the model predictions, and it is recommended to be further refined during future revisions. Specifically:

- data from several Kimberley rivers suggests that dissolved organic nitrogen (DON) may be a significant nutrient input in high flow events. Presently little is known about the composition or availability of DON or whether it is associated with the first-flush or later in the flow event. It is important to understand more about this component and what role it may play in coastal productivity;
- results from benthic mapping could be used to better configure spatial regions within the model domain with distinct sediment properties and/or benthic structures and communities;
- improved focus on sediment resuspension and sedimentation will allow for improved prediction of suspended sediment and turbidity. Outputs from remote sensing efforts can be used to help calibrate such a model to better capture the turbidity gradient from the coast to offshore. Additional effort is required to better understand the rate of particulate carbon resuspension;
- sediment nutrient fluxes, including estimates of denitrification and nitrate/ammonium fluxes are important to better resolve the sediment loading to the water column. This includes recommendations for laboratory based sediment flux studies, and additional effort to apply/develop an improved sediment biogeochemical model; and
- further work is required to better elucidate the production, fate and role of algal derived carbon as well as the fate of the apparent large amounts of terrestrial material (twigs, leaves etc.) observed to enter the inlet.

Despite the paucity of data and resulting uncertainties in the simulations this project has revealed the unique nature of the Kimberley coast and its estuarine systems and it will be important to further enhance and refine these to support future management of the region.

7 References

Allen SE, Dinniman M, Klinck J, Gorby D, Hewett A, Hickey B (2003) On vertical advection truncation errors in terrain-following numerical models: Comparison to a laboratory model for upwelling over submarine canyons. J Geophys Res 108

Bligh EG, Dyer WJ (1959) A rapid method of total lipid extraction and purification. Canadian Journal of Biochemistry and Physiology 37:911-917

Charles SP, Fu G, Silberstein RP, Mpelasoka F, McFarlane D, Hodgson G, Teng J, Gabrovsek C, Ali R, Barron O, Aryal SK, Dawes W (2015) Hydroclimate of the Pilbara: past, present and future. A report to the Government of Western Australia and industry partners from the CSIRO Pilbara Water Resource Assessment. CSIRO Land and Water Flagship, Australia

Chiew FHS, Kirono DGC, Kent DM, Frost AJ, Charles SP, Timbal B, Nguyen KC, Fu G (2010) Comparison of runoff modelled using rainfall from different downscaling methods for historical and future climates. Journal of Hydrology 387:10-23

Chiew FHS, Leahy C (2003) Comparison of evapotranspiration variables in Evapotranspiration Maps of Australia with commonly used evapotranspiration variables. Australian Journal of Water Resources 7:1–11

Chiew FHS, McMahon TA (2002) Modelling the impacts of climate change on Australian streamflow. Hydrological Processes 16:1235–1245

Chiew FHS, Peel MC, Western AW (2002) Application and testing of the simple rainfall-runoff model SIMHYD. In: Singh VP, Frevert DK (eds) Mathematical Models of Small Watershed Hydrology and Applications. Water Resources Publication, Littleton, Colorado

Chiew FHS, Siriwardena L (2005) Estimation of SIMHYD parameter values for application in ungauged catchments. Congress on Modelling and Simulation (MODSIM 2005), Melbourne, Australia

Chiew FHS, Teng J, Vaze J, Kirono DGC (2009a) Influence of Global Climate Model selection on runoff impact assessment. Journal of Hydrology 379:172-180

Chiew FHS, Teng J, Vaze J, Post DA, Perraud JM, Kirono DGC, Viney NR (2009b) Estimating climate change impact on runoff across southeast Australia: Method, results, and implications of the modeling method. Water Resources Research 45:W10414

CSIRO (2009) Water in northern Australia. Summary of reports to the Australian Government from the CSIRO Northern Australia Sustainable Yields Project. CSIRO, Australia

CSIRO (2012) Proposed project methods. A report to the West Australian Government and industry partners from the CSIRO Pilbara Water resource Resource Assessment, Australia. CSIRO Water for a Healthy Country Flagship, Australia

DoW (2008) The Kimberley river environment. Water notes for river management. Department of Water, Perth, WA

Duan Q, Gupta VK, Sorooshian S (1992) Effective and efficient global optimization for conceptual rainfall-runoff models. Water Resources Research 28:1015-1031

Harrington GA, Stelfox L, Gardner WP, Davies P, Doble R, Cook PG (2011) Surface water – groundwater interactions in the lower Fitzroy River, Western Australia. CSIRO: Water for a Healthy Country National Research Flagship

Jeffrey SJ, Carter JO, Moodie KB, Beswick AR (2001) Using spatial interpolation to construct a comprehensive archive of Australian climate data. Environmental Modelling and Software 16:309-330

Lerczak JA, Geyer WR, Chant RJ (2006) Mechanisms Driving the Time-Dependent Salt Flux in a Partially Stratified Estuary*. J Phys Oceanogr 36:2296-2311

Lindsay RP, Commander DP (2005) Hydrogeological assessment of the Fitzroy alluvium, Western Australia. Department of Water, Perth, Western Australia

MacCready P (2011) Calculating estuarine exchange flow using isohaline coordinates*. J Phys Oceanogr 41:1116-1124

Morton FI (1983) Operational estimates of areal evapotranspiration and their significance to the science and practice of hydrology. Journal of Hydrology 66:1-76

Nash JE, Sutcliffe JV (1970) River flow forecasting through conceptual models. Part 1 - A discussion of principles. Journal of Hydrology 10:282-290

Petheram C, Rustomji P, Chiew FHS, Vleeshouwer J (2012) Rainfall-runoff modelling in northern Australia: A guide to modelling strategies in the tropics. Journal of Hydrology 462:28-41

Silberstein RP, Aryal SK (2015a) Appendix A: Technical details of the Rainfall-runoff modelling. In: McFarlane DM (ed) Pilbara Water Resource Assessment: Upper Fortescue region A report to the West Australian Government and industry partners from the CSIRO Pilbara Water Resource Assessment. CSIRO Land and Water Flagship, Australia

Silberstein RP, Aryal SK (2015b) Chapter 4: Rainfall-runoff. In: McFarlane DM (ed.) (2015) Pilbara Water Resource Assessment. A report to the West Australian Government and industry partners from the CSIRO Pilbara Water Resource Assessment, CSIRO Land and Water Flagship, Australia.

Tan KS, Chiew FHS, Grayson RB, Scanlon PJ, Siriwardena L (2005) Calibration of a daily rainfall-runoff model to estimate high daily flows. MODSIM 2005 International Congress on Modelling and

Simulation, Modelling and Simulation Society of Australia and New Zealand, December 2005, 2960-2966 ISBN: 0-9758400-2-9

Verardo DJ, Froelich PN, Mcintyre A (1990) Determination of Organic-Carbon and Nitrogen in Marine-Sediments Using the Carlo-Erba-Na-1500 Analyzer. Deep-Sea Research Part a-Oceanographic Research Papers 37:157-165

Volkman JK, Revill AT, Bonham PI, Clementson LA (2007) Sources of Organic Matter in Sediments From the Ord River in Tropical Northern Australia. Organic Geochemistry 38:1039-1060

Warner JC, Geyer WR, Lerczak JA (2005a) Numerical modeling of an estuary: A comprehensive skill assessment. Journal of Geophysical Research-Oceans 110

Warner JC, Sherwood CR, Arango HG, Signell RP (2005b) Performance of four turbulence closure models implemented using a generic length scale method. Ocean Model 8:81-113

Zhang YQ, Chiew FHS (2009) Relative merits of different methods for runoff predictions in ungauged catchments. Water Resources Research 45:W07412

8 Key Communication Activities – Summary

Students supported Wencai Zhou, PhD student, UWA, anticipated to graduate in August 2017 Josh Garlepp, Oceanography of the Kimberley: A preliminary study of circulation patterns of Walcott Inlet and the surrounding Camden Sound, Final year project at UWA (2014)
Journal publications Jones NL, Patten NL, Krikke DL, Lowe RJ, Waite AM, Ivey GM (2014) Biophysical characteristics of a morphologically-complex macrotidal tropical coastal system during a dry season, Estuar. Coast. Shelf S. 149(0): 96-108
Proceedings/Technical Reports Zhou W, Espinosa-Gayosso A, Jones NL, Hipsey MR (2016) Numerical Study of the Wet-season Hydrodynamics of a Macrotidally forced Bay with Complex Topography: Collier Bay, Kimberley, Western Australia. 20th Australasian Fluid Mechanics Conference, Perth December 2016
Submitted manuscripts As above
Presentations Zhou W, Espinosa-Gayosso A, Jones NL, Hipsey MR (2016). Numerical Study of the Wet-season Hydrodynamics of a Macrotidally forced Bay with Complex Topography: Collier Bay, Kimberley, Western Australia. 20th Australasian Fluid Mechanics Conference, Perth, December 2016 Hipsey M (2016) Hydrodynamic and Biogeochemical Controls on Productivity in the Kimberley Coast. Presentation to the Department of Parks and Wildlife lunch and learn session, June 2016 Revill A (2015) Terrestrial-Ocean Linkages: the role of rivers and estuaries in sustaining marine productivity in the Kimberley. WAMSI Research Conference, Perth, March 2015
Other communications achievements 2016 June 27: WAMSI News, Kimberley coastal system: links from the land to the deep sea: http://www.wamsi.org.au/news/kimberley-coastal-system-links-land-deep-sea
Knock on opportunities created as a result of this project
Key methods for uptake (i.e. advisory committee, working group, website compendium of best practice.) Lunch and Learn presentation at Parks and Wildlife – June 2016 Meeting with Node Leader and KMRP Advisory Group to discuss management needs and application – June 2016
Other KMRP 2.2.6 Summary (June) – Terrestrial – Ocean Linkages: the role of rivers and estuaries in sustaining marine productivity in the Kimberley (released June 2016) **https://indd.adobe.com/view/19d8180e-bbb0-4c27-b932-30902027d9aa**

9 Appendices

Appendix 1: This project directly addresses the following questions outlined in the Kimberley Marine Research Program Science Plan.

Key Question Informed Response
1. What is the relative significance of terrestrially-derived nutrient in sustaining inshore marine food webs? Terrestrially derived nutrients can constitute around 50% of total nutrients in Walcott Inlet and around 15% of those in Collier Bay. At this stage it is difficult to directly trace these through to food webs but as the models become more refined these linkages should become clearer.
2. How does seasonal and cyclonic riverine discharge (e.g. nutrient, freshwater and sediments) influence inshore marine ecosystems? Seasonal cyclonic events and the associated high river flows bring sediments and nutrients into the coastal environment in a way that doesn't happen at other times of the year. Deposition of these sediments may influence habitat availability – habitat and there is evidence that significant quantities of nutrients may also be delivered, particularly dissolved organic nitrogen (DON) about which little is known. In addition, we know very little about the distribution of nutrients during a flow event, for example first flush vs later in the flow.
3. How do human use of rivers and catchments affect estuarine and inshore marine ecosystems? If catchment derived nutrients are a significant contribution to nearshore coastal environments, then any changes in catchment use or flow restrictions could impact on delivery of this material. Until we better understand the linkages with coastal production it is unclear what the ecosystem level impact could be.
4. What is the biodiversity significance of estuarine habitats and communities? This project didn't assess biodiversity
5. How will climate change impact on catchment to ocean interactions The climate change scenarios assessed in this project suggest that while the amount of rainfall may not change, the way in which it is delivered may. This could result in changes to nutrient loads.
NEW QUESTIONS POSED BY MANAGERS
What is the relative importance of the major and minor river systems across the Kimberley and how is this identified? This study has focussed on one coastal catchment thus it isn't possible to make any inference on the relative relevance of this or other river systems across the Kimberley. However, the nutrient data we present for fourteen riverine inputs during one wet season survey does imply that there is significant variability in inputs between the different river systems, something that requires further investigation. Furthermore, our study has highlighted the paucity of historical data available for flow and nutrient concentrations in the Kimberley rivers. Additional data would be required in order to assess the relative importance of different river systems.
What makes a river system important? Are some parts more important than others or is it the whole that is most important? It is likely the whole river system, including the estuary is important as material will enter the river along its length while the estuary is a place that material transformations occur.
Is traditional knowledge incorporated into this project (i.e. nutrient flow)? Traditional owner knowledge was incorporated into the planning phase of the project and attempts were made

to include rangers during the field campaigns. Unfortunately due to the limited space on the vessel and lack of their own boat at the time this wasn't possible. However, there is scope for rangers to take on the next phase of the project and incorporate their knowledge going forward.
Does agricultural use also have an influence and, if so, what level (scale) of impact/influence? Preliminary results from this project suggests catchment derived nutrients may be important in coastal productivity. If this is the case then any changes to catchment use, including agriculture, may change this process by changing catchment soil content.
Fire research - What are the implications for inputs into marine ecosystem from managed and unmanaged fires? Should this influence how we manage fires, similar to changes made based on terrestrial ecology? We have little knowledge on how fire management may impact nutrient delivery to rivers.
What are the implications/impacts to the system of inputs from cattle vs agricultural sources into system? How do these affect marine coastal environments? This project didn't assess this question but it is likely there would be differences. Cattle tend to be more dispersed though can lead to enhanced sediment delivery through activity close to riverbanks. Agriculture could lead to alteration of water flows and nutrients. However, without specific scenarios it is difficult to assess the likely implications.
What are the impacts from changing land use (e.g. extra nutrients onto land flows, through RAMSAR wetlands)? (link to 1.4 - changing colours in mudflats) At this stage this is unclear but it is a question that potentially could be answered utilising the models that have been developed.